Determining day length and temperature regulation of flowering: a molecular and modelling approach

Hannah A. Kinmonth-Schultz

A dissertation

Submitted in partial fulfillment of the

Requirements for the degree of

Doctor of Philosophy

University of Washington

2016

Reading Committee:

Takato Imaizumi, Chair

Soo-Hyung Kim

Jennifer Nemhauser

Program Authorized to Offer Degree:

Biology

University of Washington

Abstract

Determining day length and temperature regulation of flowering: a molecular and modelling approach

Hannah A. Kinmonth-Schultz

Chair of the Supervisory Committee:

Associate Professor Takato Imaizumi

Biology

In nature, plants are exposed to numerous abiotic and biotic pressures. Temperature, day length, light quality, length of winter, herbivors, nutrients, and pathogens all affect plant development and change throughout the growing season. Plants have evolved to act proactively or reflexively to mitigate negative effects and to time their development to favorable times of the year. The molecular mechanisms for many of these pressures in isolation are well understood; however, we do not yet understand how plants may perceive and integrate multiple environmental factors at once. In light of climate change, understanding plant responses in natural settings is especially crucial. Here, I review how the molecular pathways controlling the circadian clock interact with pathways involved in perceiving environmental cues to modulate circadian-regulated phenomena such as flowering, diurnal leaf growth, and the cold response. I discuss how several pathways converge to regulate a few key genes, and that this may be how plants are able to integrate multiple environmental pressures. I, then, explore the molecular responses of two key flowering

genes – *FLOWERING LOCUS T* (*FT*) and *CONSTANS* – to assess the combined influence of day length changes and temperature cycles on flowering. I show that cool temperatures can both suppress and induce *FT*, and that *FT* levels are highly predictive of flowering across a range conditions. Next, I incorporate these mechanisms into an existing model, which already included day length regulation of *FT* and temperature regulation of leaf tissue production. I show that incorporating the mechanisms of temperature regulation on *FT* coupled with accumulating *FT* with increasing leaf tissue as the plant grows can improve model predictions in fluctuating temperature environments. I discuss how such an approach might be used to improve the predictions of crop models. Finally, I discuss questions that still remain and provide recommendations for future study.

Chapter 1

Understanding plant response in complex environments

Chapter 1

Understanding plant response in complex environments

In natural environments, several biotic and abiotic factors exist – day length, light quality, length of winter, ambient temperatures, temperature cycles, pollinators, herbivores, drought, and nutrients – and most are known to affect plant development (Michaels & Amasino, 1999; Michael *et al.*, 2003; Imaizumi *et al.*, 2003; Rizhsky *et al.*, 2004; Searle *et al.*, 2006; Aerts, 2009; Bernhardsson & Ingvarsson, 2012). Considering each of these factors in isolation, plants can either preemptively or reflexively respond to alter their development to improve resource acquisition and ensure development when conditions are most favorable. For example, plants can sense available nutrients and adjust root growth so that more root tissue is produced in nutrient rich pockets (Ruffel *et al.*, 2011). Because of their internal circadian clock, plants can monitor seasonal cues such as day length to coordinate development with times when the climate is most favorable (Golembeski *et al.*, 2014). How to plant coordinate their response when they perceive multiple cues? How can we predict the response of agriculturally or ecologically important species in complex environments?

These questions become more pressing in light of climate change. Warming could increase the length of the growing season and seems to have done so over the past few decades (Iizumi *et al.*, 2014). However, spring temperatures can still dip down to freezing even after the snow melts, damaging plants that have germinated or re-initiated growth early (IPCC, 2014). Later, high heat and drought can impact plant development and stunt yield. Growers aim to time sowing and harvest such that critical points in plant development coincide with adequate rainfall while avoiding damage from stress (Wenden & Rameau, 2009).

When predicting plant response, one hypothesis is that plants perceive two simultaneous stresses or cues as a third stress or cue entirely different from the two alone (Prasch & Sonnewald, 2015,

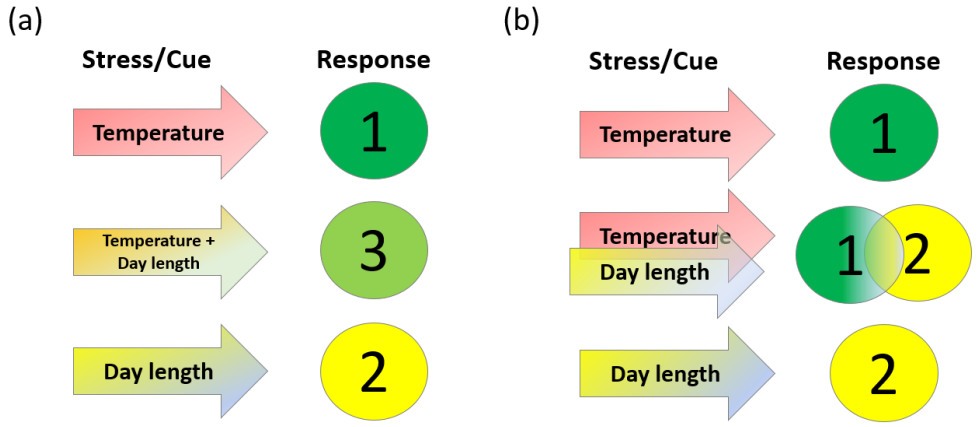

Figure 1.1. Conceptual models of plant response to complex environments. Plants could perceive two stresses or cues (temperature and day length) as an entirely different cue when perceived together, eliciting an entirely different response from either cue alone (a). The combined response could be decomposed into two separate responses than can be predicted from the cues individually (b).

Figure 1.1a). As a consequence, they produce a response that cannot be predicted from the responses from each stress or cue individually. For example, some transcriptomics comparisons revealed only a few genes that were regulated in response to heat combined with drought or light stress as well as in response to the individual stresses (Prasch & Sonnewald, 2015). The expression levels of several more genes seemed to be regulated only by the combined stress, indicating a unique response. The recommendation, then, is to test plant response to multiple combinations of stresses. I agree that exploring plant responses to complex environments is necessary. However, through such analyses, it may be possible to decompose a plant response to complex environmental interactions into separate, predictable plant processes (Figure 1.1b).

To aid farmers and seed distributors in determining which cultivars to grow and when to plant, mathematical models are often used. By and large, these are based on empirical observations that the timing of plant development coordinates well with temperature (Lehenbauer, 1914), leading to the concept of thermal time. These models can take many forms (Kumudini *et al.*, 2014), but in all cases, the effect of temperature accumulates over time. Within a range of non-stressing temperatures, more thermal units, or degrees Celsius per unit time, will accumulate during a warm growing season than a cool one, causing plants to develop faster. In some cases, these models factor in declines in the rate of development beyond a certain maximum temperature (Kumudini *et al.*, 2014). Thermal time models may need to be re-parameterized for new planting dates or locations because cool winter temperatures and the length of the day can accelerate or delay when phenological shifts occur. The degree of influence of these factors is generally relativized into a number between zero and one that modifies the rate of thermal time accumulation (reviewed in Brown *et al.*, 2013). However, it is not always easy to determine the factors driving plant response in different locations (Piper *et al.*, 1996). Is it possible to improve the predictive capacity of these models?

Thermal time is based on the concept of metabolic rate (Brown *et al.*, 2004). That is, metabolism is driven by temperature rather than responding proactively to it. However, different cultivars may respond very differently even when planted in the same location (Kozlowski, 1964; Lechowicz, 1984), and models need to be reparameterized accordingly. This implies that there are mechanistic, species-specific underpinnings of plant response. Some researchers propose that incorporating the underlying mechanisms could enable more accurate model predictions for situations in which the model was not parameterized (Hammer *et al.*, 2002; White, 2009; Boote *et al.*, 2013). And in fact, some model have incorporated the mechanistic underpinnings of day length and vernalization to accurately predict plant response as well as to ambient temperature (Welch *et al.*, 2003; Wenden *et al.*, 2009; Wilczek *et al.*, 2010; Brown *et al.*, 2013; Chew *et al.*, 2014).

In the following chapters, I discuss the complex interplay between the environment and circadian clock plant outputs such as diurnal leaf growth and flowering (Kinmonth-Schultz *et al.*, 2013), discussing how multiple cues could be integrated at the molecular level to control development. I then explore molecular and physiological plant responses to two different cues imposed at once: day length and temperature fluctuations (Kinmonth-Schultz *et al.*, 2016), and show that plant response can be decomposed into separate processes that can be predicted from different

environmental cues. In my forth chapter, I incorporate the mechanistic response to temperature at the molecular and whole-plant scale into an existing model of plant development (Chew *et al.*, 2014), and show that doing so can improve model predictions over traditional thermal unit models in some conditions. Finally, I review what I have learned and discuss new avenues for assessing plant response in complex natural environments.

References

Aerts R. **2009**. Nitrogen supply effects on leaf dynamics and nutrient input into the soil of plant species in a sub-arctic tundra ecosystem. *Polar Biology* **32**: 207–214.

Bernhardsson C, Ingvarsson PK. **2012**. Geographical structure and adaptive population differentiation in herbivore defence genes in European aspen (*Populus tremula* L., Salicaceae). *Molecular Ecology* **21**: 2197–2207.

Boote KJ, Jones JW, White JW, Asseng S, Lizaso JI. **2013**. Putting mechanisms into crop production models. *Plant, Cell and Environment* **36**: 1658–1672.

Brown JH, Gillooly JF, Allen AP, Savage VM, West GB. **2004**. Toward a metabolic theory of ecology. *Ecology* **85**: 1771–1789.

Brown HE, Jamieson PD, Brooking IR, Moot DJ, Huth NI. **2013**. Integration of molecular and physiological models to explain time of anthesis in wheat. *Annals of Botany* **112**: 1683–1703.

Chew YH, Wenden B, Flis A, Mengin V, Taylor J, Davey CL, Tindal C, Thomas H, Ougham HJ, Reffye P de, *et al.* 2014. Multiscale digital Arabidopsis predicts individual organ and whole-organism growth. *Proceedings of the National Academy of Sciences* **111**: E4127–E4136.

Golembeski GS, Kinmonth-Schultz HA, Song YH, Imaizumi T. **2014**. Photoperiodic flowering regulation in *Arabidopsis thaliana*. In: Fornara F, ed. *Molecular Genetics of Floral Transition and Flower Development*. London, UK: Academic Press Ltd-Elsevier Science Ltd, 1–28.

Hammer GL, Kropff MJ, Sinclair TR, Porter JR. **2002**. Future contributions of crop modelling--from heuristics and supporting decision making to understanding genetic regulation and aiding crop improvement. *European Journal of Agronomy* **18**: 15–31.

Iizumi T, Sakurai G, Yokozawa M. **2014**. Contributions of historical changes in sowing date and climate to U.S. maize yield trend: An evaluation using large-area crop modeling and data assimilation. *Journal of Agricultural Meteorology* **70**: 73–90.

Imaizumi T, Tran HG, Swartz TE, Briggs WR, Kay SA. **2003**. FKF1 is essential for photoperiodic-specific light signaling in *Arabidopsis*. *Nature* **426**: 302–306.

IPCC. **2014**. *Climate Change 2014: Synthesis Report. Contribution of Working Groups I, II and III to the Fifth Assessment Report of the Intergovernmental Panel of Climate Change*. Geneva, Switzerland.

Kinmonth-Schultz HA, Golembeski GS, Imaizumi T. **2013**. Circadian clock-regulated physiological outputs: dynamic responses in nature. *Seminars in cell & developmental biology* **24**: 407–413.

Kinmonth-Schultz HA, Tong X, Lee J, Song YH, Ito S, Kim S-H, Imaizumi T. **2016**. Cool night-time temperatures induce the expression of *CONSTANS* and *FLOWERING LOCUS T* to regulate flowering in *Arabidopsis*. *New Phytologist* **211**: 208–224.

Kozlowski TT. **1964**. Shoot growth in woody plants. *The Botanical Review* **30**: 335–392.

Kumudini S, Andrade FH, Boote KJ, Brown GA, Dzotsi KA, Edmeades GO, Gocken T, Goodwin M, Halter AL, Hammer GL, *et al.* 2014. Predicting Maize Phenology: Intercomparison of Functions for Developmental Response to Temperature. *Agronomy Journal* **106**: 2087.

Lechowicz M. **1984**. Why Do Temperate Deciduous Trees Leaf Out at Different Times? Adaptation and Ecology of Forest Communities. *American Naturalist* **124**: 821–842.

Lehenbauer PA. **1914**. Growth of maize seedlings in relation to temperature. *Physiological Researches* **1**: 247–288.

Michael TP, Salomé PA, McClung CR. **2003**. Two *Arabidopsis* circadian oscillators can be distinguished by differential temperature sensitivity. *Proceedings of the National Academy of Sciences* **100**: 6878–6883.

Michaels S, Amasino R. **1999**. *FLOWERING LOCUS C* encodes a novel MADS domain protein that acts as a repressor of flowering. *Plant Cell* **11**: 949–956.

Piper EL, Smit MA, Boote KJ, Jones JW. **1996**. The role of daily minimum temperature in modulating the development rate to flowering in soybean. *Field Crops Research* **47**: 211–220.

Prasch CM, Sonnewald U. **2015**. Signaling events in plants: stress factors in combination change the picture. *Environmental and Experimental Botany* **114**: 4–14.

Rizhsky L, Liang H, Shuman J, Shulaev V, Davletova S, Mittler R. **2004**. When defense pathways collide. The response of Arabidopsis to a combination of drought and heat stress. *Plant Physiology* **134**: 1683–1696.

Ruffel S, Krouk G, Ristova D, Shasha D, Birnbaum KD, Coruzzi GM. **2011**. Nitrogen economics of root foraging: Transitive closure of the nitrate–cytokinin relay and distinct systemic signaling for N supply vs. demand. *Proceedings of the National Academy of Sciences* **108**: 18524–18529.

Searle I, He Y, Turck F, Vincent C, Fornara F, Kröber S, Amasino RA, Coupland G. **2006**. The transcription factor FLC confers a flowering response to vernalization by repressing meristem competence and systemic signaling in Arabidopsis. *Genes & Development* **20**: 898–912.

Welch SM, Roe JL, Dong Z. **2003**. A genetic neural network model of flowering time control in Arabidopsis thaliana. *Agronomy Journal* **95**: 71--81.

Wenden B, Dun EA, Hanan J, Andrieu B, Weller JL, Beveridge CA, Rameau C. **2009**. Computational analysis of flowering in pea (Pisum sativum). *New Phytologist* **184**: 153–167.

Wenden B, Rameau C. **2009**. Systems biology for plant breeding: the example of flowering time in pea. *Comptes Rendus Biologies* **332**: 998–1006.

White JW. **2009**. Combining ecophysiological models and genomics to decipher the GEM-to-P problem. *NJAS - Wageningen Journal of Life Sciences* **57**: 53–58.

Wilczek AM, Burghardt LT, Cobb AR, Cooper MD, Welch SM, Schmitt J. **2010**. Genetic and physiological bases for phenological responses to current and predicted climates. *Philosophical Transactions of the Royal Society B: Biological Sciences* **365**: 3129–3147.

Chapter 2

Circadian clock-regulated physiological outputs: Dynamic responses in nature

As published in *Seminars in Cell & Developmental Biology*

2013

v24(5): 407-413

http://www.sciencedirect.com/science/article/pii/S1084952113000244

Seminars in Cell & Developmental Biology 24 (2013) 407–413

Contents lists available at SciVerse ScienceDirect

Seminars in Cell & Developmental Biology

journal homepage: www.elsevier.com/locate/semcdb

Review

Circadian clock-regulated physiological outputs: Dynamic responses in nature

Hannah A. Kinmonth-Schultz, Greg S. Golembeski, Takato Imaizumi*

Department of Biology, University of Washington, Seattle, WA 98195-1800, USA

ARTICLE INFO

Article history:
Available online 20 February 2013

Keywords:
Circadian clock
Photoperiodic flowering
Phenology
Diurnal growth
Cold acclimation
Adaptation

ABSTRACT

The plant circadian clock is involved in the regulation of numerous processes. It serves as a timekeeper to ensure that the onset of key developmental events coincides with the appropriate conditions. Although internal oscillating clock mechanisms likely evolved in response to the earth's predictable day and night cycles, organisms must integrate a range of external and internal cues to adjust development and physiology. Here we introduce three different clock outputs to illustrate the complexity of clock control. Clock-regulated diurnal growth is altered by environmental stimuli. The complexity of the photoperiodic flowering pathway highlights numerous nodes through which plants may integrate information to modulate the timing of flowering. Comparative analyses among ecotypes that differ in flowering response reveal additional environmental cues and molecular processes that have developed to influence flowering. We also explore the process of cold acclimation, where circadian inputs, light quality, and stress responses converge to improve freezing tolerance in anticipation of colder temperatures.

Contents

1. Introduction

Numerous physiological and growth processes show daily oscillation patterns, which are often controlled by the circadian clock. In *Arabidopsis*, about one third of all genes are clock regulated [1]. Likely to have evolved initially in response to the earth's predictable day and night cycles [2], the circadian clock sets the timing of various transcriptional and posttranscriptional events to specific times of day. This mechanism changes the organisms' sensitivities and/or responses to various external stimuli throughout the day, thus enabling them to extract specific information that occurred at certain times of the day or year. This clock role is called circadian gating. A well-understood example of this is the external coincidence model of photoperiodic flowering control. To accurately measure differences in day length in the facultative long-day plant, *Arabidopsis*, regulation of the timing of diurnal *CONSTANS* (*CO*) expression is crucial [3]. The circadian clock sets the timing of *CO* transcription to the late afternoon and night. During the short days of winter, the *CO* peak occurs at night, and its protein is degraded. In early summer's long days, the peak coincides with daylight, and CO protein is stabilized to activate transcription of *FLOWERING LOCUS T* (*FT*), resulting in earlier flowering [3,4]. This type of time-keeping mechanism helps guarantee that phenological changes like flowering occur during favorable times of the year.

The circadian-clock-regulated biological processes are stable but also adaptable. Dicot leaves maintain a consistent oscillatory

* Corresponding author. Tel.: +1 206 543 8709.
E-mail address: takato@u.washington.edu (T. Imaizumi).

1084-9521/$ – see front matter © 2013 Elsevier Ltd. All rights reserved.
http://dx.doi.org/10.1016/j.semcdb.2013.02.006

diurnal growth pattern despite external temperature changes [5]. Yet, there is growing recognition that diurnal growth oscillations are changeable within the lifetime of a plant, susceptible to external and internal limitations [6,7]. Among populations and across generations within the same species, clock outputs like flowering, bud break, or onset of dormancy differ [8–10]. The differences persist when growing conditions are the same, indicating genetic adaptations to regional environmental variation. We have a general molecular understanding of how each output is induced as well as how the circadian clock affects them. We still lack information on how endogenous control of clock outputs is adjusted from individual to individual and species to species.

The aim of this review is to address these complexities. We utilize diurnal plant growth to highlight the plasticity of endogenous circadian control and to illustrate that the degree of control is dependent on variation in the immediate environment. We capitalize on the in-depth mechanistic knowledge of seasonal flowering control to explore how numerous external and endogenous cues can modulate a clock-mediated output. We use recent multi-population, genome-wide analyses, which demonstrate underlying genetic differences among phenotypically different populations, to highlight genes and molecular pathways under selective pressure. Finally, we explore the molecular processes of cold-tolerance and highlight areas of uncertainty regarding stress-induced versus clock-mediated cryoprotection.

2. Diurnal plant growth: plasticity of circadian control

The sensitivity of plants to external and internal stimuli, which regulate diurnal growth, can change depending on growth conditions, plant age, type of organ, and time of day. Dicot leaves and stems display diurnal rhythmic growth that is maintained under constant environmental conditions, indicating the involvement of the circadian clock [5,11,12]. However, the timing of peak growth changes from day to night with the developmental age of the leaf, attributable to a shift from metabolic-limited growth in younger leaves to hydraulic-limited growth in mature leaves [13]. Dicot leaves maintain a stable oscillatory growth pattern even under daily temperature cycles [5], perhaps through the ability of the circadian clock to adjust metabolic rates throughout the day. Roots do not show the same degree of circadian growth-rate regulation, as they must quickly alter growth to take advantage of available soil resources and water [14]. The daily rate and pattern of leaf growth is also maintained similarly even under low-light conditions where the carbon source is limited [13]. *Arabidopsis* can continue growing with carbon limitations by decreasing leaf thickness and maintaining surface area. Conversely, water stress causes growth to slow during the day such that peak growth occurs at night even in very young leaves. Under this condition, decreasing leaf surface area by slowing growth can help reduce water lost through transpiration [13]. The molecular mechanisms by which external and internal factors coordinate to regulate leaf growth and development and how the circadian clock affects this regulation remain largely unknown.

In comparison to the diurnal leaf growth mechanism, we have a better understanding of the mechanisms of diurnal hypocotyl growth. Seedlings respond to changes in light quality and quantity, carbon reserves, and temperature in a time-dependent fashion. During the growth phase, in which *Arabidopsis* cotyledons fully expand, a change in light intensity most affects hypocotyl growth around dusk (Fig. 1A) [7]. In contrast, the effect of sucrose in the growth media is most pronounced around dawn (Fig. 1B). The mechanisms for diurnal control of growth, best understood in *Arabidopsis* hypocotyls and reviewed extensively [12,15], are beginning to shed light on changes in sensitivity over the course of the day to parameters regulated by the circadian clock (Fig. 1C). The

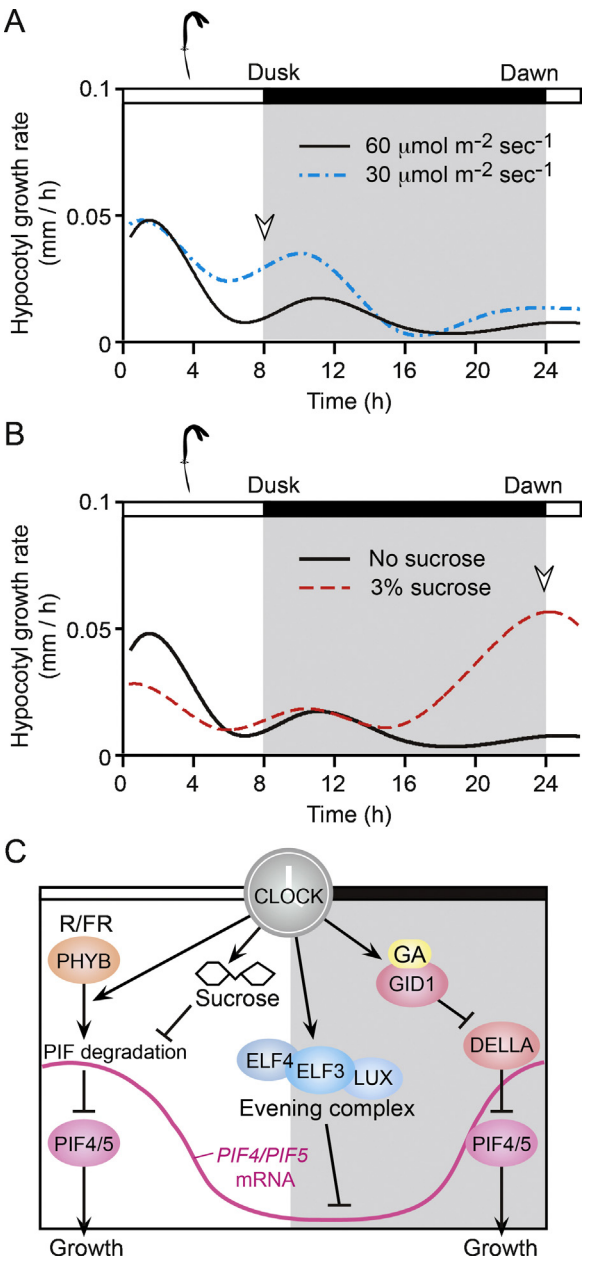

Fig. 1. Circadian clock-mediated diurnal hypocotyl growth (A and B) *Arabidopsis* hypocotyl growth for 4 to 5-day-old seedlings, before their cotyledons are fully expanded, is regulated by different inputs at different parts of the day. (A) Hypocotyl growth rate is most affected by light intensity at dusk. (B) Carbon source availability most affects the growth rate at dawn (dusk and dawn are indicated by open arrowheads). The graphs were modified from [7]. (C) The circadian clock coordinates various pathways involved in diurnal growth regulation. These pathways include phytochrome, sucrose and GA signaling, and the components (ELF3, ELF4, and LUX) of the evening complex, ultimately resulting in transcriptional or post-translational regulation of PIF4 and PIF5. Higher sucrose levels reduce the degradation rate of PIF5 resulting in an enlarged morning response to growth. PHYB signals keep PIF levels low under light. The evening complex represses the expression of *PIF4* and *PIF5* at dusk. Higher amounts of GA-GID1 complex around dawn induces degradation of DELLA proteins, which prevent PIF4 (and possibly PIF5) from binding to target DNA. *PIF4*/*PIF5* mRNA profile is shown by a pink line. Coordinated regulation by the clock contributes to temporally-confined growth that occurs at dawn and dusk through convergence of light, hormone, and metabolic signaling.

bHLH transcription factors known as *PHYTOCHROME INTERACTING FACTORs* (*PIFs*) are expressed in a clock-dependent manner [16]. The circadian clock components, EARLY FLOWERING 3 (ELF3), ELF4, and LUX ARRHYTHMO (LUX, also known as PHYTOCLOCK1) directly regulate the expression of *PIF4* and *PIF5* transcription [17]. ELF3,

ELF4, and LUX form a protein complex named the evening complex, which directly represses the expression of *PIF4* and *PIF5* transcripts around dusk, limiting the expression of *PIF4* and *PIF5* to dawn [17] (Fig. 1C).

In addition to clock-dependent transcriptional regulation, time-dependent posttranslational regulation also plays a role. PIF4 and PIF5 proteins are degraded under red light, which is absorbed by PHYTOCHROME B (PHYB) photoreceptor. This light-dependent regulation restricts the activity of these growth-promoting PIF transcription factors to shaded conditions in long days or a period around dawn in short days (reviewed in [12]). The PIF4 proteins are further activated during the night in short days, partly due to the interaction of gibberellin (GA) and its receptor GIBBERELLIN INSENSITIVE DWARF1 (GID1), both of which are modulated by the circadian clock. The clock regulates the timing of expression of GA synthetic enzyme gene *GA20ox1* and *GID1* gene [18,19]. GID1 binds to GA and this interaction triggers DELLA proteins for proteasomal degradation [20]. The DELLA proteins bind to PIF4 and inhibit its DNA binding ability [21]. DELLA proteins are degraded around dawn in short days [19]. Thus, removing the DELLA proteins enables PIF4 to bind to the G-box to induce the expression of genes involved in hypocotyl growth around dawn [21] (Fig. 1C). Sucrose also stabilizes PIF5 protein throughout the day [7]. This, together with transcriptional regulation, ensures that diurnal hypocotyl growth occurs at a certain time of day (Fig. 1C).

Hypocotyl growth is also susceptible to changes in ambient temperature. High ambient temperatures cause pre-dawn expression of *PIF4* in long days similar to that observed for short days, helping to explain why hypocotyl growth occurs in such conditions [16]. The presence of PIF4 and PIF5 proteins are required both in short days and in 28 °C long days for pre-dawn expression of a suite of genes associated with gibberellin, auxin, brassinosteroid, ethylene, and cytokinin, and which are also important for the shade avoidance response [16,22]. In sum, we are beginning to get a picture of a flexible, clock-mediated system that coordinates growth-regulating genes, turgor, and resource availability with external and internal stimuli.

3. Seasonal flowering

3.1. The photoperiodic flowering pathway in Arabidopsis

In addition to diurnal growth regulation, the circadian clock plays an important role in the regulation of photoperiodic flowering. The photoperiodic flowering pathway controls the amount of florigen, which determines flowering time. In *Arabidopsis*, FT protein is a major part of florigen synthesized in the leaf vasculature [23]. FT protein is translocated to the shoot apical meristem and, together with FD and 14-3-3 [24], initiates transcription of floral identity genes that regulate floral development [23,25]. To selectively induce *FT* transcription in long days, restricting *CO* expression by the circadian clock to the long-day afternoon is essential. In the morning, CYCLING DOF FACTORs (CDFs) are highly expressed and directly repress *CO* transcription [26,27]. At the same time, the core clock components, CCA1 and LHY, repress the transcription of *FLAVIN-BINDING, KELCH REPEAT, F-BOX 1* (*FKF1*) and *GIGANTEA* (*GI*), both of which negatively regulate CDFs [28]. FKF1 and GI proteins peak in the afternoon and form a complex in a blue-light dependent manner [28]. The FKF1-GI complex removes CDF repressors by proteasomal degradation in the long-day afternoon [28]. Simultaneously, the levels of *CDF* transcripts also decrease due to repression by other clock components, PSEUDO RESPONSE REGULATOR 9 (PRR9), PRR7, and PRR5 [29,30]. These mechanisms determine the timing of daytime *CO* gene expression in long days. Recently, four transcriptional activators of *CO*, named FLOWERING BHLH (FBH), were identified [31]. Interestingly, FBH transcriptional activators control the amplitude of *CO* expression, which also affects the expression levels of *FT* [31].

Another important mechanism for day-length sensing is specific stabilization of CO protein [4]. Light signals perceived by phytochromes (PHY) and cryptochromes (CRY) stabilize CO protein only in long-day afternoons [4]. This time-dependent stabilization of CO protein is regulated by the combinational regulation of light and the clock. The PHYB signal and the E3 ubiquitin ligase HIGH EXPRESSION OF OSMOTICALLY RESPONSIVE GENES1 (HOS1) are involved in the degradation of CO during the morning [4,32], although it is not known whether the PHYB signal regulates CO through HOS1. CRY2 binds to SUPPRESSOR OF PHYA-105 1 (SPA1) and the CONSTITUTIVE PHOTOMORPHOGENIC 1 (COP1) E3 ubiquitin ligase complex under blue light to suppress the activity of the complex [33]. In the dark, even though *CO* mRNA is highly accumulated, CO protein is actively degraded by the COP1/SPA1 complex [4,34,35]. The clock-regulated blue-light photoreceptor, FKF1, stabilizes CO in the long-day afternoon. When FKF1 is expressed under light, FKF1 binds to and stabilizes CO protein in a blue light-dependent manner [36]. The complex interplay between light and clock ensures that CO protein exists only in long day afternoons when *FT* is induced. Thus, the circadian clock controls *CO* transcriptional and posttranscriptional mechanisms to achieve proper day-length sensing for flowering.

The photoperiodic pathway also serves to integrate numerous signals, and many of these signals act through independent or partially independent pathways to regulate flowering. Members of the PHY and CRY photoreceptor families not only regulate flowering under different light conditions, but also differentially control flowering depending on ambient temperature (reviewed in [37]). One of the components that integrates photoreceptor signaling with flowering time regulation is PHYTOCHROME AND FLOWERING TIME 1 (PFT1). Acting downstream of PHYB, PHYD, and PHYE, PFT1, a component (MED25) of the Mediator complex, integrates light quality and possibly temperature signals for a subset of flowering genes [38]. In response to changes in ambient temperature, HOS1 regulates *FT* and *TWIN SISTER OF FT* (*TSF*) independently of CO through the autonomous pathway genes, *FVE* and *FLK* [39]. The expression of some of the genes listed above is regulated by abiotic and biotic stimuli. For instance, the simultaneous application of drought and heat stresses induces the expression of *FBH3* [40]. A carbon supplement in the growth media reduces *PRR5* and *CDF2* expression [41]. Metabolic sucrose seems to adjust the circadian clock through GI activity [42]. As the addition of 5% sucrose to the growth media represses *FT* expression and delays flowering [43], GI may also regulate flowering via sucrose signaling (see details in Haydon et al. in this issue). These findings indicate that precise environmental information can be integrated into the photoperiodic flowering pathway to fine tune flowering time in nature.

3.2. Differences in flowering time within and between populations

Numerous field studies have reported variations among individuals and populations in the timing of key phenological events. Early studies noted significant site and regional differences in the timing of bud break [8,9], which in *Populus* shares components of the *Arabidopsis* photoperiodic flowering pathway [44]. Some of these differences could be explained by environmental differences like photoperiod or temperature [8,9]. Others persisted when plants of the same species were collected from different sites and grown together [8,9]. These observations indicate that adaptation to regional climates contributes to genetic variation in internal regulatory mechanisms among populations. The capacity of a population to adapt depends on the genetic material available, and some studies have noted within population variation as

well. *Mertensia fusiformis* correlates its flowering to snowmelt, displaying a skewed population distribution [10]. End-of-season drought selects for early-flowering plants, while the chance of late spring frost favors maintenance of a few that flower later.

Much remains to be learned about the mechanisms underlying flowering time modulation by parameters other than photoperiod and vernalization. However, it is likely the circadian clock plays a role in regulating responses to other predictable environmental cues. For instance, daytime temperatures better correlate with flowering times than nighttime temperatures for *Arabidopsis* strains planted in the field, except for populations sown in fall [45]. This implies that the clock may influence the timing of temperature sensitivity within a day, and that the circadian gating function differs by season. Plant size, which itself is affected by the environment, also impacts timing of flowering in biennial species (see [46] for further discussion). For biennial species, plant size likely correlates to a threshold level of resources needed to induce flowering. Consistent with this idea, flowering in *Arabidopsis* and *Sinapis alba* is coupled with an increase in sucrose and the carbon:nitrogen ratio at the shoot apical meristem [47,48]. Taken together, these examples indicate there are adaptations among individuals and populations that modulate clock outputs. Yet few studies have demonstrated concrete mechanistic differences among them [44].

With the available data of single nucleotide polymorphisms (SNPs) from a large number of wild-type *Arabidopsis* accessions, comparative analyses of natural populations provide clues by which to understand the environmental drivers of adaptation [49–51]. Several environmental parameters correlate with an enrichment of amino acid-changing SNPs [50,51]. After removing SNPs related to specific geographic locations, representative SNPs in early-flowering plant populations correlated to summer precipitation, whereas growing-season temperatures drove most of the explained SNP variation in late-flowering plants [50]. These findings are supported by a reciprocal transplant between Swedish and Italian *Arabidopsis* populations [52]. The strains had higher fitness in their home sites than representatives from the other population. The authors postulate that the Swedish plants were better able to tolerate cold temperatures while Italian plants could flower early to avoid late-season droughts. Similar early- and late-flowering differentiation can occur within a population over time. Seeds of *Brassica Rapa* plants collected from the same site after multi-year periods of above- then below-average rainfall were grown together in a common garden experiment [53,54]. The drought years selected for plants that flowered earlier when they were smaller in stature. These results demonstrate that selection can rapidly occur, and that flowering times are affected when growing seasons are curtailed by drought. These data also provide clues by which to understand the molecular events that plants must simultaneously integrate when they flower in natural settings.

3.3. Flowering and the clock: molecular targets of selection

Comparative analyses of natural populations that vary in their phenotypic responses to environmental cues are tools by which to identify molecular pathways under selective pressure in nature [49–51]. Hormone signaling pathways may be targets for natural selection and have some links to the circadian clock. A recent comprehensive microarray study compared the expression levels in response to photoperiod among three *Arabidopsis* populations from locales with different photoperiods, light quality, winter severity, and precipitation in Norway [55]. They differed in their photoperiodic sensitivity when grown together, indicating underlying genetic differences in phenological regulation. Genes involved in biosynthesis of and response to abscisic acid (ABA), a drought-signaling molecule, were differentially regulated among populations. There are also surprising correlations among the expression patterns of genes involved in ethylene and auxin response and flowering [55]. The transcription of *EIN3-BINDING F-BOX PROTEIN 1* (*EBF1*) and *EBF2*, both involved in ethylene response [56], was the highest in the population showing the greatest sensitivity to photoperiod [55].

Not surprisingly, known components of the photoperiod pathway are represented in population studies that examine flowering [49,55]. *CRY2*, *GI*, *LHY*, *FKF1*, *FT* and *PHYA*, *PHYB*, and *PHYC*, as well as *SPA2* and *SPA4* are highlighted. *PHYA*, *GI*, and *FT* are mentioned in more than one study. As we described above, many of these play roles in temperature and light quality perception along with photoperiod. *DWARF IN LIGHT 2* (*DFL2*) has no known role in flowering; however, it was implicated as a target candidate in two studies [49,55]. Both studies also highlight *SHORT VEGETATIVE PHASE* (*SVP*). SVP, a MADS-domain transcription factor, is a known mediator of ambient temperature response and an upstream regulator of *FT* [57]. An area of interest for molecular studies is analyzing the molecular natures of representative synonymous and non-synonymous (=amino-acid-changing) SNPs associated with climate [50,51]. Synonymous mutations represent changes in DNA sequence that could affect *cis*-acting elements, whereas non-synonymous mutations may alter protein function. Many downstream flowering integrators are differentially expressed among populations of *Arabidopsis* [55], thus this is an area warranting further research.

4. Diurnal and seasonal cold response

4.1. Circadian regulation of cold response

Cold temperatures have a drastic impact on survival for plants in temperate or boreal environments. While the adaptive response that allows plants to survive freezing conditions is well understood, only recently has a comprehensive mechanism for cold acclimation come into focus. Circadian regulation, light quality perception, and stress responses all converge to activate cold response. Adaptation to freezing temperatures is accomplished through cold acclimation, the process by which exposure to cold, non-freezing temperatures instills subsequent freezing tolerance. The canonical cold-response pathway has been studied extensively [58] and involves the *C-REPEAT BINDING FACTOR* (*CBF* also known as *DREB*) genes, which are transcriptional activators of their *COLD REGULATED* (*COR*) downstream targets [59] (Fig. 2A). Overexpression of the three *CBF* genes in *Arabidopsis* resulted in enhanced freezing tolerance upon induction of cold treatment [58]. A global transcriptome analysis revealed that nearly a quarter of cold inducible genes have CBF/DREB *cis*-regulatory elements in their promoters, implying that *CBF*s have a broad class of targets in initiating cold tolerance [60]. The cold-inducible transcriptome contains genes involved in processes including biosynthesis of secondary metabolites (raffinose, proline, antioxidants, etc.), lipid desaturation and biosynthesis, cryoprotective compounds as well as drought stress [58,60].

Recent studies have highlighted the importance of the circadian clock in gating cold acclimation in *Arabidopsis*. Clock control in genome-wide cold response was first inferred when transcriptome surveys differed significantly based on time of sampling [61]. Expanded analysis of the promoter regions of cold-inducible genes showed the prevalence of Evening Elements (EE), *cis*-elements recognized by CCA1 and LHY. The EE elements in *CBF* promoters are often coupled to ABA responsive *cis*-elements (ABRE) and both elements are necessary for cold-inducibility of *COR* genes [62], indicating the clock components are indispensible pieces in the cold response mechanism (Fig. 2A). *CBF* expression levels oscillate throughout the day with a peak at midday [63]. In *cca1 lhy* double mutant backgrounds, *CBF* genes have significantly reduced

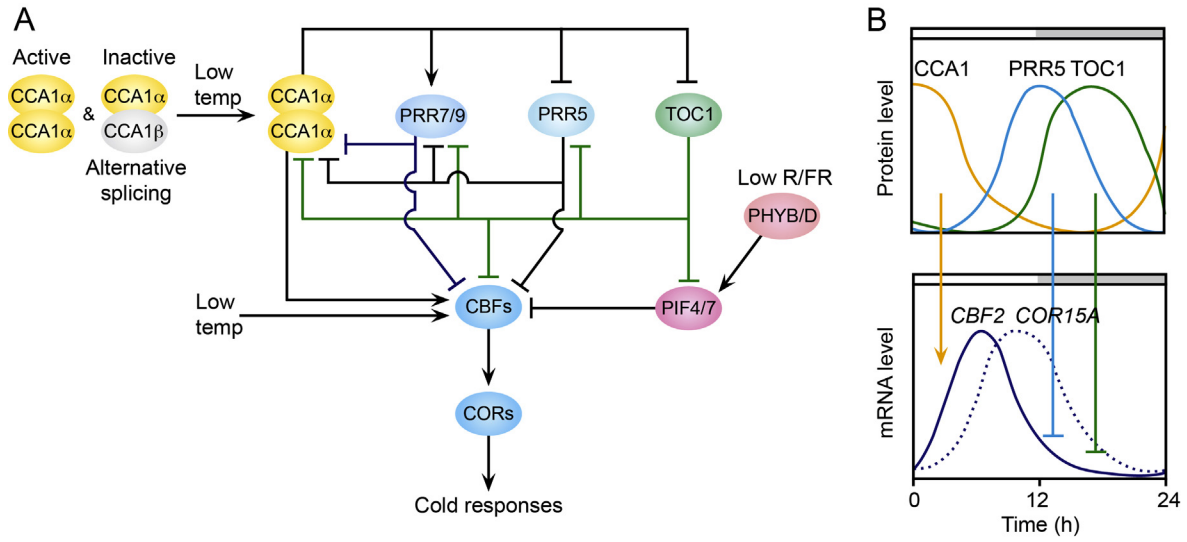

Fig. 2. Circadian clock regulation of the cold acclimation pathway in *Arabidopsis* (A) Inputs from the circadian clock, light signaling, and temperature activate *COR* genes through the *CBF* transcriptional activators, which induce the process of cold acclimation in *Arabidopsis*. In the diagram, colored lines are given to help distinguish interactions between different components. Cold temperatures induce *CBF* expression through *CCA1* alternative splicing. The accumulation of the functional CCA1α splice variant in low temperatures increases *CBF* expression. Competition for the non-functional CCA1β variant at higher temperatures attenuates the cold response. TOC1 and PRR5 directly repress *CBF* expression in the evening and PRR7 and PRR9 likely act in a similar manner. Changes in the red/far-red light ratio are sensed through PHYB and PHYD, which in low red/far-red conditions drive transcriptional activation of *CBF* genes through PIF4 and PIF7. TOC1 protein binds to the *PIF4* promoter and may physically interact with PIF7 protein [70,74]. Through these mechanisms, the circadian clock, temperature, and light inputs mediate and amplify environmental signals to induce cold acclimation. (B) Relative abundance of clock component proteins at different times of the day dictates temporal *CBF* expression. In the morning, CCA1 activates *CBF*s, which in turn activate *COR* downstream genes. In the evening, TOC1 and PRR5 repress *CBF* expression. Schematic protein and mRNA levels are drawn from data in which plants were grown in continuous light conditions [64,76,77].

expression, which results in diminished freezing tolerance [64]. Temperature-dependent alternative splicing of *CCA1* also plays a role in the establishment of cold tolerance [65]. CCA1 and LHY form homodimers or CCA1/LHY heterodimers; the formation of the paired transcriptional complex increases their DNA binding affinity and ability to activate or repress transcription through the EE. Functional *CCA1* alternative splice variants are preferentially produced at lower temperatures, which allows for increased induction of *CBF* genes under cold acclimation conditions [65]. *LHY* is also affected by temperature dependent alternative splicing, but the active variant is preferentially transcribed at higher temperatures [66]. How the alternative splicing of these genes in concert functionally affects the cold acclimation process is not known (for further discussion, see Henriquez and Mas in this issue).

While *CCA1*/*LHY* is the best-characterized link between the clock and cold-acclimation, other clock genes also affect the response. PRR5 binds to the *CBF* promoter regions and represses their transcription (Fig. 2A and B) [30]. In addition, *prr5 prr7 prr9* triple mutants, which have an arrhythmic clock phenotype, constitutively express *CBF*s and have increased freezing tolerance [67]. The *gi-3* mutants have freezing susceptibility, which may be linked to a decrease in endogenous sugar concentrations [68]. The circadian clock-regulated *CONSTANS-LIKE* genes, *COL1* and *COL2*, are implicated in cold-tolerance in genome-wide transcriptome studies [60]. Furthermore, ABA responses, which influence cold acclimation, are also regulated by the core clock protein TOC1 [69]. TOC1 also directly binds to the *CBF1* and *CBF2* promoters [70], so TOC1 may regulate *CBF*s in both an ABA-dependent and independent manner (Fig. 2A and B). Additional connections between known clock components and cold acclimation are likely to be established.

4.2. Photoperiod, light quality, and cold response

In addition to the circadian clock, light perceived by PHYs affects cold response. Sensing changes in the red/far-red ratio may be important for coordinating cold responses in anticipation of cold nighttime temperatures or seasonally cold temperatures. Interestingly, a 16 °C growth condition coupled with a low red/far-red ratio is sufficient to induce *CBF* expression [63]. PHYB and PHYD mediate this light specific *CBF* induction at ambient temperatures [63]. PHYB regulation of the transcription of *CBF* genes occurs through PIF4 and PIF7 [71] (Fig. 2A). Additionally, exposure to shorter photoperiods also induces the cold acclimation response in temperate zone perennial species [72,73]. Even in *Arabidopsis*, the amplitude of *CBF* gene oscillations in short days is higher than in long days [71]. Either the *phyB* or the *pif4 pif7* double mutations abolish the higher amplitude in *CBF* expression in short days, indicating the same components were recruited to sense changes in red/far-red ratio, temperature and day length, all of which occur when winter is approaching [71]. Furthermore, PIF7 binds to G-box elements in *CBF* promoters [71,74]. Thus, integration between light, temperature and clock output pathways at the *CBF* promoter through EE and G-box elements constitutes a novel mechanism by which these pathways assimilate various environmental information to prepare for winter by initiating cold acclimation.

5. Conclusion

Each clock output that we have described provides insight into the complexity and adaptability of circadian control tempered by external and internal stimuli. To help us understand how external and internal limitations interact in modulating circadian outputs, an interesting avenue of research would be to pair ecophysiological estimates of respiration and stomatal conductance with diurnal growth and molecular assays. As different climate variables affect early- versus late-flowering accessions of *Arabidopsis*, genome-wide association studies that separate these groups could be useful [49,55]. Several downstream flowering integrators have been implicated in population-based studies, and both synonymous and non-synonymous SNPs are enriched with climate [50,51]. It is possible this is due to linkage disequilibrium among synonymous

and non-synonymous mutations. However, QTL analysis of two parental lines mapped ambient temperature and photoperiod sensitivity to the *FT* promoter [75]. A feasible next step is to sequence the promoters of these genes as well as measure the expression levels of these genes to determine whether these SNPs alter gene expression by mutating *cis*-acting elements. We do not understand how the circadian clock works in the ABA pathway to directly or indirectly affect cold acclimation, nor do we understand how ABA, the circadian clock, and light-quality sensing through PHYB interact to regulate cold response. It is likely that each factor of the cold-response pathway plays a greater or lesser role in activation of *CBF*s depending on the length of cold exposure. Mechanistic studies that assess the effects of both short- and long-term cold treatments on each of these components could help clarify their roles. In nature, plants must integrate information about external variables like climate, light intensity and surrounding vegetation, as well as endogenous carbon, nutrients, hydraulic status, and developmental age. To understand the complex regulation of physiology and development that occurs in nature, further experiments should be carried out under a wide variety of conditions, including those that more closely reflect the natural environment.

Acknowledgements

This work was supported by funding from the National Institutes of Health (GM079712) and the University of Washington Royalty Research Fund to T.I., and the National Science Foundation Graduate Research Fellowship Program to H.K.S.

References

[1] Covington MF, Maloof JN, Straume M, Kay SA, Harmer SL. Global transcriptome analysis reveals circadian regulation of key pathways in plant growth and development. Genome Biology 2008;9:R130.
[2] Edgar RS, Green EW, Zhao Y, van Ooijen G, Olmedo M, Qin X, et al. Peroxiredoxins are conserved markers of circadian rhythms. Nature 2012;485:459–64.
[3] Yanovsky MJ, Kay SA. Molecular basis of seasonal time measurement in *Arabidopsis*. Nature 2002;419:308–12.
[4] Valverde F, Mouradov A, Soppe W, Ravenscroft D, Samach A, Coupland G. Photoreceptor regulation of CONSTANS protein in photoperiodic flowering. Science 2004;303:1003–6.
[5] Poire R, Wiese-Klinkenberg A, Parent B, Mielewczik M, Schurr U, Tardieu F, et al. Diel time-courses of leaf growth in monocot and dicot species: endogenous rhythms and temperature effects. Journal of Experimental Botany 2010;61:1751–9.
[6] Pantin F, Simonneau T, Muller B. Coming of leaf age: control of growth by hydraulics and metabolics during leaf ontogeny. New Phytologist 2012;196:349–66.
[7] Stewart JL, Maloof JN, Nemhauser JL. PIF genes mediate the effect of sucrose on seedling growth dynamics. PLoS ONE 2011;6:e19894.
[8] Kozlowski TT. Shoot growth in woody plants. Botanical Review 1964;30:335–92.
[9] Lechowicz M. Why do temperate deciduous trees leaf out at different times? Adaptation and ecology of forest communities. The American Naturalist 1984;124:821–42.
[10] Forrest J, Thomson JD. Consequences of variation in flowering time within and among individuals of *Mertensia fusiformis* (Boraginaceae), an early spring wildflower. American Journal of Botany 2009;97:38–48.
[11] Walter A. Dynamics of leaf and root growth: endogenous control versus environmental impact. Annals of Botany 2005;95:891–900.
[12] Farré EM. The regulation of plant growth by the circadian clock. Plant Biology 2012;14:401–10.
[13] Pantin F, Simonneau T, Rolland G, Dauzat M, Muller B. Control of leaf expansion: a developmental switch from metabolics to hydraulics. Plant Physiology 2011;156:803–15.
[14] Walter A, Silk WK, Schurr U. Environmental effects on spatial and temporal patterns of leaf and root growth. Annual Review of Plant Biology 2009;60:279–304.
[15] Ruts T, Matsubara S, Wiese-Klinkenberg A, Walter A. Diel patterns of leaf and root growth: endogenous rhythmicity or environmental response? Journal of Experimental Botany 2012;63:3339–51.
[16] Nomoto Y, Kubozono S, Yamashino T, Nakamichi N, Mizuno T. Circadian clock and PIF4-controlled plant growth: a coincidence mechanism directly integrates a hormones-signaling network into the photoperiodic control of plant architectures in *Arabidopsis thaliana*. Plant and Cell Physiology 2012;53:1950–64.
[17] Nusinow DA, Helfer A, Hamilton EE, King JJ, Imaizumi T, Schultz TF, et al. The ELF4–ELF3–LUX complex links the circadian clock to diurnal control of hypocotyl growth. Nature 2011;475:398–402.
[18] Hisamatsu T, King RW, Helliwell CA, Koshioka M. The involvement of gibberellin 20-oxidase genes in phytochrome-regulated petiole elongation of *Arabidopsis*. Plant Physiology 2005;138:1106–16.
[19] Arana MV, Marin-de la Rosa N, Maloof JN, Blazquez MA, Alabadi D. Circadian oscillation of gibberellin signaling in *Arabidopsis*. Proceedings of the National Academy of Sciences of the United States of America 2011;108:9292–7.
[20] Ueguchi-Tanaka M, Nakajima M, Motoyuki A, Matsuoka M. Gibberellin receptor and its role in gibberellin signaling in plants. Annual Review of Plant Biology 2007;58:183–98.
[21] de Lucas M, Daviere JM, Rodriguez-Falcon M, Pontin M, Iglesias-Pedraz JM, Lorrain S, et al. A molecular framework for light and gibberellin control of cell elongation. Nature 2008;451:480–4.
[22] Nomoto Y, Kubozono S, Miyachi M, Yamashino T, Nakamichi N, Mizuno T. A circadian clock- and PIF4-mediated double coincidence mechanism is implicated in the thermosensitive photoperiodic control of plant architectures in *Arabidopsis thaliana*. Plant and Cell Physiology 2012;53:1965–73.
[23] Corbesier L, Vincent C, Jang S, Fornara F, Fan Q, Searle I, et al. FT protein movement contributes to long-distance signaling in floral induction of *Arabidopsis*. Science 2007;316:1030–3.
[24] Taoka K, Ohki I, Tsuji H, Furuita K, Hayashi K, Yanase T, et al. 14-3-3 proteins act as intracellular receptors for rice Hd3a florigen. Nature 2011;476:332–5.
[25] Abe M, Kobayashi Y, Yamamoto S, Daimon Y, Yamaguchi A, Ikeda Y, et al. FD, a bZIP protein mediating signals from the floral pathway integrator FT at the shoot apex. Science 2005;309:1052–6.
[26] Imaizumi T, Schultz TF, Harmon FG, Ho LA, Kay SA. FKF1 F-box protein mediates cyclic degradation of a repressor of *CONSTANS* in *Arabidopsis*. Science 2005;309:293–7.
[27] Fornara F, Panigrahi KC, Gissot L, Sauerbrunn N, Rühl M, Jarillo JA, et al. *Arabidopsis* DOF transcription factors act redundantly to reduce *CONSTANS* expression and are essential for a photoperiodic flowering response. Developmental Cell 2009;17:75–86.
[28] Sawa M, Nusinow DA, Kay SA, Imaizumi T. FKF1 and GIGANTEA complex formation is required for day-length measurement in *Arabidopsis*. Science 2007;318:261–5.
[29] Nakamichi N, Kita M, Niimura K, Ito S, Yamashino T, Mizoguchi T, et al. *Arabidopsis* clock-associated pseudo-response regulators PRR9, PRR7 and PRR5 coordinately and positively regulate flowering time through the canonical CONSTANS-dependent photoperiodic pathway. Plant and Cell Physiology 2007;48:822–32.
[30] Nakamichi N, Kiba T, Kamioka M, Suzuki T, Yamashino T, Higashiyama T, et al. Transcriptional repressor PRR5 directly regulates clock-output pathways. Proceedings of the National Academy of Sciences of the United States of America 2012;109:17123–8.
[31] Ito S, Song YH, Josephson-Day AR, Miller RJ, Breton G, Olmstead RG, et al. FLOWERING BHLH transcriptional activators control expression of the photoperiodic flowering regulator *CONSTANS* in *Arabidopsis*. Proceedings of the National Academy of Sciences of the United States of America 2012;109:3582–7.
[32] Lazaro A, Valverde F, Pineiro M, Jarillo JA. The *Arabidopsis* E3 ubiquitin ligase HOS1 negatively regulates CONSTANS abundance in the photoperiodic control of flowering. Plant Cell 2012;24:982–99.
[33] Zuo Z, Liu H, Liu B, Liu X, Lin C. Blue light-dependent interaction of CRY2 with SPA1 regulates COP1 activity and floral initiation in Arabidopsis. Current Biology 2011;21:841–7.
[34] Laubinger S, Marchal V, Gentilhomme J, Wenkel S, Adrian J, Jang S, et al. *Arabidopsis* SPA proteins regulate photoperiodic flowering and interact with the floral inducer CONSTANS to regulate its stability. Development 2006;133:3213–22.
[35] Jang S, Marchal V, Panigrahi KC, Wenkel S, Soppe W, Deng XW, et al. *Arabidopsis* COP1 shapes the temporal pattern of CO accumulation conferring a photoperiodic flowering response. EMBO Journal 2008;27:1277–88.
[36] Song YH, Smith RW, To BJ, Millar AJ, Imaizumi T. FKF1 conveys timing information for CONSTANS stabilization in photoperiodic flowering. Science 2012;336:1045–9.
[37] Franklin KA. Light and temperature signal crosstalk in plant development. Current Opinion in Plant Biology 2009;12:63–8.
[38] Inigo S, Alvarez MJ, Strasser B, Califano A, Cerdan PD. PFT1, the MED25 subunit of the plant Mediator complex, promotes flowering through CONSTANS dependent and independent mechanisms in Arabidopsis. Plant Journal 2012;69:601–12.
[39] Lee JH, Kim JJ, Kim SH, Cho HJ, Kim J, Ahn JH. The E3 ubiquitin ligase HOS1 regulates low ambient temperature-responsive flowering in *Arabidopsis thaliana*. Plant and Cell Physiology 2012;53:1802–14.
[40] Rizhsky L, Liang H, Shuman J, Shulaev V, Davletova S, Mittler R. When defense pathways collide. The response of Arabidopsis to a combination of drought and heat stress. Plant Physiology 2004;134:1683–96.
[41] Usadel B, Blasing OE, Gibon Y, Retzlaff K, Hohne M, Gunther M, et al. Global transcript levels respond to small changes of the carbon status during progressive exhaustion of carbohydrates in *Arabidopsis rosettes*. Plant Physiology 2008;146:1834–61.
[42] Dalchau N, Baek SJ, Briggs HM, Robertson FC, Dodd AN, Gardner MJ, et al. The circadian oscillator gene *GIGANTEA* mediates a long-term response of the *Arabidopsis thaliana* circadian clock to sucrose. Proceedings of the National Academy of Sciences of the United States of America 2011;108:5104–9.

[43] Ohto M, Onai K, Furukawa Y, Aoki E, Araki T, Nakamura K. Effects of sugar on vegetative development and floral transition in Arabidopsis. Plant Physiology 2001;127:252–61.
[44] Böhlenius H, Huang T, Charbonnel-Campaa L, Brunner AM, Jansson S, Strauss SH, et al. *CO*/*FT* regulatory module controls timing of flowering and seasonal growth cessation in trees. Science 2006;312:1040–3.
[45] Chew YH, Wilczek AM, Williams M, Welch SM, Schmitt J, Halliday KJ. An augmented Arabidopsis phenology model reveals seasonal temperature control of flowering time. New Phytologist 2012;194:654–65.
[46] Bernier G, Périlleux C. A physiological overview of the genetics of flowering time control. Plant Biotechnology Journal 2005;3:3–16.
[47] Corbesier L, Bernier G, Perilleux C. C:N ratio increases in the phloem sap during floral transition of the long-day plants *Sinapis alba* and *Arabidopsis thaliana*. Plant and Cell Physiology 2002;43:684–8.
[48] Bernier G, Havelange A, Houssa C, Petitjean A, Lejeune P. Physiological signals that induce flowering. Plant Cell 1993;5:1147–55.
[49] Atwell S, Huang YS, Vilhjálmsson BJ, Willems G, Horton M, Li Y, et al. Genome-wide association study of 107 phenotypes in *Arabidopsis thaliana* inbred lines. Nature 2010;465:627–31.
[50] Lasky JR, Des Marais DL, McKay JK, Richards JH, Juenger TE, Keitt TH. Characterizing genomic variation of *Arabidopsis thaliana:* the roles of geography and climate. Molecular Ecology 2012;21:5512–29.
[51] Hancock AM, Brachi B, Faure N, Horton MW, Jarymowycz LB, Sperone FG, et al. Adaptation to climate across the *Arabidopsis thaliana* genome. Science 2011;334:83–6.
[52] Ågren J, Schemske DW. Reciprocal transplants demonstrate strong adaptive differentiation of the model organism *Arabidopsis thaliana* in its native range. New Phytologist 2012;194:1112–22.
[53] Franks SJ, Sim S, Weis AE. Rapid evolution of flowering time by an annual plant in response to a climate fluctuation. Proceedings of the National Academy of Sciences of the United States of America 2007;104:1278–82.
[54] Franks SJ, Weis AE. A change in climate causes rapid evolution of multiple life-history traits and their interactions in an annual plant. Journal of Evolutionary Biology 2008;21:1321–34.
[55] Lewandowska-Sabat AM, Winge P, Fjellheim S, Dørum G, Bones AM, Rognli OA. Genome wide transcriptional profiling of acclimation to photoperiod in high-latitude accessions of *Arabidopsis thaliana*. Plant Science 2012;185–186:143–55.
[56] Binder BM, Walker JM, Gagne JM, Emborg TJ, Hemmann G, Bleecker AB, et al. The *Arabidopsis* EIN3 binding F-Box proteins EBF1 and EBF2 have distinct but overlapping roles in ethylene signaling. Plant Cell 2007;19:509–23.
[57] Lee JH, Yoo SJ, Park SH, Hwang I, Lee JS, Ahn JH. Role of SVP in the control of flowering time by ambient temperature in *Arabidopsis*. Genes & Development 2007;21:397–402.
[58] Van Buskirk HA, Thomashow MF. Arabidopsis transcription factors regulating cold acclimation. Physiologia Plantarum 2006;126:72–80.
[59] Jaglo-Ottosen KR, Gilmour SJ, Zarka DG, Schabenberger O, Thomashow MF. *Arabidopsis CBF1* overexpression induces *COR* genes and enhances freezing tolerance. Science 1998;280:104–6.
[60] Hannah MA, Heyer AG, Hincha DK. A global survey of gene regulation during cold acclimation in *Arabidopsis thaliana*. PLOS Genetics 2005;1:e26.
[61] Bieniawska Z, Espinoza C, Schlereth A, Sulpice R, Hincha DK, Hannah MA. Disruption of the *Arabidopsis* circadian clock is responsible for extensive variation in the cold-responsive transcriptome. Plant Physiology 2008;147:263–79.
[62] Mikkelsen MD, Thomashow MF. A role for circadian evening elements in cold-regulated gene expression in *Arabidopsis*. Plant Journal 2009;60:328–39.
[63] Franklin KA, Whitelam GC. Light-quality regulation of freezing tolerance in *Arabidopsis thaliana*. Nature Genetics 2007;39:1410–3.
[64] Dong MA, Farré EM, Thomashow MF. CIRCADIAN CLOCK-ASSOCIATED 1 and LATE ELONGATED HYPOCOTYL regulate expression of the C-REPEAT BINDING FACTOR (CBF) pathway in *Arabidopsis*. Proceedings of the National Academy of Sciences of the United States of America 2011;108:7241–6.
[65] Seo PJ, Park M-J, Lim M-H, Kim S-G, Lee M, Baldwin IT, et al. A self-regulatory circuit of CIRCADIAN CLOCK-ASSOCIATED1 underlies the circadian clock regulation of temperature responses in *Arabidopsis*. Plant Cell 2012;24:2427–42.
[66] James AB, Syed NH, Bordage S, Marshall J, Nimmo GA, Jenkins GI, et al. Alternative splicing mediates responses of the *Arabidopsis* circadian clock to temperature changes. Plant Cell 2012;24:961–81.
[67] Nakamichi N, Kusano M, Fukushima A, Kita M, Ito S, Yamashino T, et al. Transcript profiling of an *Arabidopsis PSEUDO RESPONSE REGULATOR* arrhythmic triple mutant reveals a role for the circadian clock in cold stress response. Plant and Cell Physiology 2009;50:447–62.
[68] Cao SQ, Song YQ, Su L. Freezing sensitivity in the *gigantea* mutant of *Arabidopsis* is associated with sugar deficiency. Biologia Plantarum 2007;51:359–62.
[69] Legnaioli T, Cuevas J, Mas P. TOC1 functions as a molecular switch connecting the circadian clock with plant responses to drought. EMBO Journal 2009;28:3745–57.
[70] Huang W, Perez-Garcia P, Pokhilko A, Millar AJ, Antoshechkin I, Riechmann JL, et al. Mapping the core of the *Arabidopsis* circadian clock defines the network structure of the oscillator. Science 2012;336:75–9.
[71] Lee CM, Thomashow MF. Photoperiodic regulation of the C-repeat binding factor (CBF) cold acclimation pathway and freezing tolerance in *Arabidopsis thaliana*. Proceedings of the National Academy of Sciences of the United States of America 2012;109:15054–9.
[72] Welling A, Moritz T, Palva ET, Junttila O. Independent activation of cold acclimation by low temperature and short photoperiod in hybrid aspen. Plant Physiology 2002;129:1633–41.
[73] Puhakainen T, Li C, Boije-Malm M, Kangasjärvi J, Heino P, Palva ET. Short-day potentiation of low temperature-induced gene expression of a C-repeat-binding factor-controlled gene during cold acclimation in silver birch. Plant Physiology 2004;136:4299–307.
[74] Kidokoro S, Maruyama K, Nakashima K, Imura Y, Narusaka Y, Shinwari ZK, et al. The phytochrome-interacting factor PIF7 negatively regulates *DREB1* expression under circadian control in Arabidopsis. Plant Physiology 2009;151:2046–57.
[75] Schwartz C, Balasubramanian S, Warthmann N, Michael TP, Lempe J, Sureshkumar S, et al. *Cis*-regulatory changes at *FLOWERING LOCUS T* mediate natural variation in flowering responses of *Arabidopsis thaliana*. Genetics 2009;183:723–32.
[76] Wang ZY, Tobin EM. Constitutive expression of the *CIRCADIAN CLOCK ASSOCIATED 1* (*CCA1*) gene disrupts circadian rhythms and suppresses its own expression. Cell 1998;93:1207–17.
[77] Baudry A, Ito S, Song YH, Strait AA, Kiba T, Lu S, et al. F-box proteins FKF1 and LKP2 act in concert with ZEITLUPE to control *Arabidopsis* clock progression. Plant Cell 2010;22:606–22.

Chapter 3

Cool night-time temperatures induce the expression of *CONSTANS* and *FLOWERING LOCUS T* to regulate flowering in *Arabidopsis*

As published in *New Phytologist*

2016

v211(1): 208-224

http://onlinelibrary.wiley.com/doi/10.1111/nph.13883/full

New Phytologist

Cool night-time temperatures induce the expression of *CONSTANS* and *FLOWERING LOCUS T* to regulate flowering in *Arabidopsis*

Hannah A. Kinmonth-Schultz[1], Xinran Tong[1], Jae Lee[1], Young Hun Song[1,2], Shogo Ito[1], Soo-Hyung Kim[3] and Takato Imaizumi[1]

[1]Department of Biology, University of Washington, Seattle, WA 98195-1800, USA; [2]Department of Life Sciences, Ajou University, Suwon 443-749, Korea; [3]School of Environmental and Forest Sciences, University of Washington, Seattle, WA 98195-2100, USA

Author for correspondence:
Takato Imaizumi
Tel: +1 206 543 8709
Email: takato@u.washington.edu

Received: *2 November 2015*
Accepted: *6 January 2016*

New Phytologist (2016) **211:** 208–224
doi: 10.1111/nph.13883

Key words: ambient temperature, *Arabidopsis thaliana*, CONSTANS, FLOWERING LOCUS T, flowering time, photoperiod, signal integration.

Summary

• Day length and ambient temperature are major stimuli controlling flowering time. To understand flowering mechanisms in more natural conditions, we explored the effect of daily light and temperature changes on *Arabidopsis thaliana*.

• Seedlings were exposed to different day/night temperature and day-length treatments to assess expression changes in flowering genes.

• Cooler temperature treatments increased *CONSTANS* (*CO*) transcript levels at night. Night-time *CO* induction was diminished in *flowering bhlh* (*fbh*)-quadruple mutants. *FLOWERING LOCUS T* (*FT*) transcript levels were reduced at dusk, but increased at the end of cooler nights. The dusk suppression, which was alleviated in *short vegetative phase* (*svp*) mutants, occurred particularly in younger seedlings, whereas the increase during the night continued over 2 wk. Cooler temperature treatments altered the levels of *FLOWERING LOCUS M-β* (*FLM-β*) and *FLM-δ* splice variants. *FT* levels correlated strongly with flowering time across treatments.

• Day/night temperature changes modulate photoperiodic flowering by changing *FT* accumulation patterns. Cooler night-time temperatures enhance FLOWERING BHLH (FBH)-dependent induction of *CO* and consequently increase CO protein. When plants are young, cooler temperatures suppress *FT* at dusk through SHORT VEGETATIVE PHASE (SVP) function, perhaps to suppress precocious flowering. Our results suggest day length and diurnal temperature changes combine to modulate *FT* and flowering time.

Introduction

In nature, plants experience temperature fluctuations coinciding with day and night, and daily temperature fluctuations affect plant development (Myster & Moe, 1995). When exposed to day/night temperature cycles, flowering of rice and barley can be accelerated or delayed relative to constant-temperature conditions (Yin & Kropff, 1996; Karsai *et al.*, 2008). Time-of-day information is important for a range of physiological responses as sensitivity to temperature is modulated by the circadian clock throughout the day (McClung, 2006). Further, plant responses to combined environmental stimuli cannot be easily predicted from the responses to each alone (Prasch & Sonnewald, 2015). Therefore, to study the mechanisms that operate in nature, it is useful to assess the combinational influence of day length and day-to-night temperature fluctuations on seasonal flowering.

The day-length dependent (photoperiodic) flowering pathway has been well studied in *Arabidopsis thaliana* (Golembeski *et al.*, 2014; Osugi & Izawa, 2014; Shrestha *et al.*, 2014). Components of this pathway are implicated in ambient-temperature-dependent flowering (Song *et al.*, 2013), indicating that light and temperature signals can be integrated into the same pathway. Photoperiod information is processed through regulation of the *CONSTANS* (*CO*) gene. *CO* peaks in the afternoon and evening during long days (LD) (Suárez-López *et al.*, 2001). CO protein production follows the same pattern during the day; however, it is degraded during the night by CONSTITUTIVE PHOTOMORPHOGENIC 1 (COP1)/SUPPRESSOR OF *PHYA-105* (SPA) E3 ubiquitin ligase complex (Laubinger *et al.*, 2006; Jang *et al.*, 2008; Liu *et al.*, 2011). In LD afternoons, two types of blue-light photoreceptors CRYPTOCHROME (CRY) and FLAVIN-BINDING, KELCH REPEAT, F-BOX 1 (FKF1) stabilize CO protein inducing *FLOWERING LOCUS T* (*FT*) at the end of the day to promote flowering (Zuo *et al.*, 2011; Song *et al.*, 2012, 2014; Tan *et al.*, 2013).

Temperature affects flowering by modulating *FT* levels through *CO*-dependent and -independent mechanisms (Lee *et al.*, 2007; Jung *et al.*, 2012; Lazaro *et al.*, 2012; Nomoto *et al.*,

2013). At constant lower (16°C) temperatures in 12 h : 12 h light : dark days and LD, *FT* levels are reduced and plants flower later compared with 23°C conditions (Blazquez *et al.*, 2003; Lee *et al.*, 2007). However, in *short vegetative phase* (*svp*) mutants, the *FT* level remains high even at a constant 16°C (Lee *et al.*, 2007). At both 16°C and 23°C, *svp* mutants flower at similar times, indicating that SVP represses *FT* and delays flowering under cool temperatures. SVP interacts with the FLOWERING LOCUS M (FLM) splice variant, FLM-β, to bind the *FT* promoter (Posé *et al.*, 2013). Intermittent drops to cold (4°C) temperatures during the day may act through CO to repress flowering (Jung *et al.*, 2012). A temperature drop from 23°C to 4°C from Zeitgeber time (ZT) 10 to ZT16 in LD leads to *FT* repression and a delay of flowering. The decline in *FT* mRNA strongly parallels a decline in CO protein abundance.

Colder temperatures within a day do not always reduce *FT* levels. In constant light, a 22°C/12°C temperature cycle over a 24-h period causes a strong induction of *FT* during the cool periods of the cycle, and temperature cycles are likely associated with early flowering (Schwartz *et al.*, 2009). Under 12-h light and 12-h dark conditions, having warmer temperatures (28°C) at night but not in the day (22°C) causes upregulation of *FT* (Thines *et al.*, 2014). Therefore, depending on light conditions, temperature changes occurring at different times of the day differentially regulate *FT* expression patterns and do so through several mechanisms.

In *Arabidopsis thaliana*, small numbers of consecutive LD treatments are sufficient to induce early flowering, and *FT* is immediately upregulated after plants are moved from short days (SD) to LD, but declines to basal levels shortly after plants are returned to SD (Corbesier *et al.*, 1996, 2007; Krzymuski *et al.*, 2015). This accumulation of a discrete amount of *FT* correlates with early flowering and suggests that environmental cues which modulate *FT* levels will affect flowering time. To better assess the mechanisms that occur in natural conditions, we analyzed the combined influence of temperature and day-length changes on photoperiodic-flowering-pathway genes and tested the extent to which *FT* gene expression levels can explain flowering times across a range of treatments.

Materials and Methods

Plant material and growth conditions

Wild-type (WT) accessions of *Arabidopsis thaliana* (L.) Heynh, Columbia-0 (Col-0), Landsberg *erecta* (L*er*), and Wassilewskija-2 (Ws-2), were used. All mutants and transgenic lines were in the Col-0 background and described previously: *co-101* and *ft-101* (Takada & Goto, 2003); *fbh*-quadruple mutant (*fbh-q #2*) and *FBH1:FLAG-FBH1* (Ito *et al.*, 2012); *CO:HA-CO* and *35S:3HA-CO* (Song *et al.*, 2012); and *svp-31* (Lee *et al.*, 2007) and *SVP:SVP-6HA* (Shen *et al.*, 2011). For flowering experiments, seeds were sown on soil (Sunshine #3 Mix; Sun Gro Horticulture, Agawam, MA, USA) containing Osmocote Classic time-release fertilizer (Scotts, Marysville, OH, USA) and Systemic Granules: Insect Control (Bionide, Oriskany, NY, USA). For gene and protein expression, GUS activity, and the 14-d, LD-to-SD-transfer flowering experiment, seeds were placed on plates containing 1× Linsmaier and Skoog (LS) media (Caisson, Smithfield, UT, USA) and 3% sucrose. Plants were grown in LD (16-h light/8-h dark) or SD (8-h light/16-h dark) conditions for 7, 14, or 21 d to avoid temperature effects on germination and early development, then moved to constant 12°C or 22°C, or to temperature cycles of 22°C (light) and 12°C or 17°C (dark) in SD, 12-h light/12-h dark (MD) or LD conditions. HOBO Pendant temperature/light data loggers (Onset, Bourne, MA, USA) were used to ensure that temperature deviated 0.5°C or less from the target temperatures. Full-spectrum fluorescent light (Octron F032/950/48; Osram-Sylvania, Wilmington, MA, USA) intensities in the growth chambers averaged *c.* 100 μmol m^{-2} s^{-1} in SD and 60 μmol m^{-2} s^{-1} in LD. For flowering experiments, individuals from each strain were assigned random positions within 32-pot flats. The flats were repositioned at least weekly within and between chambers to avoid chamber and positional affects. For the 14-d transfer experiment, one representative of each age (1–14 d) was randomized and put into a single flat to account for differences resulting from watering or fertilization. For the remaining analyses, temperature treatments were randomly assigned different incubators for each replicate. Flowering time was measured by recording the number of rosette leaves on the main stem. To assess rate of leaf production, new leaves at least 2 mm long were counted once a week.

Gene expression analysis (qPCR)

For most experiments, plants were grown for 7 d in SD conditions before being transferred to treatments and harvested every 4 h beginning at dawn (ZT0) on Day 4 of treatment. For the 48-h time courses, seedlings were harvested starting at ZT12 on Day 3 of treatment, when the seedlings were 10 d old. For the 14-d time courses, seedlings were harvested at ZT0, ZT8 and ZT16 on days 1–14 of treatment. RNA isolation, cDNA synthesis and qPCR were carried out as described (Ito *et al.*, 2012). All genes were normalized against *ISOPENTENYL PYROPHOSPHATE/DIMETHYLALLYL PYROPHOSPHATE ISOMERASE* (*IPP2*) (Hazen *et al.*, 2005). We confirmed that diurnal *IPP2* was expressed uniformly across our temperature conditions compared to other potential internal control genes, *SERINE/THREONINE PROTEIN PHOSPHATASE 2A* (*PP2A*) (Hong *et al.*, 2010) and *ACTIN 2* (*ACT2*) (Sawa *et al.*, 2007) (Supporting Information Fig. S1). Primers and PCR conditions for *FT*, *CO*, *SUPPRESSOR OF OVEREXPRESSION OF CONSTANS* (*SOC1*), *FLC* (Ito *et al.*, 2012), *ACT2* and *PP2A* were described previously (Sawa *et al.*, 2007; Hong *et al.*, 2010). The primers for *SVP* are 5′-ACGGAAGAGAACGAGCGACTTG-3′ and 5′-CTCGTACACAGCAGCGTTCTCC-3′. qPCR was done using the following program: 1 min 95°C denaturation, then 45 cycles of 10 s at 95°C, 20 s at 59°C and 20 s at 72°C.

Protein expression analysis (Western blot)

Extraction and detection of FLAG-FBH1 and SVP-6HA proteins, and of nuclear HA-CO were performed as described (Ito

et al., 2012; Song *et al.*, 2012). FLAG-FBH1 and SVP-6HA and HA-CO protein were detected by anti-FLAG antibody (Sigma) or anti-HA conjugated to horseradish-peroxidase (Roche). Actin, HSP90 and Histone H3, detected by anti-Actin, anti-HSP90 or anti-Histone H3 antibodies (Song *et al.*, 2012), respectively, were used as loading controls. Relative expression levels were normalized by the values of loading controls.

GUS activity visualization

pFT:GUS and *pCO:GUS* lines were described previously (Takada & Goto, 2003). Eleven-day-old seedlings were harvested at ZT24 on Day 4 of the temperature and day-length treatment. Tissue preparation and staining were as described previously (Ito *et al.*, 2012). Seedlings were prepared for visualization with a series of washes of 70%, 50% and 30% ethanol, H_2O, then 25% and 50% glycerol.

Statistical analyses

Statistical analyses were done using R Statistical Computing software (v3.1.1 and earlier; R Core Team, 2015). The statistical significance of final rosette leaf numbers at bolt was determined using ANOVA with temperature treatment and strain as main effects. Pairwise comparisons were determined using Tukey's Honest Statistical Difference (R Core Team, 2015). In some cases the replicate and/or tray was introduced as a covariate to account for pseudo-replication. Statistical significance of leaf production over time was analyzed using linear mixed-effects regression (Bates *et al.*, 2015), which accounted for repeated measures of the same individuals, with temperature, strain and time (weeks) included as the main effects. This was followed by Satterthwaite approximation to generate *P*-values (Satterthwaite, 1946). For leaf production, we considered only data recorded before the appearance of visible bolts. Data were transformed as needed based on Box–Cox analysis (Box & Cox, 1964) and visual comparisons of residuals to ensure equal variance. Most flowering experiments were replicated at least twice, with at least 10 individuals per strain and treatment in each replicate. The 14-d, LD-to-SD transfer experiment was replicated twice with five individuals per treatment per replicate.

Gene expression data displayed heteroskedastic residuals, so effects of temperature and time were compared using the Generalized Estimating Equation (Carey, 2015), which computes robust standard errors and test statistics, followed by pairwise Tukey's comparisons using lsmeans (Lenth, 2015). To improve normality and equal variance among treatments, time (ZT) was transformed by finding the cosine, and, if necessary, day and night segregation was included as a covariate to account for oscillatory patterns. All gene and protein experiments were replicated at least three times, and we obtained similar results. Effects were considered significant when both of the following conditions were met: *P*-value $\leq$ significance level and the 95% Confidence Interval (CI) for the difference between a pair did not contain zero. The significance level was 0.05. For highly nonlinear data, subsets (by time) were tested and the significance level was lowered using Bonferonni correction for multiple comparisons.

Results

Cool night-time temperatures result in delay of flowering, and altered accumulation profiles of *CO* and *FT* transcripts

Outdoors, diurnal light and temperature cycles occur together. How do plants integrate these cues? Using as a guide the 21.1°C-high/11.7°C-low temperature range of the summer solstices in Seattle, Washington, USA (averages from 1971 to 2000, day length: 15 h 59 min), we overlaid a 22°C/12°C temperature cycle onto a 16-h-light, 8-h-dark LD cycle, such that the cool period occurred throughout the night (referred to as LD22/12°C) and assessed the timing of flowering. As temperature influences numerous plant processes (Parent *et al.*, 2010), we mitigated its influence on early development by growing all seedlings in non-flowering-inductive SD conditions at 22°C for 7 d before moving them to temperature treatments. Growth in cool night-time temperatures resulted in a delay in flowering (20.84 ± 0.64 leaves) and a 40.46% increase in the number of leaves produced at bolt in Col-0 plants relative to plants grown in the constant-temperature conditions usually used in studies of photoperiodic flowering in *Arabidopsis* (LD22/22°C) (14.96 ± 0.42 leaves, $P \leq 0.001$; Fig. 1a; Table 1).

In order to determine the mechanisms responsible for this delay, we analyzed the profiles of several flowering-regulator gene transcripts (Yant *et al.*, 2009). We found a significant increase of *CO* transcript accumulation at night in LD22/12°C conditions relative to plants grown in the LD22/22°C control (Fig. 1b). *FT* transcript levels in LD22/12°C were also significantly altered compared to the control. *FT* levels were reduced at dusk, but higher at dawn (Fig. 1c). A smaller (5°C) difference between day and night-time temperatures (LD22/17°C) resulted in an intermediate response relative to the control. *CO* was induced at night in LD22/17°C conditions, but to a lesser extent than in LD22/12°C (Fig. 1b). The *FT* profile in LD22/17°C conditions was similar at dusk and dawn to the control, but higher than either the control or LD22/12°C in the middle of the night (ZT20, Fig. 1c). Therefore, diurnal temperature cycles, in conjunction with day and night, influence the profiles of *CO* and *FT* transcript accumulation.

SOC1 is downstream of *FT* and acts at the shoot apex to induce *LEAFY* (*LFY*) to promote flowering (Lee *et al.*, 2008). *SOC1* level was reduced during the morning in LD22/12°C conditions relative to the control (Fig. 1d), consistent with a delay in flowering. The expression of the strong *FT* repressor, *FLOWERING LOCUS C* (*FLC*) gene (Michaels & Amasino, 1999), did not respond to our temperature treatments (Fig. 1e), suggesting that if day/night temperature fluctuations affect flowering through *FLC*, it is not through altered mRNA levels. SVP represses *FT* and delays flowering time under lower temperatures (i.e. 16°C) (Lee *et al.*, 2007). The daily patterns of *SVP* transcript accumulation were not significantly changed between our two conditions (Fig. 1f).

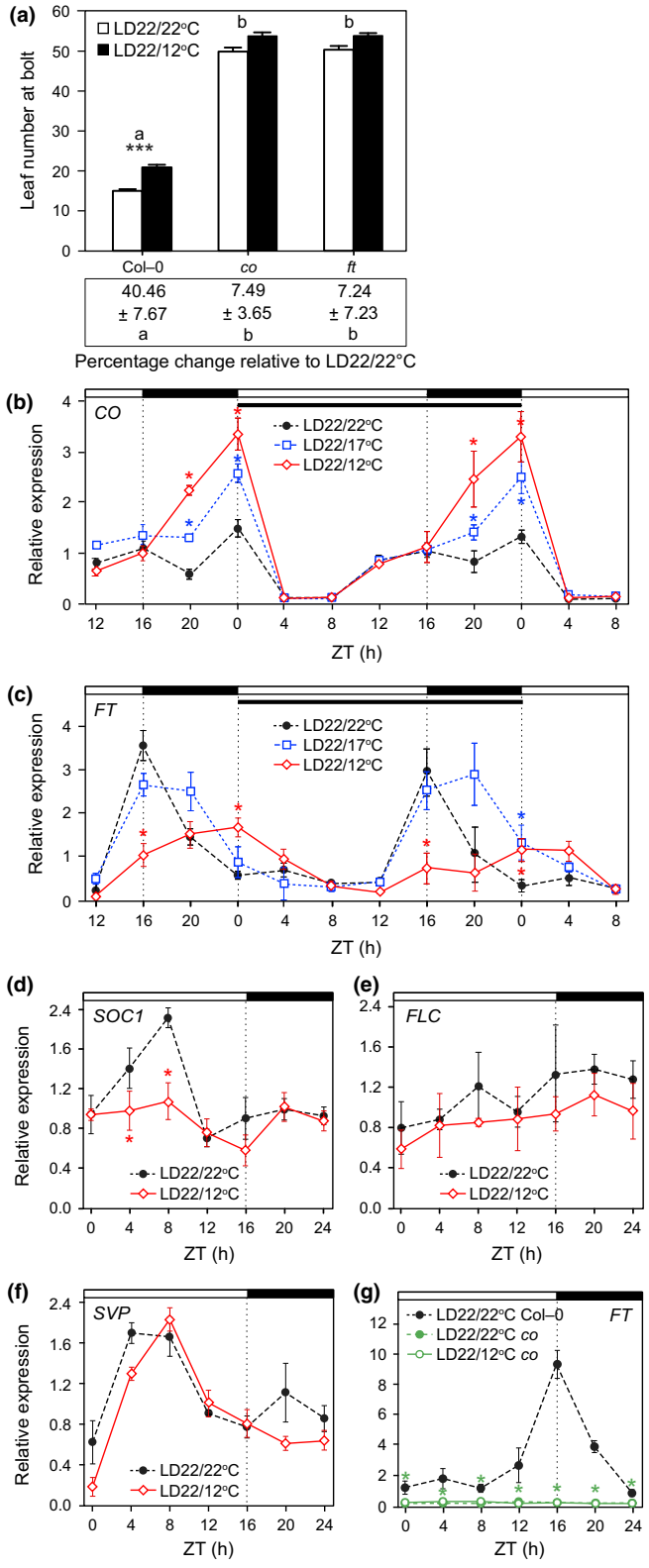

Fig. 1 Flowering is delayed and transcript accumulation patterns of *CONSTANS* (*CO*) and *FLOWERING LOCUS T* (*FT*) are altered in response to day : night temperature fluctuations. (a) Rosette leaf number of Columbia-0 (Col-0) wild-type *Arabidopsis thaliana* plants, *co-101*, and *ft-101* mutants (top) and percentage change in rosette leaf number between treatment means within a replicate (bottom) in long-day treatments with 22°C daytime temperatures and 22°C or 12°C night-time temperatures (LD22/22°C and LD22/12°C). Letters represent significant differences among strains of $P < 0.05$. Asterisks (***) indicate significance between treatments within Col-0 ($P < 0.001$), mean and 95% Confidence Interval (CI, 0.329, 0.232, 0.425). Treatment differences of *co-101* and *ft-101* (top) were not significantly different ($P = 0.199$ and 0.375), mean and 95% CI (0.081, −0.015, 0.177) and (0.072, −0.025, 0.169), respectively; for differences in percentage change from that of Col-0 (bottom), mean and 95% CI (−3.681, −5.095, −2.267) and (−3.489, −4.903, −2.075), respectively ($n = 10$, replicate = 5). (b, c) *CO* and *FT* transcript accumulation patterns in LD treatments with different night-time temperatures (LD22/22°C, LD22/17°C, and LD22/12°C). Topmost white and black bars designate day and night, respectively. Dotted vertical lines are times of lights on or off. Narrow black bar designates Day 4 of treatment. (d) *SUPPRESSOR OF OVEREXPRESSION OF CONSTANS* (*SOC1*), (e) *FLOWERING LOCUS C* (*FLC*), and (f) *SHORT VEGETATIVE PHASE* (*SVP*) gene transcript accumulation patterns in Col-0, and (g) *FT* transcript accumulation in *co-101* mutant line from seedlings harvested on Day 4 in LD22/22°C and LD22/12°C. Data represent means ± SEM derived from at least three biological replicates. (b–g) Asterisks (*) indicate $P < 0.05$ and 95% CI of difference between pair did not contain zero in statistical comparisons made against the LD22/22°C control. ZT, zeitgeber time (h after light onset).

FT and *CO* are upstream of *SOC1* and several studies suggest that *FT* levels are predictive of flowering (Kobayashi *et al.*, 1999; Blazquez *et al.*, 2003; Corbesier *et al.*, 2007; Salazar *et al.*, 2009; Krzymuski *et al.*, 2015; Seaton *et al.*, 2015), therefore, we chose to explore whether *FT* and *CO* profile changes could account for the delay in flowering we observed. We tested the flowering time of *co* and *ft* mutants. The final leaf numbers at bolt of *ft* and *co* mutant plants were not significantly different between the LD22/22°C control and LD22/12°C temperature treatments (Fig. 1a; Table 1), indicating that *CO* and *FT* may be involved in the temperature-dependent delay of flowering. CO is a chief activator of daytime *FT* expression (Yanovsky & Kay, 2002). We tested whether CO is required for the cooler-night-temperature-induced *FT* changes. In the *co* mutant line, we found that *FT* remained at basal levels throughout the day in both LD22/22°C and LD22/12°C conditions relative to *FT* in WT plants (Fig. 1g), indicating that night-time expression of *FT* under LD22/12°C conditions still requires the *CO* gene.

In order to analyze whether these night-time-temperature-induced responses are conserved in other WT accessions, we measured flowering time and gene expression in two common lab strains, L*er* and Ws-2. Both showed delayed flowering in LD22/12°C conditions relative to LD22/22°C that were similar to Col-0 (Fig. 2a; Table 1). As with Col-0, they both displayed night-time induction of *CO* (Fig. 2b,c), suppression of *FT* at dusk and higher levels of *FT* at dawn (Fig. 2d,e) in the LD22/12°C conditions relative to the LD22/22°C control, indicating that this response was not accession-specific.

We wondered whether the changes in *CO* and *FT* transcript accumulation were due to changes in the spatial accumulation patterns of these genes, which are expressed in the leaf vasculature in the LD22/22°C conditions (Takada & Goto, 2003). We examined the spatial patterns of *CO* and *FT* and found that the tissue-specific accumulation of *pFT:GUS* and *pCO:GUS* were not affected by LD22/12°C treatments relative to the control

Table 1 Means, variances, 95% Confidence Intervals and *P*-values for final rosette leaf number at bolt of *Arabidopsis thaliana* strains in response to constant (22°C) temperatures or warm (22°C) days and cool (12°C) nights in LD

Strain	Night temp. (°C)	Mean (leaf number)	Standard deviation	SE	Mean (log(leaf number))	95% CI		adjusted *P**
						upper	lower	
Col-0†	22	14.96	2.91	0.42	0.3289	0.2323	0.4254	0.0000
	12	20.84	4.51	0.64				
co-101	22	49.76	6.99	1.01	0.0809	−0.0152	0.1769	0.1987
	12	53.70	5.98	0.85				
ft-101	22	50.22	6.52	0.94	0.0720	−0.0245	0.1686	0.3748
	12	53.78	4.19	0.60				
svp-31	22	7.30	1.44	0.23	0.1874	0.0784	0.2964	0.0000
	12	8.84	1.74	0.29				
Ler	22	7.40	2.07	0.33	0.3131	0.2062	0.4199	0.0000
	12	9.98	1.75	0.28				
Ws-2	22	8.00	1.04	0.17	0.2902	0.1833	0.3971	0.0000
	12	10.73	1.74	0.28				
Col-0†	22	15.79	2.11	0.33	0.3144	0.2127	0.4162	0.0000
	12	22.23	5.04	0.94				
fbh-quadruple #2	22	22.80	2.99	0.55	0.2241	0.0972	0.3510	0.0000
	12	27.72	3.71	0.90				

**P*-value adjusted to account for multiple comparisons.
†Col-0 included as a wild-type control in all experiments.
The results shown above and below the dotted line were obtained from different experiments.

(Fig. 3a–d), indicating that temperature fluctuations only alter the temporal accumulation patterns of these genes.

FT induction is dependent on the presence of light in the afternoon at constant temperatures (Yanovsky & Kay, 2002). In order to investigate whether night-time *CO* induction and the altered *FT* profile were day-length dependent, we tested accumulation profiles of *CO* and *FT* transcripts in SD and MD. In both cases, the seedlings were exposed to 12°C for the duration of the night. Induction of *CO* in response to 12°C night-time temperatures occurred in both day lengths (Fig. 3e,f). However, *FT* was not appreciably induced in SD, whereas *FT* did not differ significantly between treatments in MD (Fig. 3g,h), indicating that cool night-time temperatures do not override the requirement of *FT* for afternoon light.

Induction of *CO* and *FT* in response to cool night-time temperatures is reproduced over 2 wk of treatment

Peak expression of *FT* increases as plants age from 5 to 15 d (Mathieu *et al.*, 2009). We wondered whether the rate of increase would be slower in LD22/12°C conditions, helping to explain the delay in flowering, and whether the diurnal transcript accumulation patterns we observed remained consistent over time. We extended the LD22/22°C control and LD22/12°C treatment for 14 d (from 7- to 21-d-old plants), harvesting at dawn (ZT0), during the middle of the day (ZT8) when *CO* and *FT* transcripts are at trough levels, and at dusk (ZT16) for the full 2 wk. In LD22/12°C conditions, night-time induction of *CO* and upregulation of *FT* at dawn were reproduced for the full 14 d (Fig. 4a,b). However, dusk suppression of *FT* in LD22/12°C disappeared over time (Fig. 4b). Could suppression of *FT* at dusk be a transient response to cool nights, perhaps acting to buffer development to short-term temperature modulations? If correct, we would expect dusk suppression of *FT* even in plants first exposed to the LD22/12°C treatment later in development. We sampled 18- and 25-d-old seedlings, each having been exposed to the temperature treatments for 4 d, to determine whether we observed *FT* accumulation at dusk. Interestingly, in 25-d-old plants but not in 18-d-old plants, dusk levels of *FT* were not significantly different from those of the control (Fig. 4c,d), indicating that dusk suppression can be a transient response, dependent on developmental age, potentially suppressing flowering in young plants when temperatures are unfavorable.

FT expression correlates with flowering across treatments

A discrete number of LDs and amount of *FT* expression is required to induce flowering (Krzymuski *et al.*, 2015). We confirmed that such a distinct switch occurs in our conditions. After 7 d in SD, seedlings were moved to LD22/22°C conditions. For 2 wk, after each LD treatment, we transferred some seedlings back to SD conditions and recorded leaf number at bolt. Seedlings exposed to 1–4 d of LD flowered similarly to plants grown in SD (leaf number 57.7 ± 11.68 (standard deviation)) (Fig. 5a). After five consecutive LDs, most seedlings flowered early (leaf number 9.35 ± 8.03). Together with previous research, this implies that flowering occurs after *FT* reaches a threshold and that alterations in *FT* levels in response to environmental perturbations can be predictive of flowering time.

However, cool temperature affects several plant processes and slows leaf production (Parent *et al.*, 2010). It is difficult to separate temperature effects mediated through *CO* and *FT* from other factors. To assess whether leaf production slowed in LD22/12°C

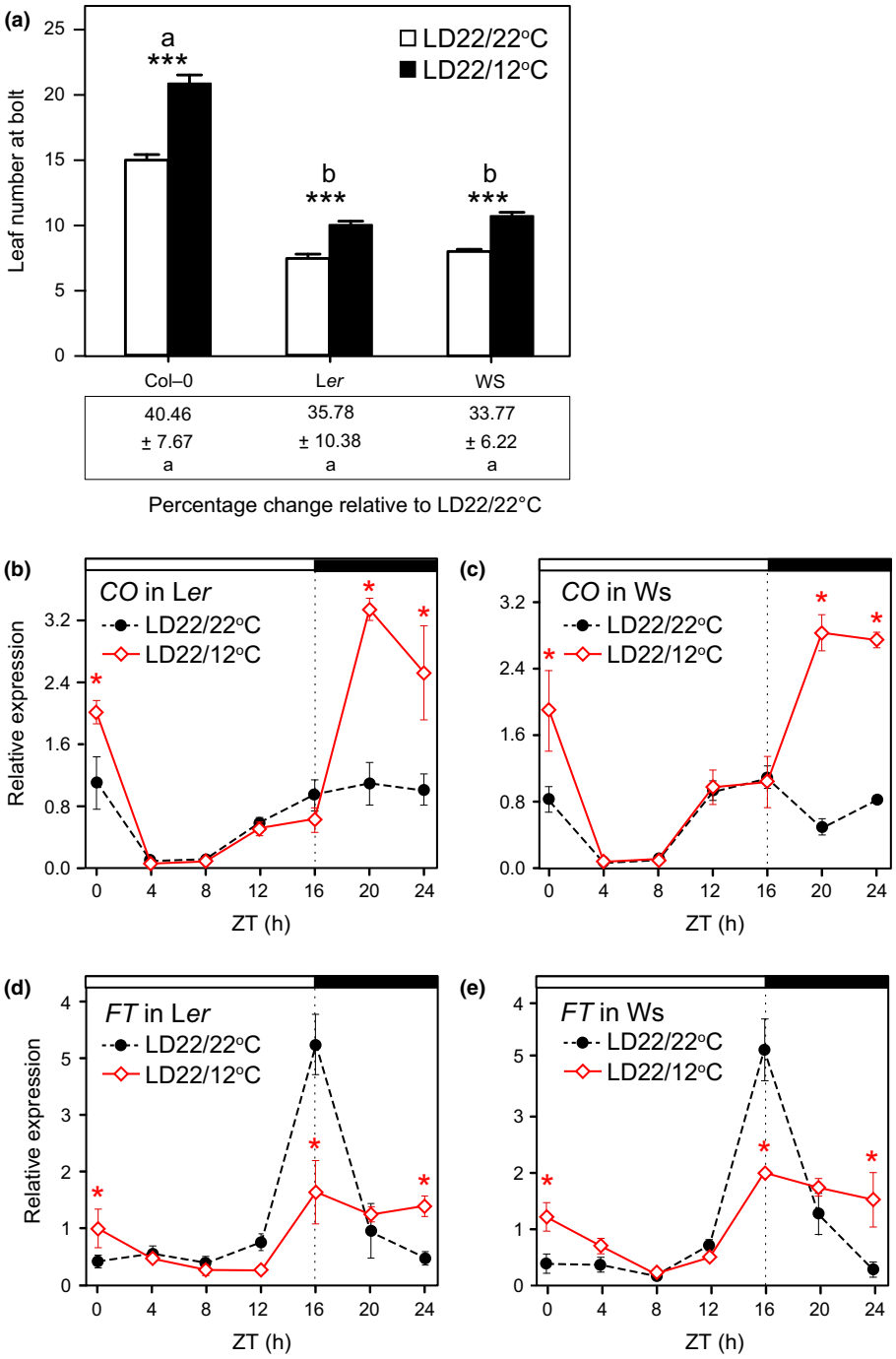

Fig. 2 Flowering and transcript accumulation patterns of *CONSTANS* (*CO*) and *FLOWERING LOCUS T* (*FT*) in different *Arabidopsis thaliana* ecotypes in response to day : night temperature fluctuations are similar to those in the Columbia-0 (Col-0) *Arabidopsis thaliana* accession. (a) Rosette leaf number of Col-0, Landsberg *erecta* (L*er*) and Wassilewskija-2 (Ws-2) (top) and percentage change in rosette leaf number between treatment means within a replicate (bottom) in LD22/22°C (long days with day : night temperatures = 22°C : 22°C) and LD22/12°C conditions. (Top) Asterisks (***) indicate significance between treatments ($P < 0.001$), mean and 95% Confidence Interval (CI, 0.329, 0.232, 0.425), (0.313, 0.206, 0.419) and (0.290, 0.183, 0.397), respectively. (Bottom) Differences in percentage change from that of Col-0 for L*er* and Ws ($P = 0.949$ and 0.844, respectively), mean and 95% CI (−0.408, −1.908, 1.092) and (−0.549, −2.049, 0.951), respectively ($n = 10$, replicate = 5). (b, c) *CO* transcript accumulation and (d, e) *FT* transcript accumulation in L*er* and Ws in LD22/22°C and LD22/12°C conditions. Seedlings were grown under the same conditions used for the experiments shown in Fig. 1. Data represent means ± SEM derived from at least three biological replicates. (b–e) Asterisks (*) indicate significance $P < 0.05$ and that 95% CI of difference between pair did not contain zero. ZT, zeitgeber time (h after light onset).

temperature cycle conditions relative to the LD22/22°C control, we counted the number of leaves produced each week for several WT and mutant strains. When considering only leaves produced before production of visible bolts, there was a slightly lower overall leaf number across strains in LD22/12°C conditions relative to the LD22/22°C control ($P < 0.001$, Fig. 5b). However, the 95% CI (−0.134, 0.1497) of the difference between treatments contained zero and so is not significant. This was true even when considering only late flowering strains, which were exposed to cool night-time temperatures the longest, suggesting that our temperature-cycle treatments do not appreciably affect leaf production.

We then investigated how well the relative *FT* levels in each strain and treatment explain final leaf numbers at bolt. Because the *FT* transcript profiles remain relatively consistent in LD (Fig. 4b), we assumed that the pattern of *FT* on Day 4 of our treatments was representative of the amount of *FT* produced before plants reached an LD threshold. We found that leaf numbers declined with increasing levels of *FT*, when accumulated Day 4 *FT* transcript was found by integrating under the curve (Fig. 5c, closed circles). After the data were linearized, *FT* levels explained much of the variation in flowering across day length and temperature treatments and WT and mutant strains within the Col-0 background. Recent work indicated that *FT* generated

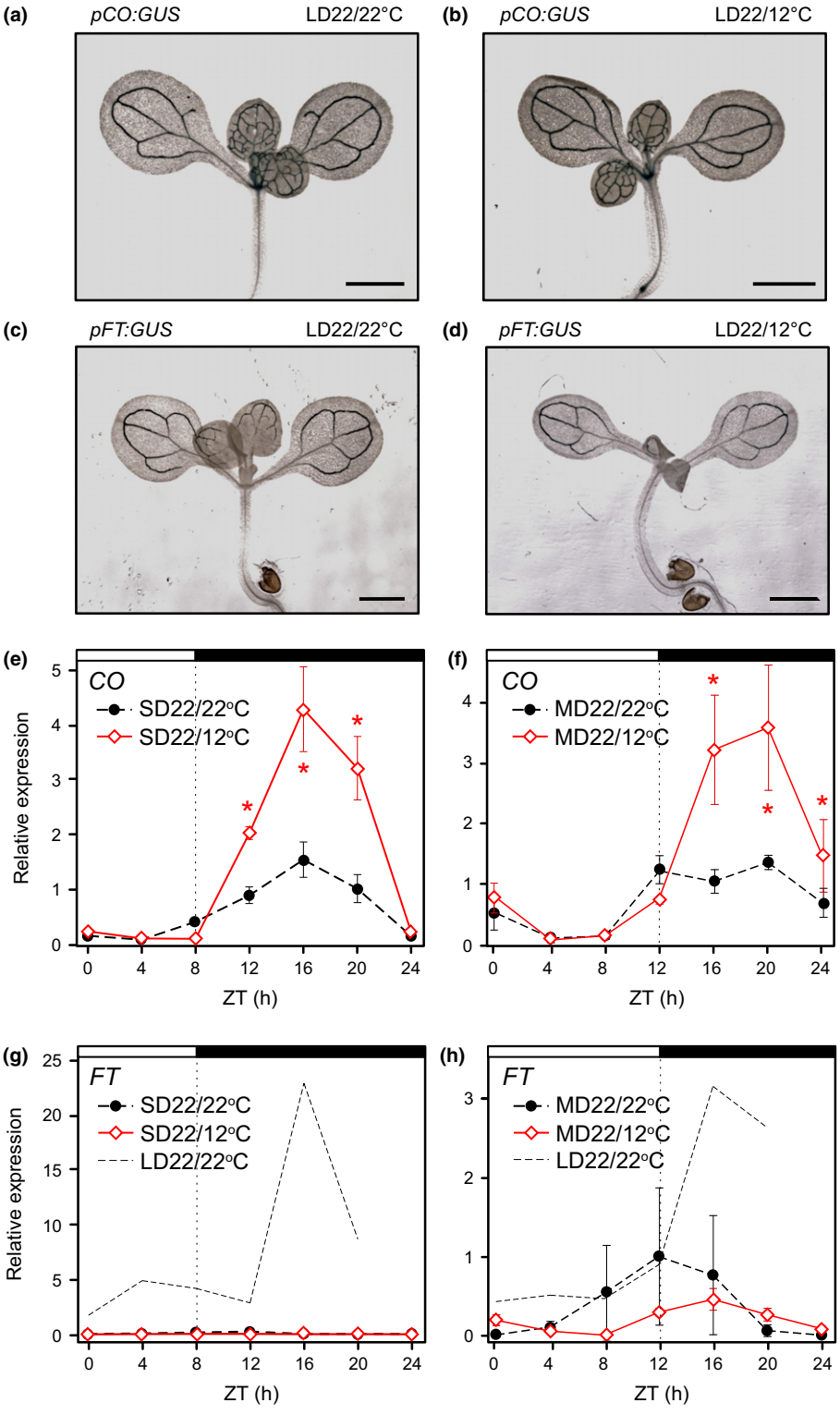

Fig. 3 Spatial transcript accumulation patterns of *CONSTANS* (*CO*) and *FLOWERING LOCUS T* (*FT*) are not altered in response to day : night temperature fluctuations in *Arabidopsis thaliana* (Columbia-0 (Col-0)). Night-time induction of *CO* in response to cool night-time temperatures occurs regardless of day length; *FT* induction by cool temperatures does not occur in short day (SD). (a–d) Tissue-specific patterns of GUS activity in *pCO:GUS* (a, b) and *pFT:GUS* (c, d) plants grown in LD22/22°C (long days with day : night temperatures = 22°C : 22°C) and LD22/12°C conditions for 5 d. Scale bars, 1 mm. (e, f) *CO* transcript accumulation and (g, h) *FT* transcript accumulation on Day 4 in SD or 12-h, mid-length-day (MD) treatments with 22°C daytime temperatures and 22°C or 12°C night-time temperatures. Replicate of *FT* transcript accumulation in LD22/22°C conditions is included for comparison. Data represent means ± SEM derived from at least three biological replicates. (e–h) Asterisks (*) indicate significance $P < 0.05$ and that 95% CI of difference between pair did not contain zero. ZT, zeitgeber time (h after light onset).

around dusk (ZT12–ZT20; Krzymuski *et al.*, 2015) is more effective for inducing flowering, and suppression of *FT* at dusk likely accounts for the delays in flowering induced by our warm-day/cool-night conditions. The correlation between *FT* amounts over this timeframe and flowering time was strong in our conditions as well, showing the same correlation as for total *FT* ($R^2 = 0.88$, RMSE = 0.25 log(leaves)). However, the correlation was strongest when daytime *FT* from samples collected at ZT0, ZT8 and ZT16 were considered (Fig. 5c inset, $R^2 = 0.92$, RMSE = 0.21 log(leaves)), indicating that morning levels of *FT* may contribute to flowering time. L*er* and Ws-2 showed a similar negative correlation between *FT* and flowering between the LD22/22°C control and LD22/12°C treatments; however, the intercept was different from that of Col-0, perhaps indicating a

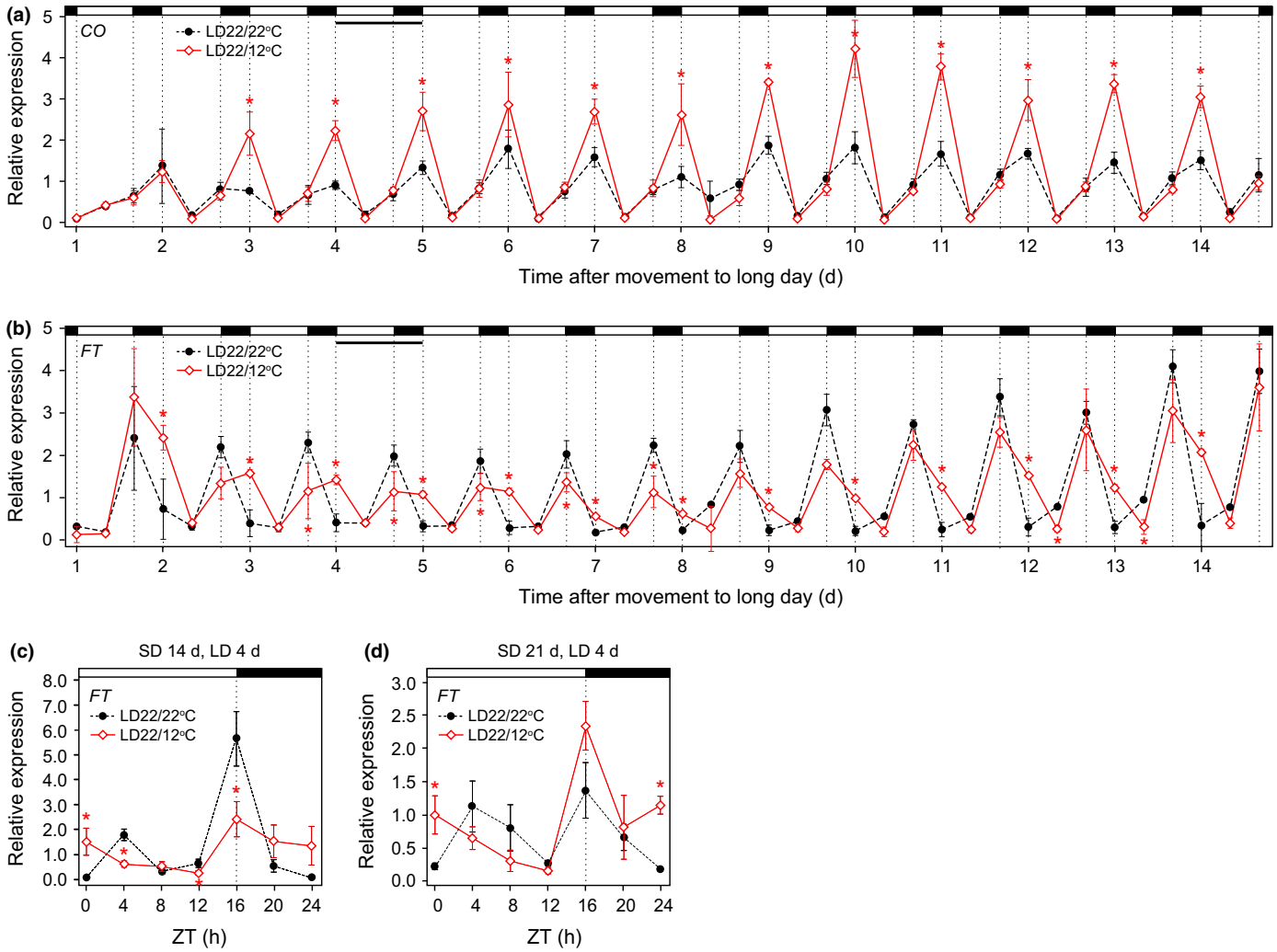

Fig. 4 Late night/dawn inductions of *CONSTANS* (*CO*) and *FLOWERING LOCUS T* (*FT*) transcript accumulation are conserved over 2 wk, dusk suppression declines as plants age in *Arabidopsis thaliana* (Columbia-0 (Col-0)). (a) *CO* and (b) *FT* transcript accumulation in LD22/22°C (long days with day : night temperatures = 22°C : 22°C) and LD22/12°C conditions for two consecutive weeks. Narrow, horizontal black bar indicates Day 4 of treatment. Seedlings were harvested at zeitgeber time (ZT, h after light onset) 0, ZT8 and ZT16. Seedlings were grown for 7 d in short days (SD) before being transferred to LD temperature treatments; harvest began on Day 1 of treatments. Data represent means ± SEM derived from five biological replicates. (c, d) *FT* transcript accumulation on Day 4 of LD temperature treatments in 18-d-old seedlings (c), and in 25-d-old (d) seedlings harvested at the same time. Seedlings were kept in SD until moved to the treatments. Data represent means ± SEM derived from at least three biological replicates. (a–d) Asterisks (*) indicate significance $P < 0.05$ and that 95% CI of difference between pair did not contain zero.

lower requirement of *FT* for flowering in these accessions (Fig. 5c, open circles). These data imply that alterations to *FT* levels in response to environmental changes can be predictive of flowering time across multiple conditions.

Induction of *CO* requires a decrease in temperature

Once we had determined that *FT* transcript accumulation levels were predictive of flowering across a range of conditions, we explored the mechanisms responsible for the transcript profile which we observed. As CO is a major activator of *FT*, we examined whether night-time induction of *CO* by cool temperatures showed time-dependent differences. Seedlings were exposed to cool temperatures (12°C) for 4-h durations at the beginning, middle or end of the night in LD. Cool temperatures induced *CO* regardless of when during the night they occurred, and *CO* declined again to control levels during the warm periods of the night (Fig. 6a–c). It appeared as if a change in temperature from 22°C to 12°C induced night-time *CO*, but it was possible that *CO* was simply high at 12°C. Would *CO* be induced in plants grown in constant 12°C (LD12/12°C) conditions? The pattern of *CO* for plants grown in SD22/22°C then moved to LD12/12°C for 4 d was slightly higher but similar to the LD22/22°C control and did not show strong night-time induction (Fig. 6d). These results suggest that a drop in temperature during the night results in immediate upregulation of *CO*, and that there is no obvious circadian-gating effect for *CO* induction at night.

By contrast, the response of *FT* showed time-dependent differences. Cool temperatures at the beginning of the night resulted in an *FT* transcript accumulation profile that was similar to the

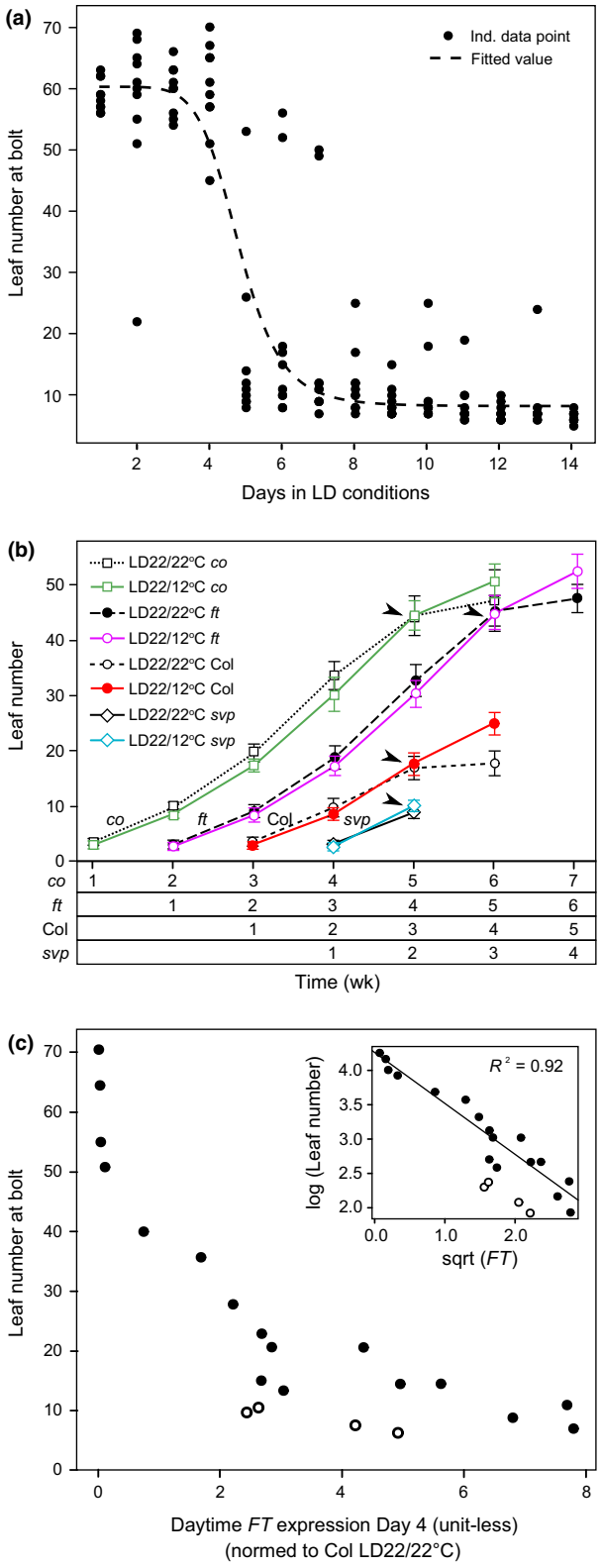

Fig. 5 Short-term exposure to long days rapidly induces flowering in *Arabidopsis thaliana* (Columbia-0 (Col-0)), and *FLOWERING LOCUS T* (*FT*) transcript accumulation correlates with final rosette leaf number across treatments and mutant strains within the Col-0 background. (a) Seven-day-old seedlings were transferred to LD22/22°C (long days with day : night temperatures = 22°C : 22°C) and LD22/12°C for 14 d. After each LD, beginning on Day 1, a subset of seedlings was transferred to short days (SD) and allowed to grow until bolts were observed (closed circles). A Hill function (dashed line) describing the final rosette leaf number (*LfNmbr*) at bolt as a function of days exposed to LD (*days*) was fitted to the flowering data : $LfNmbr = \{(Bmax(tc\hat{}n))/(tc\hat{}n + days\hat{}n)\} + Bmin$, where *Bmax* is highest fitted leaf number at bolt (= 52.17 leaves), *Bmin* is lowest fitted leaf number at bolt (= 8.23 leaves), *tc* is day at which transition occurs (= 4.86), *n* is modifier affecting abruptness of the transition (= 8.31) ($P < 0.0001$ for fit of all parameters). (b) Number of rosette leaves added each week for Col-0 wild-type plants, *co-101*, *ft-101* and *svp-31* in LD22/22°C and LD22/12°C conditions. Black arrows indicate when transition to bolting occurred. Error bars; means ± standard deviation. Overall temperature effect ($P < 0.001$), mean for difference between temperature treatments and 95% Confidence Interval (CI, 0.008, −0.134, 0.1497). The strains are plotted adjacent to the others for ease of comparison; however, all were planted at the same time. At time Week 1, seedlings were 7 d old and had not yet been exposed to LD temperature treatments. LMER was used to test for a delay in leaf production, followed by Satterthwaite approximation to generate *P*-values. Leaf numbers to the right of the arrow were excluded from the test as plants in the LD22/22°C treatment had begun to bolt and stopped rosette leaf production. Note that *svp-31* plants began to bolt within the first week of treatment, so do not show the same pattern as the other strains, Landsberg *erecta* (Ler), and Wassilewskija-2 (Ws-2) had patterns similar to *svp-31* and so are not shown. (c) Final rosette leaf number plotted against daytime *FT* transcript accumulation harvested from time points at zeitgeber time (ZT) 0, ZT8 and ZT16 across several photoperiod and temperature conditions, and strains within the Col-0 background (closed circles), and for Ler and Ws (open circles). Accumulated *FT* at time points ZT0, ZT8 and ZT16 (dawn, trough and dusk) was found by integrating under the curve and normalized to Col-0 harvested at ZT16 in LD22/22°C constant temperature conditions. Data were linearized by transforming as shown in inset for linear regression analysis (RMSE = 0.208 log(leaves)).

pattern observed in LD22/12°C conditions (Fig. 6e). Cool temperatures in the middle of the night resulted in a peak *FT* level at dusk (ZT16) that declined more slowly than the LD22/22°C control such that it was higher in the middle of the night (ZT20, Fig. 6f). In both cases, *FT* declined to control levels during the warm period at the end of the night (ZT24). When cool temperatures occurred at the end of the night, the *FT* profile was similar to that in the LD22/22°C conditions (Fig. 6g), suggesting that acute induction of *CO* at the beginning, but not the end, of the night is sufficient to induce night-time *FT* expression.

As previous work showed that *FT* levels are low throughout the day in 12-h-light, 12-h-dark cycles when grown from seed in constant 16°C temperatures (Blazquez *et al.*, 2003), we anticipated that *FT* levels would be suppressed when cool temperatures were applied for 4 d throughout the day (LD12/12°C). Unexpectedly, *FT* was higher throughout the day (Fig. 6h). We wondered whether the differences in *FT* levels between our study and the previous work might be caused by the growth conditions of younger seedlings, as we grew seedlings at constant SD22/22°C for a week before temperature treatments. Therefore, we grew seedlings in LD12/12°C conditions from seed and compared these to seedlings grown in LD22/22°C and in LD22/22°C for 7 d then switched to LD12/12°C for 4 d. Seedlings grown entirely in the LD12/12°C conditions had lower levels of *FT* and *CO*, and were delayed in development (Fig. S2), lacking true leaves by Day 12, whereas plants in the other treatments had two

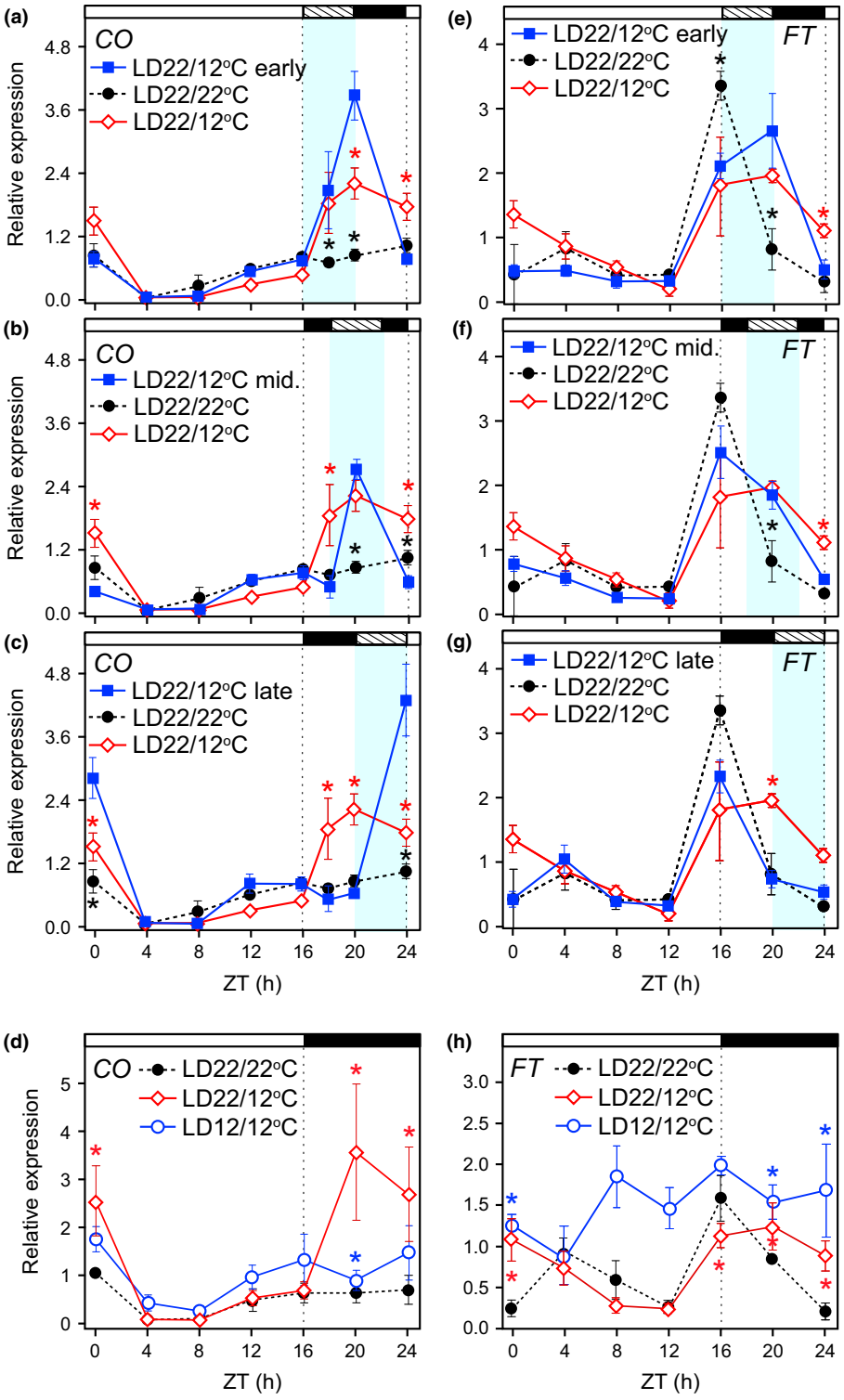

Fig. 6 Transcript accumulation of *CONSTANS* (*CO*) is induced regardless of when temperature drops occur at night in *Arabidopsis thaliana* (Columbia-0 (Col-0)); cool temperatures at the beginning of the night induce *FLOWERING LOCUS T* (*FT*). (a–c) *CO* transcript accumulation and (e–g) *FT* transcript accumulation in response to 4-h periods of 12°C at the beginning of the night from zeitgeber time (ZT) 16 to 20 (a, e *early*), middle of the night from ZT18 to 22 (b, f *mid.*), and end of the night from ZT20 to 24 (c, g *late*) in LD. (d) *CO* transcript accumulation and (h) *FT* transcript accumulation in LD with constant 12°C conditions (LD12/12°C). All panels show *CO* and *FT* transcript accumulation patterns in LD22/22°C and LD22/12°C conditions as references. Data represent means ± SEM derived from at least three biological replicates. Topmost white and black bars designate day and night, respectively. Hashed bars at the top and light blue areas on the graphs represent 4-h cool period (a–c, e–g). Asterisks (a–c, e–g) represent significance ($P < 0.05$) and 95% CI of difference between pair did not contain zero in statistical comparisons between the early, middle or late night treatments and the LD22/22°C (black) or LD22/12°C controls (red). Asterisks (*) (d, h) indicate significance $P < 0.05$ and that 95% CI of difference between pair did not contain zero in statistical comparisons made against the LD22/22°C control.

true leaves that had begun to emerge. However, plants grown from seed in LD12/12°C conditions appeared stressed, so we repeated this experiment using constant 17°C (LD17/17°C) conditions. Plants grown from seed in LD17/17°C conditions were smaller than those grown in LD22/22°C, and had lower overall levels of *FT* similar to the previously published results (Blazquez *et al.*, 2003). In the plants moved from LD22/22°C to LD17/17°C, daytime *FT* levels were higher especially in the morning (Fig. S3). Previous results also showed that lower day-time temperatures upregulate *FT*. When the daytime temperature was cooler (22°C) relative to a 28°C night, *FT* levels were *c.* 15 times higher than those in constant temperature conditions (Thines *et al.*, 2014), and *FT* was drastically induced during the 12°C phase under 22/12°C daily temperature cycles in constant lights

(Schwartz *et al.*, 2009). Taken together, our results suggest that plants respond to cooler temperatures differently depending on how and when (including which part of the day) they are applied, and some conditions can upregulate *FT*.

FBH genes regulate the cooler night-induced *CO* transcription

We next examined which genetic components might be involved in the lower-temperature-induced changes in *CO* and *FT* transcript levels. *CO* transcription is regulated by both positive and negative transcription factors (Golembeski *et al.*, 2014). CYCLING DOF FACTOR (CDF) family proteins repress *CO* during the daytime, whereas FLOWERING BHLH (FBH) family proteins induced *CO* especially during the night (Fornara *et al.*, 2009; Ito *et al.*, 2012). We examined whether FBHs are involved in the lower-temperature *CO* induction during night. The lower-temperature-induced accumulation of *CO* transcript was strongly attenuated in the *fbh* quadruple (*fbh-q*: *fbh1 fbh2 fbh3 fbh4*; Ito *et al.*, 2012) mutants when compared with the level of WT plants grown in LD22/12°C (Fig. 7a), indicating that FBH proteins play a role in the upregulation of *CO* during cooler nights. In the *fbh-q* mutant, night-time *CO* levels in LD22/12°C were still slightly higher than those of the LD22/22°C control, potentially as a result of incomplete silencing of *FBH1* and *FBH4* expression in this mutant (Ito *et al.*, 2012) or due to contribution of another unknown factor. As expected, expression of *FT* was lower overall in the *fbh-q* mutant compared to the control (Fig. 7b) and the *fbh-q* flowered later than WT under both conditions (Table 1). The patterns of *FT* were similar to those in WT, showing suppression at dusk and upregulation at the end of the night in LD22/12°C conditions (Fig. 7b), consistent with the higher levels of *CO* in these conditions.

As FBH function seemed higher under cooler night-time temperature conditions, we analyzed whether lower night temperature might alter the expression patterns of FBH protein. Using the *FBH1:FLAG-FBH1* line (Ito *et al.*, 2012), we found similar patterns of FBH1 protein accumulated throughout the day in both LD22/22°C and LD22/12°C (Fig. 7c), indicating that FBH1-mediated induction of *CO* in response to cool night-time temperatures may not be caused by changes in FBH1 protein abundance. Taken together, our results suggest that FBHs mediate cooler night-induced increases in *CO* transcription and this alters *FT* expression.

CO protein is higher under cool night-time temperatures

Post-translational regulation of CO plays an important role in the induction of *FT* (Song *et al.*, 2015). Under constant temperatures, CO protein is stable in the LD afternoon to induce *FT* (Valverde *et al.*, 2004), and is degraded at night through the activity of the COP1-SPA1/3/4 ubiquitin ligase complex (Laubinger *et al.*, 2006; Jang *et al.*, 2008; Liu *et al.*, 2011). We found that *FT* levels declined more slowly in cooler temperatures at night (Fig. 1b), and speculated that CO protein might become more stable under those conditions. We analyzed CO protein profiles in *CO:HA-CO* plants (Song *et al.*, 2012) grown in LD22/22°C or LD22/12°C conditions. We found that HA-CO protein driven by the native *CO* promoter was higher at night in LD22/12°C conditions compared to the LD22/22°C control (Fig. 8a,b). As *CO* mRNA levels are highly induced during the cooler night (Fig. 1a), it remained uncertain

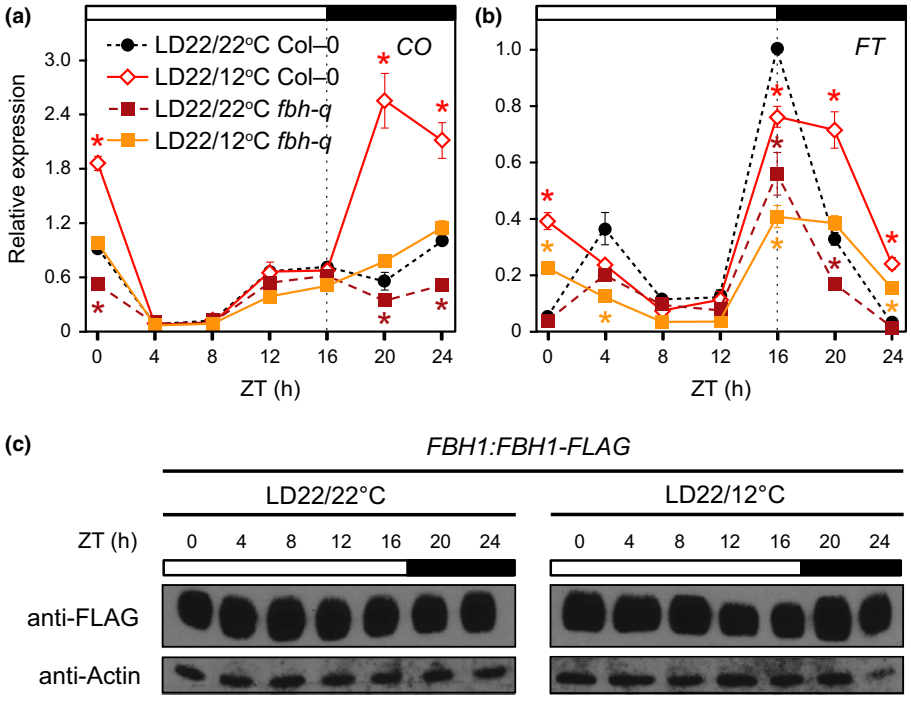

Fig. 7 The *FLOWERING BHLH* (*FBH*) family is involved in cool-night induction of *CONSTANS* (*CO*) and *FLOWERING LOCUS T* (*FT*) transcript accumulation in *Arabidopsis thaliana* (Columbia-0 (Col-0)). (a) *CO* and (b) *FT* gene transcript accumulation in *fbh*-quadruple (*fbh-q*) mutant line. Data, which are normalized to the maximum value in Col-0 wild-type control, represent means ± SEM derived from three biological replicates. Asterisks (*) represent significance $P < 0.05$ and that 95% CI of difference between pair did not contain zero in statistical comparisons made within a strain against the LD22/22°C treatment. (c) Accumulation patterns of FLAG-FBH1 protein in *FBH1:FLAG-FBH1* plants grown in LD22/22°C (long days with day : night temperatures = 22°C : 22°C) and LD22/12°C conditions. Actin serves as a loading control. ZT, zeitgeber time (h after light onset).

whether this was caused by transcriptional or post-transcriptional changes. We measured CO protein levels driven from a constitutively expressed *35S* promoter in *35S:3HA-CO* plants and found no obvious difference in CO protein profiles in the plants grown under LD22/12°C and LD22/22°C conditions (Fig. S4). This indicates that CO protein is not particularly stabilized under cooler night conditions, and suggests that CO protein levels become higher during cooler nights due mainly to increases in transcription rather than protein stability regulation.

Involvement of SVP in cool-night-time temperature induction of *FT* changes

We observed suppression of *FT* at dusk following cool nights (Fig. 4b), which may prevent precocious flowering in young plants. One possible candidate for *FT* suppression was SVP, which represses *FT* under constant 16°C LD conditions (Lee *et al.*, 2007). Are the preceding cooler nights sufficient to facilitate *FT* repression by SVP at dusk the following day? We found that the dusk peak of *FT* in *svp* mutants was similar between LD22/12°C conditions and the LD22/22°C control relative to WT (ZT16, Fig. 9a), whereas dawn *FT* levels still differed between the two conditions (ZT24, Fig. 9a), indicating that SVP is required to reduce the level of *FT* particularly around dusk. Consistent with a smaller difference in the amount of *FT* in the *svp* mutant between the two treatments, the *svp* mutants were delayed in flowering to a lesser degree than WT in LD22/12°C conditions relative to LD22/22°C (Table 1). These results imply that SVP represses *FT* around dusk under our conditions and that cooler night temperatures are sufficient to activate SVP function.

Cooler constant temperatures stabilize SVP protein (Lee *et al.*, 2013). Do cooler nights affect daily SVP protein profiles? SVP-6HA protein levels in *SVP:SVP-6HA* plants (Shen *et al.*, 2011) in LD22/12°C conditions remained higher after dusk and into the night-time than those in LD22/22°C (Fig. 9b,c), indicating that timing of SVP protein stability is altered when plants are exposed to lower night-time temperatures for part of the day. Binding of SVP to the *FT* promoter is affected when temperature alters the amounts of *FLM* splicing variants (Posé *et al.*, 2013). Under cool constant temperatures, the FLM-β variant is more prevalent, promoting DNA binding of SVP, whereas the FLM-δ variant, which lacks a functional MADS-box domain and inhibits DNA binding of SVP by forming a complex, is present in warm temperatures (Posé *et al.*, 2013). The increased ratio of FLM-β to FLM-δ was proposed to facilitate SVP-mediated flowering delays (Posé *et al.*, 2013); although a recent study indicated that *FLM-β* transcript levels correlate more strongly with flowering than those of *FLM-δ* (Lutz *et al.*, 2015). To analyze whether cooler night temperatures change the abundance of these splice variants, we measured the accumulated levels of *FLM-β* and *FLM-δ* under LD22/22°C, LD22/12°C, and LD12/12°C conditions. Consistent with previous results, *FLM-β* was higher under LD12/12°C than the LD22/22°C control (Fig. 9d); *FLM-β* in LD22/12°C did not significantly differ from the LD22/22°C control. However, the levels of *FLM-δ* in LD22/12°C, were lower during the day than in LD22/22°C, similar to that of LD12/12°C, causing a higher ratio of *FLM-β* to *FLM-δ* in both conditions (Fig. 9e). Together with the observation that SVP protein is slightly more stable around dusk, this result indicates that more SVP may form a heterodimer with functional FLM (FLM-β) to repress *FT* around dusk under LD22/12°C.

We observed dusk *FT* transcript levels to increase over 2 wk in LD22/12°C, becoming similar to those of LD22/22°C (Fig. 4b), and wondered whether this change might correlate with levels of *SVP* mRNA and/or protein over that

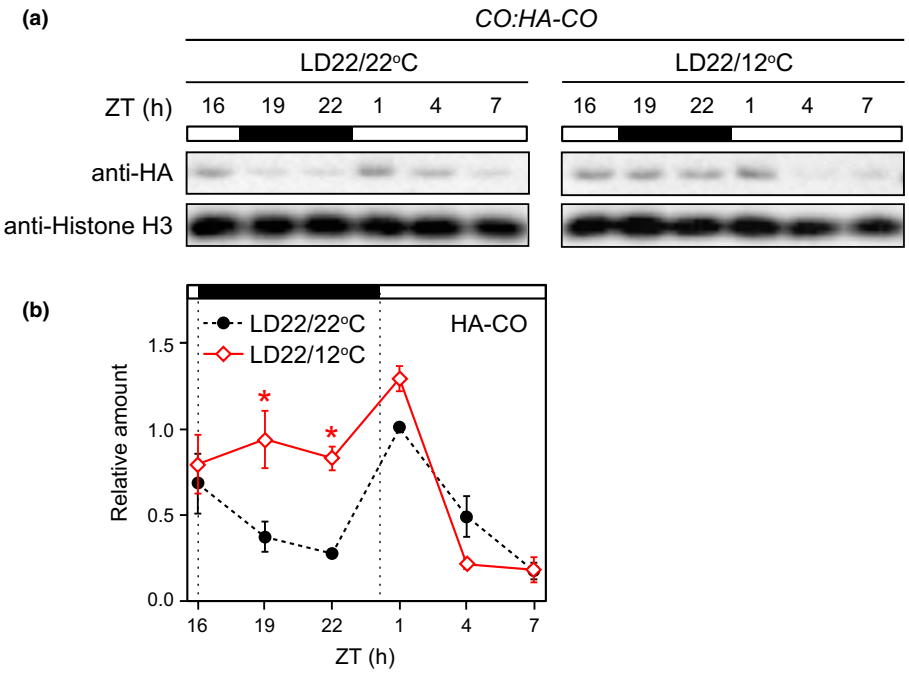

Fig. 8 CONSTANS (CO) protein is higher during cool nights in *Arabidopsis thaliana* (Columbia (Col-0)). (a, b) Accumulation patterns (a) and quantification (b) of HA-CO protein in *CO:HA-CO* plants grown in LD22/22°C (long days with day : night temperatures = 22°C : 22°C) and LD22/12°C conditions. Histone H3 serves as a loading control. (b) Data represent means ± SEM derived from three biological replicates. Asterisks (*) indicate significance $P < 0.5$ and that 95% CI of difference between pair did not contain zero in statistical comparisons made to the LD22/22°C control. ZT, zeitgeber time (h after light onset).

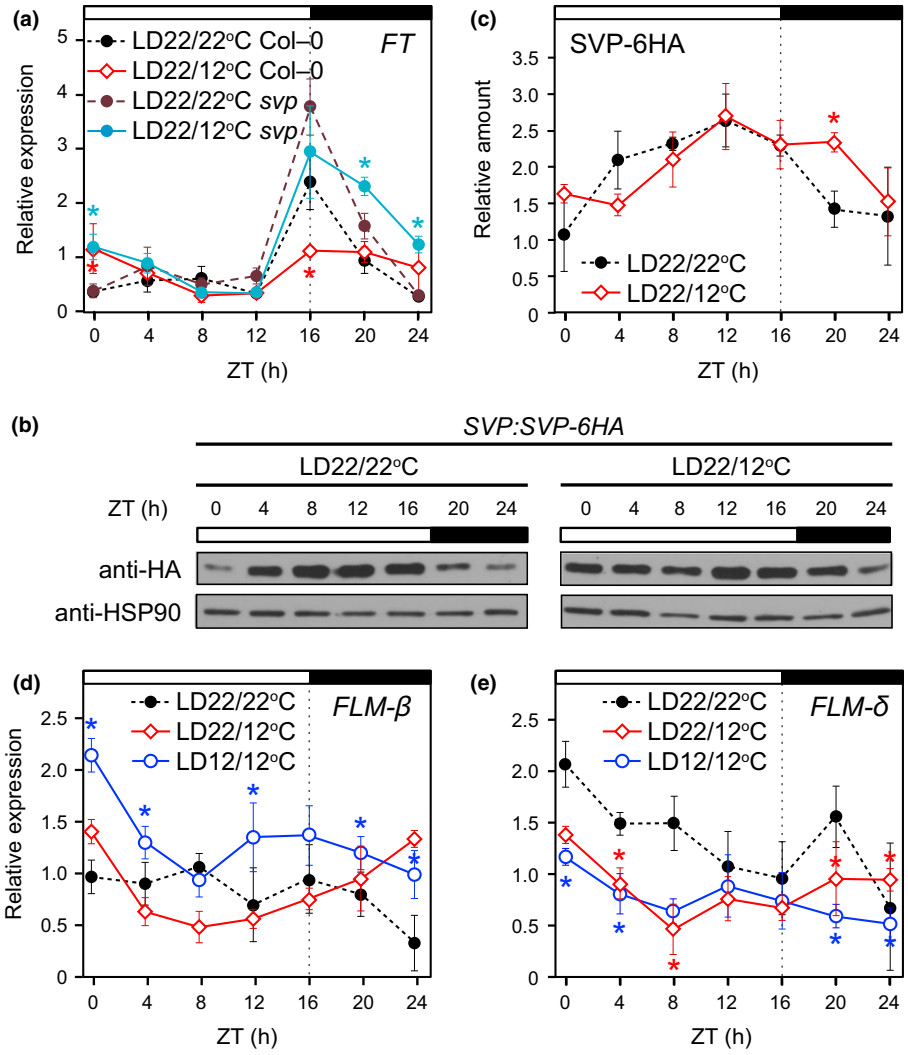

Fig. 9 *SHORT VEGETATIVE PHASE* (*SVP*) is involved in cool-night-induced dusk suppression of *FLOWERING LOCUS T* (*FT*) accumulation in *Arabidopsis thaliana* (Columbia-0 (Col-0)); suppression may be aided by a decrease in *FLOWERING LOCUS M* (*FLM*)-*δ* splice variant before dusk. (a) *FT* transcript accumulation in *svp* mutant lines. Accumulation patterns (b) and quantification (c) of SVP-6HA protein in *SVP:SVP-6HA* plants grown in LD22/22°C and LD22/12°C conditions. HEAT SHOCK PROTEIN 90 (HSP90) serves as a loading control. (d) *FLM-β* splice variant, which facilitates SVP binding, and (e) non DNA-binding *FLM-δ* transcript accumulation in wild-type plants grown in LD22/22°C (long days with day : night temperatures = 22°C : 22°C), LD22/12°C, and LD12/12°C conditions. Data represent means ± SEM derived from three biological replicates. (a, c–e) Statistical comparisons are made to the LD22/22°C control; asterisks (*) indicate $P < 0.5$ and that 95% CI of difference between pair did not contain zero. ZT, zeitgeber time (h after light onset).

period. *SVP* mRNA levels were similar between LD22/22°C and LD22/12°C treatments, although *SVP* transcript levels in LD22/12°C were slightly lower during Week 1 (Fig. 10a). SVP protein sampled before dusk (ZT13) did not differ significantly over the 2-wk period (Fig. 10b,c). We next analyzed *FLM-β* and *FLM-δ* transcript accumulation over this timeframe. *FLM-β* levels did not differ significantly between the two treatments (Fig. 10d). *FLM-δ* levels were lower in the LD22/12°C conditions relative to the LD22/22°C control (Fig. 10e). To more clearly assess the relationship between these transcripts over developmental time, we calculated the ratio of *FLM-β* relative to *FLM-δ* at each time point and then averaged across each day. The ratio of *FLM-β* to *FLM-δ* remained consistent over 2 wk in LD22/22°C (Fig. 10f). In LD22/12°C, however, the ratio of *FLM-β* to *FLM-δ* was higher than in LD22/22°C during Week 1, becoming similar to the LD22/22°C control during Week 2 (Fig. 10f). The decreased ratio of *FLM-β* relative to *FLM-δ* in LD22/12°C in Week 2 may facilitate *FT* accumulation by affecting DNA binding ability of SVP (Posé *et al.*, 2013; Lutz *et al.*, 2015).

Discussion

Diurnal temperature changes alter flowering time and *CO* and *FT* profiles

In order to understand flowering time regulation under natural conditions, we studied the effects of temperature alterations coincident with light changes, and demonstrated how two environmental cues can be integrated through the *FT* gene to influence flowering. A warm-day, cool-night temperature treatment results in upregulation of the *CO* gene and protein levels at night and an altered *FT* accumulation profile in long days (LDs). *FT* accumulates during the night and at dawn, but is suppressed at dusk through the action of SVP and FLM-β (Fig. S5). We found that *FT* levels explained much of the variance in final leaf number across several temperature and photoperiod treatments and across several mutant lines consistent with other studies (Fig. 5c and Kobayashi *et al.*, 1999; Blazquez *et al.*, 2003; Corbesier *et al.*, 2007; Salazar *et al.*, 2009; Krzymuski *et al.*, 2015; Seaton *et al.*, 2015). Therefore, although temperature influences

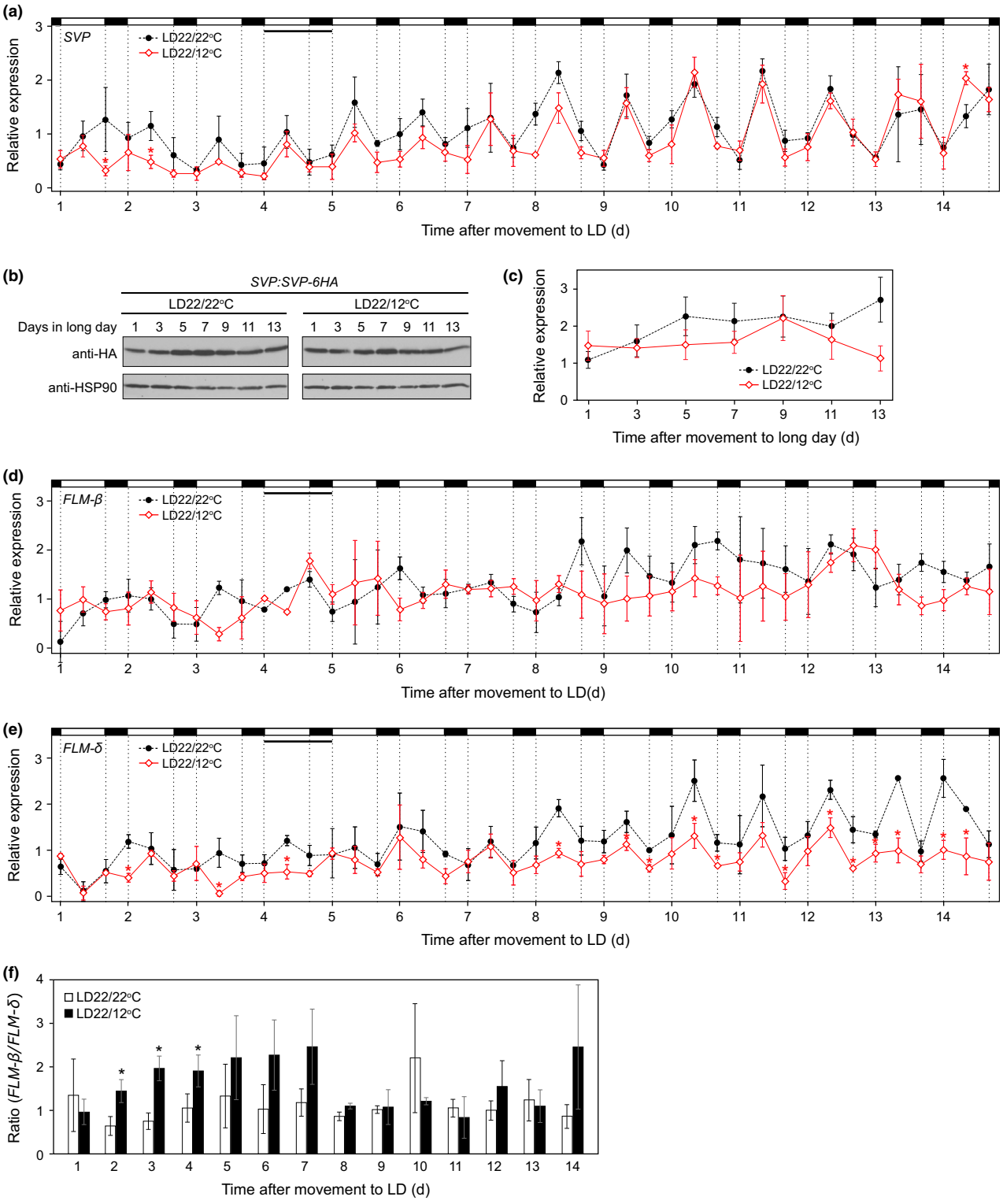

Fig. 10 Alleviation of dusk *FLOWERING LOCUS T* (*FT*) transcript suppression over 2 wk may be caused by the change in *FLOWERING LOCUS M* (*FLM*)-β and *FLM*-δ transcripts in *Arabidopsis thaliana* (Columbia-0 (Col-0)). (a) *SVP* transcript accumulation in wild-type plants grown in LD22/22°C (long days with day : night temperatures = 22°C : 22°C) and LD22/12°C conditions in wild-type plants for 14 d harvested at zeitgeber time (ZT) 0, ZT8 and ZT16 starting on Day 1 of treatment. Accumulation patterns (b) and quantification (c) of SVP-6HA protein in *SVP:SVP-6HA* plants grown in LD22/22°C and LD22/12°C conditions over the 2 wk, harvested every other day at ZT13 starting on Day 1. HSP90 serves as a loading control. (d) *FLM*-β and (e) *FLM*-δ splice variant transcript accumulation patterns and (f) the ratio of *FLM*-β to *FLM*-δ in wild-type plants grown in LD22/22°C and LD22/12°C for 14 d harvested at ZT0, ZT8 and ZT16 starting on Day 1 of treatment. The ratios (f) were calculated for each time point and then averaged over each day. In all cases plants were grown in short days (SD) for 1 wk before being transferred to treatments. Data represent means ± SEM derived from three biological replicates. (a, e, f) Asterisks (*) indicate $P < 0.05$ and that 95% CI of difference between pair did not contain zero.

myriad processes, the delay in flowering that we observed in LD22/12°C conditions is largely explained by the amount of *FT* produced. Interestingly, the strongest correlation was observed when ZT0, 8 and 16 were considered, and all three wild-type strains tested displayed both dusk suppression and dawn induction of *FT*, indicating that morning levels of *FT* may be important in the ability of plants to integrate environmental perturbations such as temperature changes.

Although this is beyond the scope of our current research, together with previous results (Schwartz *et al.*, 2009; Thines *et al.*, 2014), our results indicate that plants respond to drops in temperature differently than would be expected from studies of plants grown in constant temperature conditions (Blazquez *et al.*, 2003), and *FT* is frequently induced by lower temperatures that occur in conjunction with light (Figs 6h, S2c, S3c; Schwartz *et al.*, 2009; Thines *et al.*, 2014). The effects of cold treatment (4°C) are also more pronounced when plants are treated during the day than at night (Fowler *et al.*, 2005). Cooler temperatures occurring under light may be perceived as a signal of the changing seasons, such as a shift from summer to fall. Alterations of *FT* under these conditions may be a mechanism to accelerate flowering before unfavorable weather sets in. For instance, flowering was similarly accelerated between a 22°C-day/28°C-night treatment and a constant 28°C treatment, whereas flowering occurred later in a 28°C-day/22°C-night treatment (Thines *et al.*, 2014). Plants may have different responses to typical fluctuations (warmer day vs colder night) and changes that might associate with seasonal changes (warmer day vs colder day). If that is the case, these responses might be regulated differently for different purposes.

Roles of CO and FBH in temperature-cycle-mediated induction of *FT* at dawn

The degree of upregulation of *CO* at night is dependent upon the degree of temperature difference between day and night. The mechanism driving this phenomenon is unknown. The FBH protein family members are logical players, as we demonstrate that FBHs are required for strong night-time induction of *CO* and *FT*. However, amounts of FLAG-FBH1 did not differ between treatments. The levels of other FBH family members may vary. Alternatively, the phosphorylation states of FBHs could be altered. FBH1 is a putative substrate of several mitogen-activated protein kinases (MPKs) (Popescu *et al.*, 2009). In addition, FBH3 is phosphorylated by SNF1-RELATED PROTEIN KINASE 2 (SnRK2) in response to ABA signaling (Takahashi *et al.*, 2013), and is a putative substrate for CALMODULIN DOMAIN PROTEIN KINASE 9 (CPK9) (Yang *et al.*, 2013). *CPK9* expression is altered by ethylene, which, along with ABA, is involved in perception of numerous environmental stresses (Qiao *et al.*, 2009; Wang *et al.*, 2013; Nakashima *et al.*, 2014). Daily temperature changes may influence the amounts/activities of these kinases and, consequently, *FBH* phosphorylation states, and may be a mechanism by which plant stress modulates flowering time.

Age dependent suppression of *FT* expression at dusk by SVP

Although CO induces *FT* expression in response to warm day/ cool night conditions, this effect may be countered by suppression of *FT* by SVP at dusk in LD in < 3-wk-old plants. Our analysis indicated that SVP accounts for the *FT* repression at the end of the warmer day, and that this repression was regulated by the cooler night in a previous day. The ratio of *FLM-β* to *FLM-δ* transcript was higher during the daytime in LD22/12°C, perhaps increasing SVP binding of the *FT* promoter and decreasing *FT* accumulation at dusk, and SVP-6HA protein levels shift from daytime to around dusk and decline more slowly at night, which may also contribute to *FT* suppression.

Dusk suppression of *FT* was alleviated over 2 wk in the cool-night treatment, and we observed dusk suppression of *FT* in 11- and 18-d-old plants, not in 25-d-old plants. The cooler temperature treatments did not drastically alter the accumulation levels of *SVP* mRNA and protein over the 2-wk period, indicating that *SVP* levels likely do not cause the age-dependent alleviation of *FT* suppression. We observed the changes in both *FLM-β* and *FLM-δ* transcript levels over 2 wk. The ratio of daily *FLM-β*/*FLM-δ* levels in LD22/12°C conditions decreased after 1 wk in this treatment. A recent report indicated that the *FLM-β* level, more than the *FLM-β*/*FLM-δ* ratio, correlates with flowering time in the accessions examined (Lutz *et al.*, 2015). However, as Lutz *et al.* also stated, and because increasing the *FLM-δ* level without altering the *FLM-β* level drastically caused early flowering (Posé *et al.*, 2013), their ratio changes may partly account for the changes in *FT* repression by altering the DNA-binding-abilities of SVP under our conditions. It is possible that developmental-age-dependent suppression by *SVP/FLM* may serve to repress precocious flowering in younger plants.

Daytime and night-time temperatures differentially affect leaf number as well as flowering in other plant species (Yin & Kropff, 1996; Karsai *et al.*, 2008). Therefore, understanding the relationship between day and night-time temperatures in conjunction with day length is important. Our study highlights an interface between environmental conditions and the mechanisms controlling flowering that may become more important as local weather regimes are altered with climate change.

Acknowledgements

We thank Dr Hao Yu for *SVP:SVP-6HA* seeds, and Sheila Davis and Leema Singh for their assistance. This work was supported by funding from the National Science Foundation Graduate Research Fellowship Program to H.A.K-S., partly from Next-Generation BioGreen 21 Program (SSAC, PJ01117501 to Y.H.S. and PJ01117502 to T.I, Rural Development Administration, Republic of Korea), and from the National Institutes of Health (GM079712) and the University of Washington Royalty Research Fund to T.I.

Author contributions

H.A.K-S., S.-H.K. and T.I. planned and designed the research. H.A.K-S., X.T., J.L., Y.H.S. and S.I. performed experiments and analyzed data. H.A.K-S. and T.I. wrote the manuscript.

References

Bates D, Maechler M, Bolker B, Walker S. 2015. Fitting linear mixed-effects models using lme4. *Journal of Statistical Software* **67**: 1–48.

Blazquez M, Ahn J, Weigel D. 2003. A thermosensory pathway controlling flowering time in *Arabidopsis thaliana*. *Nature Genetics* **33**: 168–171.

Box GEP, Cox DR. 1964. An analysis of transformations. *Journal of the Royal Statistical Society* **26**: 211–252.

Carey VJ. 2015. gee: Generalized Estimation Equation Solver. *Version 4.13-19*Ported to R by Thomas Lumley (versions 3.13 and 4.4) and Brian Ripley (version 4.13). (Computer program) [WWW document] URL http://CRAN.R-project.org/package=gee [accessed 19 July 2015].

Corbesier L, Gadisseur I, Silvestre G, Jacqmard A, Bernier G. 1996. Design in *Arabidopsis thaliana* of a synchronous system of floral induction by one long day. *Plant Journal* **9**: 947–952.

Corbesier L, Vincent C, Jang S, Fornara F, Fan Q, Searle I, Giakountis A, Farrona S, Gissot L, Turnbull C *et al.* 2007. FT protein movement contributes to long-distance signaling in floral induction of *Arabidopsis thaliana*. *Science* **316**: 1030–1033.

Fornara F, Panigrahi KC, Gissot L, Sauerbrunn N, Rühl M, Jarillo JA, Coupland G. 2009. *Arabidopsis* DOF transcription factors act redundantly to reduce *CONSTANS* expression and are essential for a photoperiodic flowering response. *Developmental Cell* **17**: 75–86.

Fowler SG, Cook D, Thomashow MF. 2005. Low temperature induction of Arabidopsis *CBF1*, *2*, and *3* is gated by the circadian clock. *Plant Physiology* **137**: 961–968.

Golembeski GS, Kinmonth-Schultz HA, Song YH, Imaizumi T. 2014. Photoperiodic flowering regulation in *Arabidopsis thaliana*. In: Fornara F, ed. *Molecular genetics of floral transition and flower development*. London, UK: Academic Press/ Elsevier Science, 1–28.

Hazen SP, Schultz TF, Pruneda-Paz JL, Borevitz JO, Ecker JR, Kay SA. 2005. *LUX ARRHYTHMO* encodes a Myb domain protein essential for circadian rhythms. *Proceedings of the National Academy of Sciences, USA* **102**: 10 387–10 392.

Hong SM, Bahn SC, Lyu A, Jung HS, Ahn JH. 2010. Identification and testing of superior reference genes for a starting pool of transcript normalization in Arabidopsis. *Plant and Cell Physiology* **51**: 1694–1706.

Ito S, Song YH, Josephson-Day AR, Miller RJ, Breton G, Olmstead RG, Imaizumi T. 2012. FLOWERING BHLH transcriptional activators control expression of the photoperiodic flowering regulator *CONSTANS* in *Arabidopsis*. *Proceedings of the National Academy of Sciences, USA* **109**: 3582–3587.

Jang S, Marchal V, Panigrahi KCS, Wenkel S, Soppe W, Deng X-W, Valverde F, Coupland G. 2008. *Arabidopsis* COP1 shapes the temporal pattern of CO accumulation conferring a photoperiodic flowering response. *EMBO Journal* **27**: 1277–1288.

Jung J-H, Seo PJ, Park C-M. 2012. The E3 ubiquitin ligase HOS1 regulates *Arabidopsis* flowering by mediating CONSTANS degradation under cold stress. *Journal of Biological Chemistry* **287**: 43 277–43 287.

Karsai I, Szucs P, Koszegi B, Hayes PM, Casas A, Bedo Z, Veisz O. 2008. Effects of photo and thermo cycles on flowering time in barley: a genetical phenomics approach. *Journal of Experimental Botany* **59**: 2707–2715.

Kobayashi Y, Kaya H, Goto K, Iwabuchi M, Araki T. 1999. A pair of related genes with antagonistic roles in mediating flowering signals. *Science* **286**: 1960–1962.

Krzymuski M, Andrés F, Cagnola JI, Seonghoe J, Yanovsky M, Coupland G, Casal JJ. 2015. The dynamics of FLOWERING LOCUS T expression encodes long-day information. *Plant Journal* **83**: 952–961.

Laubinger S, Marchal V, Le Gourrierec J, Gentilhomme J, Wenkel S, Adrian J, Jang S, Kulajta C, Braun H, Coupland G *et al.* 2006. *Arabidopsis* SPA proteins regulate photoperiodic flowering and interact with the floral inducer CONSTANS to regulate its stability. *Development* **133**: 3213–3222.

Lazaro A, Valverde F, Pineiro M, Jarillo JA. 2012. The *Arabidopsis* E3 Ubiquitin Ligase HOS1 negatively regulates CONSTANS abundance in the photoperiodic control of flowering. *Plant Cell* **24**: 982–999.

Lee J, Oh M, Park H, Lee I. 2008. SOC1 translocated to the nucleus by interaction with AGL24 directly regulates *LEAFY*. *Plant Journal* **55**: 832–843.

Lee JH, Ryu H-S, Chung KS, Posé D, Kim S, Schmid M, Ahn JH. 2013. Regulation of temperature-responsive flowering by MADS-Box transcription factor repressors. *Science* **342**: 628–632.

Lee JH, Yoo SJ, Park SH, Hwang I, Lee JS, Ahn JH. 2007. Role of *SVP* in the control of flowering time by ambient temperature in *Arabidopsis*. *Genes & Development* **21**: 397–402.

Lenth R. 2015. *lsmeans: least-squares means. Version 2.21-1*. [WWW document] URL http://CRAN.R-project.org/package=lsmeans [accessed 9 August 2015].

Liu B, Zuo Z, Liu H, Liu X, Lin C. 2011. *Arabidopsis* cryptochrome 1 interacts with SPA1 to suppress COP1 activity in response to blue light. *Genes & Development* **25**: 1029–1034.

Lutz U, Posé D, Pfeifer M, Gundlach H, Hagmann J, Wang C, Weigel D, Mayer KFX, Schmid M, Schwechheimer C. 2015. Modulation of ambient temperature-dependent flowering in *Arabidopsis thaliana* by natural variation of *FLOWERING LOCUS M*. *PLoS Genetics* **11**: e1005588.

Mathieu J, Yant LJ, Mürdter F, Küttner F, Schmid M. 2009. Repression of flowering by the miR172 target SMZ. *PLoS Biology* **7**: e1000148.

McClung CR. 2006. Plant circadian rhythms. *Plant Cell* **18**: 792–803.

Michaels S, Amasino R. 1999. *FLOWERING LOCUS C* encodes a novel MADS domain protein that acts as a repressor of flowering. *Plant Cell* **11**: 949–956.

Myster J, Moe R. 1995. Effect of diurnal temperature alternations on plant morphology in some greenhouse crops – a mini review. *Scientia Horticulturae* **62**: 205–215.

Nakashima K, Yamaguchi-Shinozaki K, Shinozaki K. 2014. The transcriptional regulatory network in the drought response and its crosstalk in abiotic stress responses including drought, cold, and heat. *Frontiers in Plant Science* **5**: 1–7.

Nomoto Y, Kubozono S, Miyachi M, Yamashino T, Nakamichi N, Mizuno T. 2013. A circadian clock- and PIF4-mediated double coincidence mechanism is implicated in the thermosensitive photoperiodic control of plant architectures in *Arabidopsis thaliana*. *Plant and Cell Physiology* **54**: 643–643.

Osugi A, Izawa T. 2014. Critical gates in day-length recognition to control the photoperiodic flowering. In: Fornara F, ed. *Molecular genetics of floral transition and flower development*. London, UK: Academic Press/Elsevier Science, 103–130.

Parent B, Turc O, Gibon Y, Stitt M, Tardieu F. 2010. Modelling temperature-compensated physiological rates, based on the co-ordination of responses to temperature of developmental processes. *Journal of Experimental Botany* **61**: 2057–2069.

Popescu SC, Popescu GV, Bachan S, Zhang Z, Gerstein M, Snyder M, Dinesh-Kumar SP. 2009. MAPK target networks in *Arabidopsis thaliana* revealed using functional protein microarrays. *Genes & Development* **23**: 80–92.

Posé D, Verhage L, Ott F, Yant L, Mathieu J, Angenent GC, Immink RGH, Schmid M. 2013. Temperature-dependent regulation of flowering by antagonistic FLM variants. *Nature* **503**: 414–417.

Prasch CM, Sonnewald U. 2015. Signaling events in plants: stress factors in combination change the picture. *Environmental and Experimental Botany* **114**: 4–14.

Qiao H, Chang KN, Yazaki J, Ecker JR. 2009. Interplay between ethylene, ETP1/ETP2 F-box proteins, and degradation of EIN2 triggers ethylene responses in *Arabidopsis*. *Genes & Development* **23**: 512–521.

R Core Team. 2015. *R: a language and environment for statistical computing*. [WWW document] URL https://www.R-project.org [accessed 19 July 2015]

Salazar JD, Saithong T, Brown PE, Foreman J, Locke JC, Halliday KJ, Carre IA, Rand DA, Millar AJ. 2009. Prediction of photoperiodic regulators from quantitative gene circuit models. *Cell* **139**: 1170–1179.

Satterthwaite FE. 1946. An approximate distribution of estimates of variance components. *Biometrics Bulletin* **2**: 110–114.

Sawa M, Nusinow DA, Kay SA, Imaizumi T. 2007. FKF1 and GIGANTEA complex formation is required for day-length measurement in *Arabidopsis*. *Science* **318**: 261–265.

Schwartz C, Balasubramanian S, Warthmann N, Michael TP, Lempe J, Sureshkumar S, Kobayashi Y, Maloof JN, Borevitz JO, Chory J *et al.* 2009. Cis-regulatory changes at *FLOWERING LOCUS T* mediate natural variation in flowering responses of *Arabidopsis thaliana*. *Genetics* **183**: 723–732.

Seaton DD, Smith RW, Song YH, MacGregor DR, Stewart K, Steel G, Foreman J, Penfield S, Imaizumi T, Millar AJ *et al.* 2015. Linked circadian outputs control elongation growth and flowering in response to photoperiod and temperature. *Molecular Systems Biology* **11**: 1–19.

Shen L, Kang YGG, Liu L, Yu H. 2011. The J-Domain protein J3 mediates the integration of flowering signals in *Arabidopsis*. *Plant Cell* **23**: 499–514.

Shrestha R, Gomez-Ariza J, Brambilla V, Fornara F. 2014. Molecular control of seasonal flowering in rice, Arabidopsis and temperate cereals. *Annals of Botany* **114**: 1445–1458.

Song YH, Estrada DA, Johnson RS, Kim SK, Lee SY, MacCoss MJ, Imaizumi T. 2014. Distinct roles of FKF1, GIGANTEA, and ZEITLUPE proteins in the regulation of CONSTANS stability in *Arabidopsis* photoperiodic flowering. *Proceedings of the National Academy of Sciences, USA* **111**: 17672–17677.

Song YH, Ito S, Imaizumi T. 2013. Flowering time regulation: photoperiod- and temperature-sensing in leaves. *Trends in Plant Science* **18**: 575–583.

Song Y-H, Shim J-S, Kinmonth-Schultz HA, Imaizumi T. 2015. Photoperiodic flowering: time measurement mechanisms in leaves. *Annual Review of Plant Biology* **66**: 441–464.

Song YH, Smith RW, To BJ, Millar AJ, Imaizumi T. 2012. FKF1 conveys timing information for CONSTANS stabilization in photoperiodic flowering. *Science* **336**: 1045–1049.

Suárez-López P, Wheatley K, Robson F, Onouchi H, Valverde F, Coupland G. 2001. *CONSTANS* mediates between the circadian clock and the control of flowering in *Arabidopsis*. *Nature* **410**: 1116–1120.

Takada S, Goto K. 2003. TERMINAL FLOWER2, an Arabidopsis homolog of HETEROCHROMATIN PROTEIN1, counteracts the activation of *FLOWERING LOCUS T* by CONSTANS in the vascular tissues of leaves to regulate flowering time. *Plant Cell* **15**: 2856–2865.

Takahashi Y, Ebisu Y, Kinoshita T, Doi M, Okuma E, Murata Y, Shimazaki K. 2013. bHLH transcription factors that facilitate K^+ uptake during stomatal opening are repressed by abscisic acid through phosphorylation. *Science Signaling* **6**: ra48.

Tan S-T, Dai C, Liu H-T, Xue H-W. 2013. *Arabidopsis* casein kinase1 proteins CK1.3 and CK1.4 phosphorylate cryptochrome2 to regulate blue light signaling. *Plant Cell* **25**: 2618–2632.

Thines BC, Youn Y, Duarte MI, Harmon FG. 2014. The time of day effects of warm temperature on flowering time involve PIF4 and PIF5. *Journal of Experimental Botany* **65**: 1141–1151.

Valverde F, Mouradov A, Soppe W, Ravenscroft D, Samach A, Coupland G. 2004. Photoreceptor regulation of CONSTANS protein in photoperiodic flowering. *Science* **303**: 1003–1006.

Wang F, Cui X, Sun Y, Dong C-H. 2013. Ethylene signaling and regulation in plant growth and stress responses. *Plant Cell Reports* **32**: 1099–1109.

Yang Z, Guo G, Zhang M, Liu C, Hu Q, Lam H, Cheng H, Xue Y, Li J, Li N. 2013. Stable isotope metabolic labeling-based quantitative phosphoproteomic analysis of Arabidopsis mutants reveals ethylene- regulated time-dependent phosphoproteins and putative substrates of Constitutive Triple Response 1 Kinase. *Molecular and Cellular Proteomics* **12**: 3559–3582.

Yanovsky MJ, Kay SA. 2002. Molecular basis of seasonal time measurement in *Arabidopsis*. *Nature* **419**: 308–312.

Yant L, Mathieu J, Schmid M. 2009. Just say no: floral repressors help *Arabidopsis* bide the time. *Current Opinion in Plant Biology* **12**: 580–586.

Yin X, Kropff M. 1996. The effect of temperature on leaf appearance in rice. *Annals of Botany* 77: 215–221.

Zuo Z, Liu H, Liu B, Liu X, Lin C. 2011. Blue light-dependent interaction of CRY2 with SPA1 regulates COP1 activity and floral initiation in Arabidopsis. *Current Biology* **21**: 841–847.

Supporting Information

Additional supporting information may be found in the online version of this article.

Fig. S1 Transcript accumulation levels of *ISOPENTENYL PYROPHOSPHATE/DIMETHYLALLYL PYROPHOSPHATE ISOMERASE* (*IPP2*) remain unaltered through the day across three temperature treatments.

Fig. S2 Growth is delayed and *FLOWERING LOCUS T* (*FT*) level is depressed in seedlings exposed to constant 12°C temperatures.

Fig. S3 Growth is delayed and *FLOWERING LOCUS T* (*FT*) level is reduced in seedlings exposed to constant 17°C temperatures.

Fig. S4 CONSTANS (CO) protein stabilization is not altered during cool nights.

Fig. S5 Proposed mechanism for the transcriptional regulation of *FLOWERING LOCUS T* (*FT*) in long days with temperature changes.

Please note: Wiley Blackwell are not responsible for the content or functionality of any supporting information supplied by the authors. Any queries (other than missing material) should be directed to the *New Phytologist* Central Office.

New Phytologist

***New Phytologist* Supporting Information**

Article title: **Cool nighttime temperatures induce the expression of *CONSTANS* and *FLOWERING LOCUS T* to regulate flowering in *Arabidopsis***

Authors: Hannah A. Kinmonth-Schultz, Xinran Tong, Jae Lee, Young Hun Song, Shogo Ito, Soo-Hyung Kim and Takato Imaizumi

Article acceptance date: 06 January 2016

The following Supporting Information is available for this article:

Fig. S1 Transcript accumulation levels of *ISOPENTENYL PYROPHOSPHATE/DIMETHYLALLYL PYROPHOSPHATE ISOMERASE* (*IPP2*) remain unaltered over the day across three temperature treatments.

Fig. S2 Growth is delayed and *FLOWERING LOCUS T* (*FT*) level is depressed in seedlings exposed to constant 12°C temperatures.

Fig. S3 Growth is delayed and *FLOWERING LOCUS T* (*FT*) level is reduced in seedlings exposed to constant 17°C temperatures.

Fig. S4 CONSTANS (CO) protein stabilization is not altered during the cool night.

Fig. S5 Proposed mechanism for the transcriptional regulation of *FLOWERING LOCUS T* (*FT*) in long days with temperature changes.

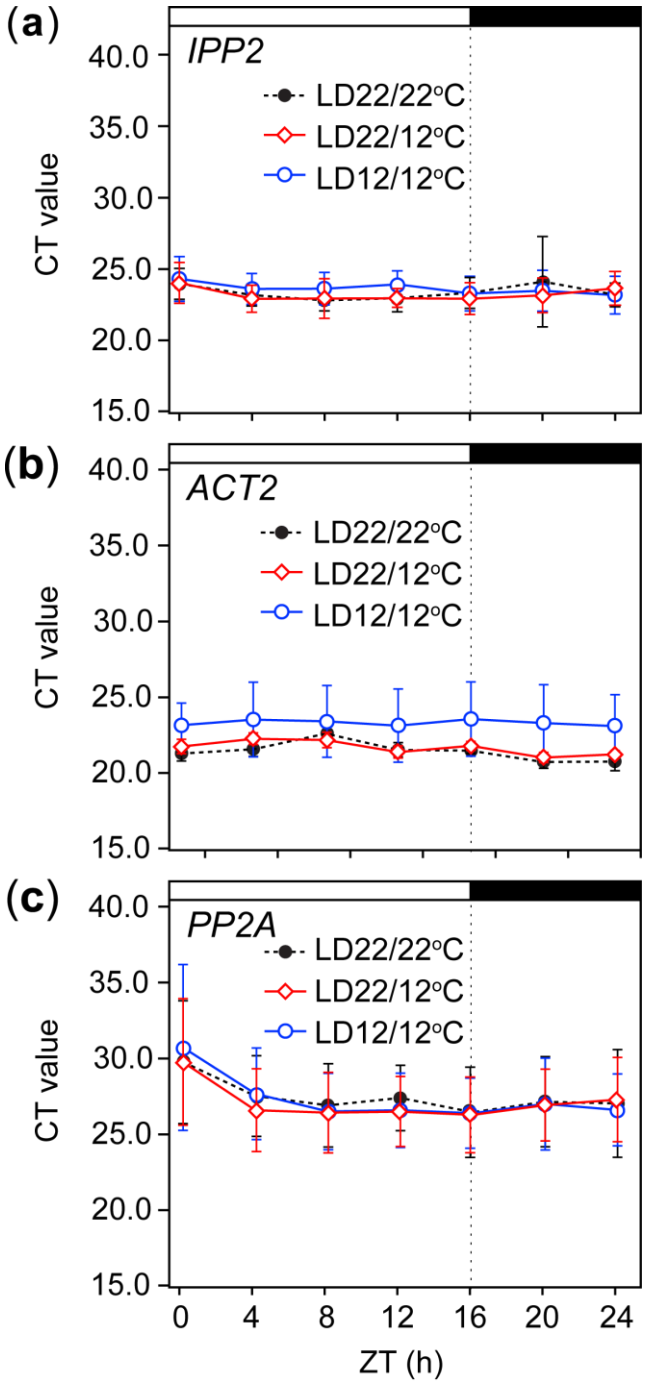

Fig. S1 Transcript accumulation levels of *ISOPENTENYL PYROPHOSPHATE/DIMETHYLALLYL PYROPHOSPHATE ISOMERASE* (*IPP2*) remain unaltered over the day across three temperature treatments. (a, b, c) Transcript accumulation patterns of *IPP2*, *ACTIN 2* (*ACT2*), and *SERINE/THREONINE PROTEIN PHOSPHATASE 2A* (*PP2A*) in 11-d-old Col-0 plants in LD22/22°C (long days with day : night temperatures = 22°C : 22°C), LD22/12°C, and LD12/12°C conditions. Seedlings were grown for 7 d in short-day conditions before being transferred to LD temperature treatments. Data represent means ± SEM derived from three biological replicates. Topmost white and black bars designate day and night, respectively. Dotted vertical lines are times of lights off.

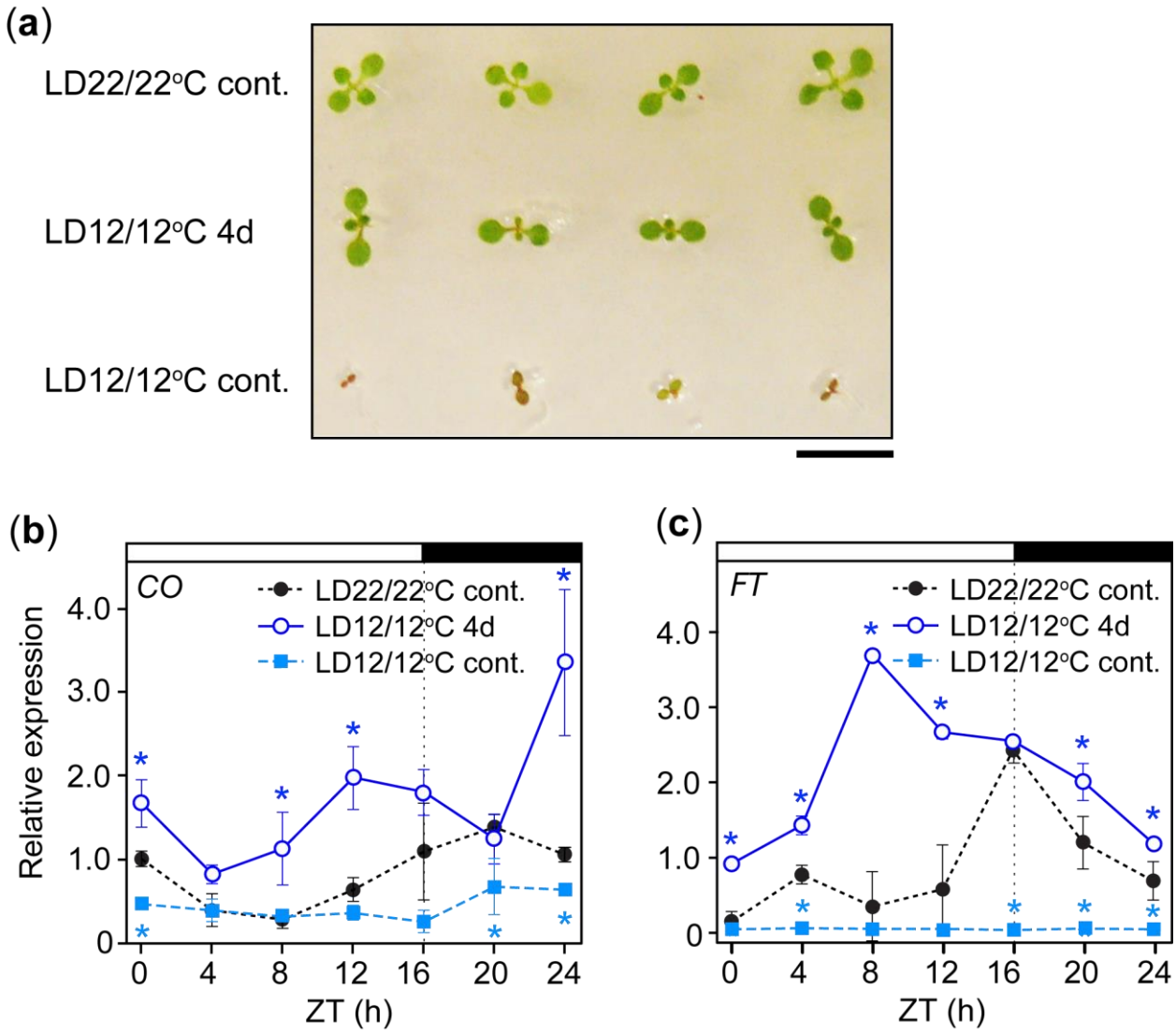

Fig. S2 Growth is delayed and *FLOWERING LOCUS T* (*FT*) level is depressed in seedlings exposed to constant 12°C temperatures. Transcript accumulation patterns of *FT* and *CONSTANS* (*CO*) are very low in seedlings exposed to cool (12°C) temperatures from seed. (a) Visual comparison of individuals grown from seed in LD22/22°C (long days with day : night temperatures = 22°C : 22°C) and LD12/12°C conditions (cont.), or in LD22/22°C for 7 d then transferred to LD12/12°C for 4 d (4d). Photos taken when seedlings were 12 d old. Scale bar, 1 cm. (b, c) Transcript accumulation patterns of *FT* and *CO* in these conditions. Harvest began at dawn when seedlings were 11 d old. Data represent means ± SEM derived from three biological replicates. Asterisks indicate $P<0.05$ and 95% CI of difference between pair did not contain zero in statistical comparisons made to the LD22/22°C control. Topmost white and black bars designate day and night, respectively. Dotted vertical lines are times of lights off.

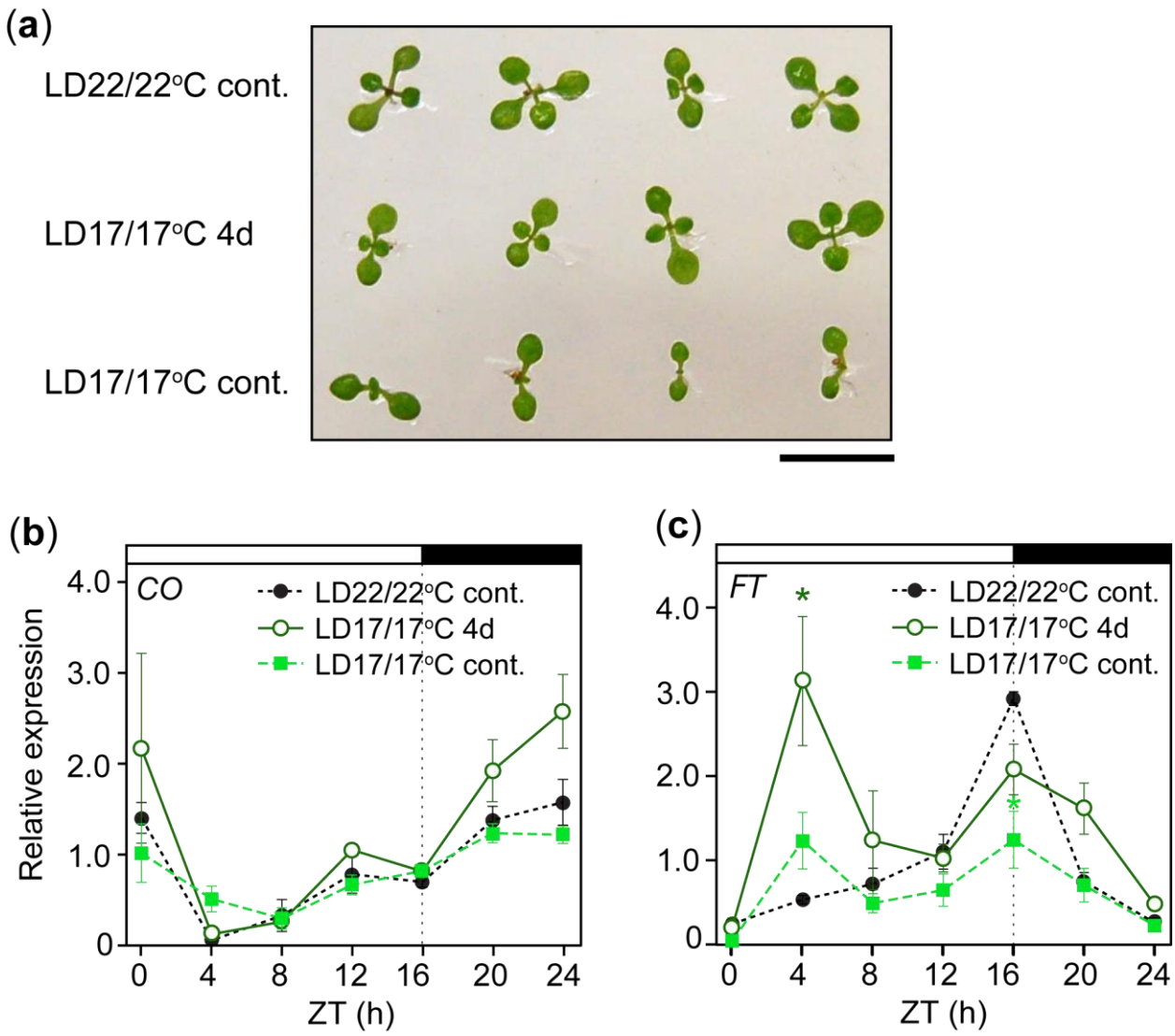

Fig. S3 Growth is delayed and *FLOWERING LOCUS T* (*FT*) level is reduced in seedlings exposed to constant 17°C temperatures. Transcript accumulation patterns of *FT* is reduced in seedlings exposed to cool (17°C) temperatures from seed. (a) Visual comparison of individuals grown from seed in LD22/22°C (long days with day : night temperatures = 22°C : 22°C) and LD17/17°C conditions (cont.), or in LD22/22°C for 7 d then transferred to LD17/17°C for 4 d (4d). Photos taken when seedlings were 12 days old. Scale bar, 1 cm. (b, c) Transcript accumulation patterns of *FT* and *CONSTANS* (*CO*) in these conditions. Harvest began at dawn when seedlings were 11 d old. Data represent means ± SEM derived from three biological replicates. Asterisks indicate $P<0.05$ and 95% CI of difference between pair did not contain zero in statistical comparisons made to the LD22/22°C control. Topmost white and black bars designate day and night, respectively. Dotted vertical lines are times of lights off.

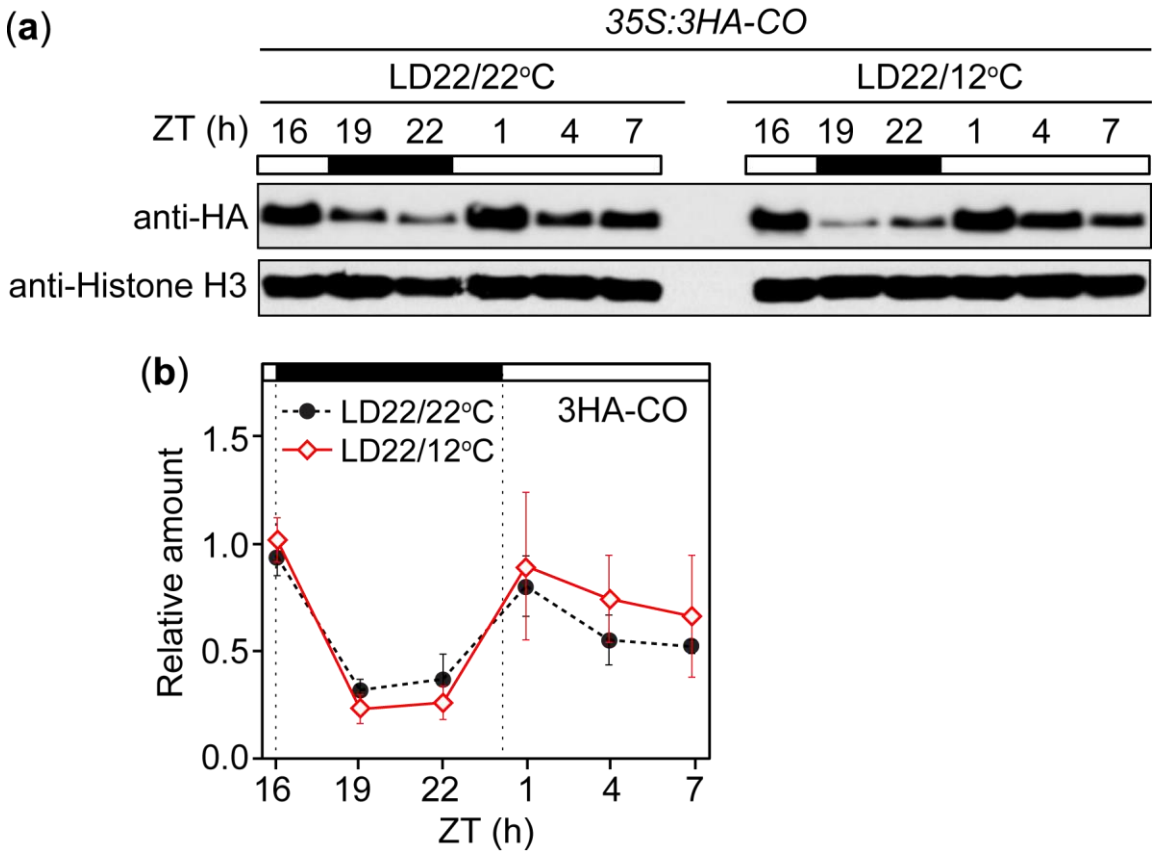

Fig. S4 CONSTANS (CO) protein stabilization is not altered during the cool night. (a, b) Accumulation patterns (a) and quantification (b) of 3HA-CO proteins in *35S:HA-CO* plants grown in LD22/22°C (long days with day : night temperatures = 22°C : 22°C) and LD22/12°C conditions. Histone H3 serves as a loading control. Data represent means ± SEM derived from three biological replicates. Topmost white and black bars designate day and night, respectively. Dotted vertical lines are times of lights off.

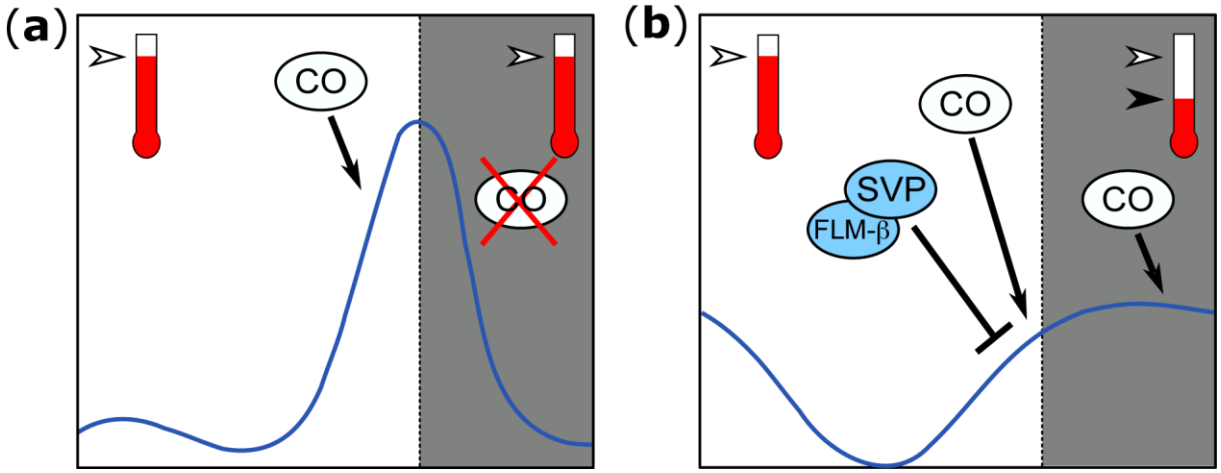

Fig. S5 Proposed mechanism for the transcriptional regulation of *FLOWERING LOCUS T* (*FT*) in long days with temperature changes. (a) As previously shown, CONSTANS (CO) protein is stabilized in the afternoon of long days and induces *FT* transcript accumulation. (b) When warm/cool temperature cycles are imposed over long days, SHORT VEGITATIVE PHASE (SVP) in conjunction with FLOWERING LOCUS M (FLM)-β suppresses *FT* at the end of the light period, whereas more CO protein is present at night (gray box) and induces *FT* transcript accumulation.

Chapter 4

Temperature and developmental regulation of *FT* can replace thermal time to predict flowering in *Arabidopsis*

As submitted for publication

Temperature and developmental regulation of *FT* can replace thermal time to predict flowering in *Arabidopsis*

Running title: Replacing thermal time with *FT* accumulation and regulation

Hannah A. Kinmonth-Schultz[1,a], Melissa J. MacEwen[1,b], Takato Imaizumi[1,c], Soo-Hyung Kim[3,d]

[1]Department of Biology, University of Washington, Seattle, WA 98195-1800, USA

[2]SynthSys and School of Biological Sciences, University of Edinburgh, Edinburgh, UK

[3]School of Environmental and Forest Sciences, University of Washington, Seattle, WA 98195-2100, USA

[a]hkinmonth@uwalumni.com

[b]mjsmacewen@gmail.com

[c]takato@uw.edu

[d]Author for correspondence: Soo-Hyung Kim

Tel: +1-206-616-4971

Email: soohkim@uw.edu

Date of Submission: 30 July 2016

Number of Tables: 3

Number of Figures: 7

Color figures in print and online: 2, Figures 1 and 3

Color figures online only: 2, Figures 1 and 3

Supplementary Data:

Number of Tables: 1

Number of Figures: 5

Word Count (Intro to Acknowledgements, max 6500): 6396

Highlight

Photoperiod, temperature, and developmental regulation of the expression of florigen, *FT*, can replace thermal time to accurately predict phenological changes in plant growth and flowering in *Arabidopsis*.

Abstract

Thermal time (degrees Celsius per unit time) is widely used to relate temperature to plant development without incorporating underlying mechanisms. Temperature influences *FLOWERING LOCUS T* (*FT*), a photoperiodic flowering regulator. *FT* correlates with flowering and is produced in the leaves. Temperature influences the leaf production rate. We hypothesized: 1) temperature regulation of *FT*, accumulated with leaf growth, is a component of thermal time, and 2) incorporating mechanistic temperature regulation of *FT* could improve model predictions in fluctuating temperatures. We assessed *FT* production in differently aged leaves and modified an existing model (Framework Model) that incorporates photoperiodic regulation of *FT* and temperature influence on leaf growth for *Arabidopsis*. We developed a *FT*-Temperature-Response module, then linked *FT* to leaf growth, eliminating the model's use of thermal time. We demonstrate that *FT* is mainly produced in the first few true leaves. Our approach could better explain flowering in fluctuating temperatures than thermal time in long days. We clarify that the final leaf number is influenced by day length and temperature through *FT*, while the leaf production affects whole-plant *FT* and flowering time. Our model provides a base on which to build a phenology model that reflects climate-responsive flowering mechanisms across developmental age.

Key words: *Arabidopsis thaliana*, flowering time, *FT*, mathematical model, temperature fluctuation, thermal time, crop simulation model

Introduction

Ambient temperature during the growing season correlates with the timing of plants' transition from vegetative to reproductive growth. Germination, organ emergence, leaf expansion, photosynthesis, and respiration display similar relationships (Parent *et al.*, 2010). These observations led to the concept of thermal time (Lehenbauer, 1914), which asserts that temperature-driven metabolic rates govern development (Zavalloni et al., 2006), and to models that use the empirical relationship between temperature and development to predict plant response (e.g., Chuine, 2000; Jones *et al.*, 2003).

Thermal time describes an aggregate response in which thermal units accumulate more quickly, and reach a predetermined threshold sooner to predict reproduction during warm growing seasons than cool ones. This implies: 1) that all processes respond similarly to temperature and 2) that fluctuating and constant temperatures have the same influence on most processes if the average temperature remains stable. However, processes do not always slow under cool temperatures. The up-regulation of cryo-protective genes (Jaglo-Ottosen *et al.*, 1998) and the

circadian clock's buffering to temperature changes (Rensing & Ruoff, 2002) are just two examples.

Predicting plant response to future climates remains imprecise when considering temperature alone or in conjunction with CO_2 (Asseng *et al.*, 2013; Makowski *et al.*, 2015). The effect of non-stressing temperatures varies considerably between cultivars (Karsai *et al.*, 2013). Plant response to constant temperatures may not accurately reflect response to daily temperature fluctuations (Yin & Kropff, 1996; Kim *et al.*, 2007; Karsai *et al.*, 2008), and potentially requires empirical calibrations for new cultivars, climates, or locations (Piper *et al.*, 1996). As most plant models incorporate some variant of thermal time (Ritchie & Otter, 1985; Jamieson *et al.*, 1998a,b; Wilczek *et al.*, 2009; He *et al.*, 2012; Kumudini *et al.*, 2014), these models may fail to capture aspects of temperature response. Incorporating the molecular mechanisms of cultivar response would likely improve models' capacity to illustrate and predict system responses.

A more mechanistic approach decomposes the influence of temperature into separate plant processes (Welch *et al.*, 2003; Kim *et al.*, 2012; Zheng *et al.*, 2013; Brown *et al.*, 2013). One strategy notes that the number of leaves produced before the reproductive transition decreases as the environmental signal's strength increases (Jamieson *et al.*, 1998b). For wheat, prolonged cold, vernalizing temperatures followed by longer days reduces the leaf number (Brown *et al.*, 2013) and affects the transition's timing. Modeling accumulation of *VRN3*, a key flowering gene, in response to vernalization and day length cues, and as a function of thermal time, can accurately predict final leaf number and timing of flowering (Brown *et al.*, 2013).

VRN3 is an orthologue of *FLOWERING LOCUS T* (*FT*) in *Arabidopsis thaliana* (Yan *et al.*, 2006), a key integrator of environmental cues in the photoperiodic flowering pathway (Song *et al.*, 2015). *FT* levels correlate strongly with the leaf number at which flowering occurs (Krzymuski *et al.*, 2015; Seaton *et al.*, 2015; Kinmonth-Schultz *et al.*, 2016). Day length, vernalization, and ambient temperature changes regulate *FT* expression (Blazquez *et al.*, 2003; Amasino, 2010; Song *et al.*, 2015). Under constant and fluctuating temperature conditions, cool temperatures suppress *FT* through the interaction of SHORT VETIGATIVE PHASE (SVP) and the FLOWERING LOCUS M (FLM)-β splice variant on the *FT* regulatory regions (Blazquez *et al.*, 2003; Posé *et al.*, 2013; Lee *et al.*, 2013; Lutz *et al.*, 2015; Kinmonth-Schultz *et al.*, 2016). However, temperature fluctuations from warm to cool induce *FT* through induction of *CONSTANS* (*CO*), a chief transcriptional activator of *FT* (Schwartz *et al.*, 2009; Kinmonth-Schultz *et al.*, 2016). As there is no simple correlation between temperature decrease and reduction of *FT* levels, the linear accumulation of flowering gene products with thermal time may not adequately capture the influence of temperature on final leaf number, especially in fluctuating temperatures.

The FT protein is expressed in the leaves and moves to the shoot apex where it complexes with FD protein to induce the transition from leaf to floral production (Abe *et al.*, 2005; Corbesier *et al.*, 2007). The amount of FT protein perceived at the shoot apex should depend on the amount of leaf tissue present; leaf production and growth is strongly temperature dependent (Parent *et al.*, 2010). We propose that a key factor underlying the accumulation of thermal time is the accumulation of gene product (e.g., FT) or the increasing capacity for transcript production as a plant grows. *FT* is likely not expressed consistently in all leaves or developmental stages. *pFT:GUS* is expressed in the tips of true leaves in young plants, but can range across the leaf in older plants (Takada & Goto, 2003). Further, whole-plant transcript levels increase from age five

to 15 days relative to an internal control, indicating a changing capacity for *FT* expression with age (Mathieu *et al.*, 2009). The concept of measuring *FT* transcript levels in leaves of different ages has neither been executed nor incorporated into flowering models, but it could improve our understanding of how day length and temperature impact *FT* to control flowering across developmental age.

FT simulated as a function of day length and accumulated as a function of thermal time can accurately predict flowering in some conditions (Chew *et al.*, 2012). To investigate whether a model could incorporate direct temperature regulation of *FT* production and *FT* accumulation with leaf growth instead of incorporating thermal time, we measured *FT* expression in leaves and plants of different ages and utilized an existing model (Framework Model; FM) capable of simulating plant growth and flowering times in response to temperature (Chew *et al.*, 2014). We replaced the thermal time module, used to predict flowering times, with an *FT*-temperature-response (FTR) module that incorporates known mechanisms of *FT* suppression in response to cool temperatures (Lee *et al.*, 2007, 2013; Posé *et al.*, 2013), as well as induction of *FT* after a change to cool temperatures (Kinmonth-Schultz *et al.*, 2016). These adjustments allowed us to mimic *FT* profile change under more natural warm-day, cool-night conditions. We then linked *FT* to leaf production and tested the model's capacity to predict flowering under a range of temperature conditions. We demonstrate that *FT* is expressed primarily in the first few true leaves produced, and that our new model can explain the flowering response mechanistically while improving model predictions in long day fluctuating temperature environments. Our model also highlights uncertainties in climate's influence on flowering as plants age.

Materials and Methods

Description of the Framework Model 1

The Framework Model (FM-1, Figure S1, Section S1, Chew *et al.*, 2014) is the only existing model that combines plant growth and mechanistic flowering regulation for *Arabidopsis*. It is a useful tool to decompose thermal time into its underlying components. The timing of flowering (Days to bolt, DtB), is determined by two modules. The Photoperiodism module describes circadian clock and day length control of *FT* (Salazar *et al.*, 2009). *FT* transcript accumulation is input into the Phenology module (Wilczek *et al.*, 2009; Chew *et al.*, 2012) to modify the rate of thermal time accumulation to produce Modified Photothermal Units (MPTUs). The number of days taken to reach the MPTU threshold determines the stopping point of vegetative growth and onset of flowering. Vegetative growth is determined by the rate of photosynthesis and carbon partitioning between roots and shoots (Carbon Dynamic module, Rasse & Tocquin, 2006), and includes the rate of organ production as a function of temperature, including production of individual leaves (Functional-Structural Plant module).

Modifications to FM-1 for use in this study

In order to utilize FM-1, we made the following alterations, shown (Figure 1, Sections S2-5):

1) As *FT* is expressed in the leaves, we made *FT* a function of the amount of leaf tissue present. Rather than running the model in two phases (Figure S1), we called the Phenology module at each time step.

    a) We considered the output of the Phenology module as representative of *FT* produced per unit leaf tissue. We, then, calculated the *FT* produced by each leaf based on the amount of leaf tissue present and on leaf and plant age, and summed this across all leaves on the plant (Figure 1, section S2). We used leaf area to determine the amount of leaf tissue present (section S3).

    b) FM-1 was unable to simulate a decrease in leaf area with decreasing temperatures in fluctuating temperature conditions, although we observed this behavior. To address this, we adjusted the specific leaf area (SLA, m^2g^{-1}) to decline with decreasing temperature (Pyl et al. 2012) and removed the temperature sensitivity of maintenance respiration which affected the carbon available for growth (section S4).

2) We removed the accumulation of MPTUs for flowering entirely, and instead set the model to cease leaf production and transition to reproduction when *FT* accumulated to a pre-determined threshold (section S3). The influence of temperature was incorporated through direct modulation of *FT* gene, and through leaf development, which affected the rate of whole-plant *FT* accumulation. We retained the day length influence on *FT* gene expression. To find the threshold level of *FT*, we utilized the model to determine the amount of *FT* expressed by two ecotypes of *Arabidopsis thaliana*, Columbia (Col-0) and Landsberg *erecta* (L*er*) that had reached 15 and eight true leaves, respectively, under the following conditions: one week in short days at 22 °C, then growth in long days at 22 °C. These leaf numbers were the observed average across several replicates in that condition (Kinmonth-Schultz et al. 2016). We assumed *FT* accumulates over time, as several consecutive days of *FT* induction are needed for flowering to occur (Corbesier *et al.*, 2007; Krzymuski *et al.*, 2015; Kinmonth-Schultz *et al.*, 2016).

3) To determine the capacity of each leaf to express *FT*, we measured the copy number of *FT* transcripts in leaves and plants of several different ages. We found that *FT* increases as leaves age, then declines as they begin to senesce. Later-emerging leaves lose the capacity to express *FT*. We simulated this using a beta function (Yin *et al.*, 1995, section S2), in which peak *FT* expression depends on the total number of leaves the plant has produced. This ensures that the first few true leaves that emerge contribute the most *FT*. As only transcript abundance, not the area of the leaf expressing *FT*, is altered by temperature in young seedlings (Kinmonth-Schultz *et al.*, 2016), we assumed this relationship did not differ with climate.

4) We incorporated the temperature influence on *FT* gene expression by adding an *FT*-Temperature-Response (FTR) module. Simulated SVP activity increases with decreasing temperature, causing suppression of *FT*, consistent with previously observed results (Blazquez *et al.*, 2003; Lee *et al.*, 2013). *CO* increases after a drop in temperature, causing induction of *FT* (Kinmonth-Schultz *et al.*, 2016). “SVP activity” encompasses

the combined activity of SVP and FLM-β, which facilitates SVP binding of the *FT* regulatory regions (Posé *et al.*, 2013), as the levels of both increase similarly with cooling temperatures (Posé *et al.*, 2013; Lee *et al.*, 2013; Kinmonth-Schultz *et al.*, 2016). To accurately simulate *FT* behavior in warm-day, cool-night conditions, in which *FT* is suppressed at dusk, but higher at dawn than the constant, warm temperature control (Kinmonth-Schultz *et al.*, 2016), we assumed that CO and SVP (in conjunction with FLM-β) act competitively on the *FT* regulatory regions. FM-1 already describes the relationship between *FT* and CO protein in the Photoperiod module (Chew *et al.*, 2014). We adjusted this interaction by modifying the Michaelis-Menten function for competitive inhibition (Segal, 1976) of *FT* transcription in FM-1, such that the induction of *FT* by CO is influenced by the SVP activity (equation [S5.3]). To simulate the suppression of *FT* at dusk, we caused the decay rate for SVP activity to be slightly lower than its production, such that it remained higher at 22 °C after a 12 °C night than in constant warm temperatures (Figure S2).

5) Dropping the temperature from night to day caused a strong induction of *FT* corresponding to higher levels of *CO* (Kinmonth-Schultz *et al.*, 2016). To ensure the relative dosages of *FT* were similar to that observed, we caused *CO* to decline over time if the temperatures remained stable after dropping initially (Figure S3, equation [S5.4). We also adjusted the rate at which CO protein is produced when temperature fluctuations occur during the day (section S5) to avoid overly strong daytime induction of *FT* in these conditions, as the model likely fails to capture some daytime regulation of *CO* and *FT*.

Model parameterization and testing

We parameterized the equations describing gene expression or protein activity (equations [S5.1] to [S5.5] using transcript accumulation data collected in long days (Kinmonth-Schultz *et al.*, 2016). We had 13 replicates performed using Col-0 that contained two temperature treatments: 22 °C days, and 22 °C or 12 °C nights. One experiment was conducted over 48 hours and included 17 °C nights as well. We assessed treatment effects in this experiment using ANOVA, including or excluding *day* as a covariate (i.e. a 24-hour period). We found no difference between models, indicating no difference in gene expression across the two days in that experiment. We considered each day separately, providing six additional replicates that contained three temperature treatments (19 total replicates). The original parameterization of the Photoperiodism module used by FM-1 normalized the gene expression levels of *FT* and its upstream promoter *CO* across experiments by peak *CO* expression in short-day conditions (Salazar *et al.*, 2009). This was done because the peak in short days is broader than that in long days and likely to provide consistent results despite different sampling times. Here, most experiments did not include short day conditions. Instead, we normalized by the average *CO* levels at dusk and in the middle of the night (ZT16 and 20).

These 19 replicates were randomly assigned to either a training or testing dataset, with nine being used to parameterize induction of *CO* by cool temperatures. We found that the amplitudes of *CO* expression were consistent across replicates and among temperature treatments, while *FT* varied considerably, although the relative differences remained intact. To parameterize *FT*, as well as the equations that affected *FT* levels, we used only those training datasets that included

the three nighttime temperatures. Our aim was to simulate overall changes in *FT* levels, and therefore assessed model fit by comparing the simulated and actual areas under the curve of *FT* expression. The area under the curve for the data and modeled outputs was calculated using the Trapz function in R Statistical Computing software (v3.1.1; R Core Team, 2015). We tested the model's capacity to predict *FT* gene expression patterns in data from warm-day, cool-night conditions not used for training, as well as in conditions in which the temperature drops during the day causing *FT* levels to accumulate higher than the control (Kinmonth-Schultz *et al.*, 2016). We then assessed the model's ability to predict flowering in these conditions. To do so, we calculated a new MPTU threshold for our conditions using Col-0 and L*er* grown in long days at 22 °C using the equation from Wilczek *et al.* 2009.

Plant growth conditions

Arabidopsis thaliana, Columbia-0 (Col-0), plants for flowering analysis and tissue specific gene expression were grown on soil as previously described (Kinmonth-Schultz et al. 2016). Plants were grown at increasing light intensities with decreasing day-length to control for differences in the amount of light received. We considered a plant as having bolted when 1 mm of the stem was visible below the cauline leaves. We controlled for variation in germination times and plant size by beginning all experiments with plants of similar size and by grouping plants by size and leaf number, such that each group contained one representative of each treatment. To reduce positional effects, these groups were also positioned in the growth chambers such that all plants in a group experienced similar chamber conditions.

Determining absolute copy number of FT transcript across leaves of different ages

Plants were grown on soil for two-, four-, or six weeks in short days, then moved to short or long days for three days. They were harvested at dusk (ZT16) on the third day. Leaves of individual plants were dissected and immediately frozen in liquid nitrogen. The leaves of the same relative age of at least six plants were pooled. We isolated RNA and ensured similar starting material. Transcript amount was determined by RT-qPCR. We excluded any samples for which we were unable to get 2µg total RNA. These samples primarily came from older leaves. Absolute copy number was determined using a known concentration of *FT* fragment spanning base pairs 1900 to 2135 from the transcriptional start site in exons three and four. The fragment was amplified by PCR and concentrated using ethanol purification. Copy number was determined using the following equation: Copy number = C x Na/M as previously described (Fernández-Aparicio *et al.*, 2013). Where Copy number = number of molecules/µl, C = concentration of the purified cDNA (g/µl), M = molecular weight of the purified region, Na = Avogadro's number = 6.023 x 10^{23} molecules/mole. This sample was diluted using an eight-step, 1:10 serial dilution. The serial dilution was run along with the plant sample during qPCR, and used to develop a linear relationship between copy number and cycle number. Replicates were normalized by the replicate average.

Tissue specific expression of FT *(GUS analysis*)

We grew *pFT:GUS* plants (Takada & Goto, 2003) under short day conditions on soil for two, three, four, or six weeks before moving them to short or long days for three days. We harvested all plants at 16 hours after dawn on the third long day, at peak *FT* in long days (Corbesier *et al.*, 2007). Immediately after harvest, we incubated the plants in chilled 90% acetone for 45 minutes before immersing them in GUS staining solution, then vacuum infiltrating them three times for ten minutes, as previously described (Sieburth and Meyerowitz, 1997). We kept the plants in the staining solution for 48 hours, and in the clearing solution for 48 hours. All plants were photographed under a dissecting scope (Leica DMC 2900). We compiled the images using GIMP. To quantify *FT* expression, we traced any locations stained blue, so they could be detected by ImageJ software, then quantified the total area of *FT* expression relative to the area of each leaf. At least three individuals were analyzed for each treatment.

Statistical analysis

Statistical analysis on flowering time was done using Generalized Estimating Equation (Carey, 2015) in R Statistical Computing Software (v3.1.1; R Core Team, 2015), which accounts for missing values and the relatedness of individuals within a group. The Robust Z and standard error, were used to calculate *P*-values and 95% confidence intervals (C.I.) of the difference between the means. Treatment effects were considered significant when the *P*-values fell below 0.05 and the C.I. did not contain zero.

Results

Assessing original model, FM-1, in different temperature conditions

FM-1 uses thermal time (i.e., MPTU) to predict flowering time. We assessed the mechanistic and developmental influences of temperature on flowering by replacing thermal time with mechanistic regulation of *FT* and whole-plant accumulation of *FT* with leaf tissue. To determine our approach's efficacy, we first assessed the behavior of the original model. We focused on long days as *FT* is upregulated in these conditions (Kobayashi *et al.*, 1999). In FM-1 and previous iterations of the Phenology module, the best prediction for plants grown outdoors occurred when nighttime temperatures were given lesser influence than daytime temperatures (Wilczek et al. 2009, and Chew et al. 2012). As cool nighttime temperatures altered the expression of *FT*, and as *FT* predicts flowering across a range of conditions (Kinmonth-Schultz *et al.* 2016), we wondered how well FM-1 could capture flowering times in warm day, cool night temperature conditions. If the MPTUs in FM-1 adequately captured the influence of temperature, then the MPTU threshold should be similar across treatments, with negligible differences between predicted and observed days to bolt for all three temperature regimes.

The model accurately captured Col-0 and L*er* grown in 22 °C nighttime temperatures and showed an expected delay in days to bolt for both 17 °C and 12 °C nighttime temperature conditions; however, the predicted number days to bolt was lower than observed (Figure 2a, Table 1). The trend for plants exposed to constant 12 °C was similar, with the model predicting flowering 6.63 days earlier than observed. FM-1 predicted fewer leaves in all cool temperature treatments than in the constant, 22 °C control (Figure 2b, Table 1), contrary to the higher leaf

number observed previously (Blazquez *et al.*, 2003; Kinmonth-Schultz *et al.*, 2016). Leaf production was slower in these conditions, so the simulation did not reach the observed final leaf number before reaching the MPTU target. FM-1 reduced the influence of nighttime temperature relative to daytime temperature (Wilczek *et al.*, 2009; Chew *et al.*, 2012), but we found that equalizing the influence of nighttime and daytime temperatures reduced the trend across temperature treatments and improved the fit (Figure 2c, Table 1).

Incorporating FT as a function of leaf production: leaf FT expression capacity changes with leaf and plant age

We proposed that whole-plant *FT* levels increase with leaf production, and could influence thermal time. To quantify this influence, we developed a method to understand each leaf's capacity to express *FT*. We quantified the *FT* transcript accumulation in individual leaves of Col-0 plants aged two, four, and six weeks. In younger plants, *FT* increased as leaves aged and then declined (Figure 3a-c). For plants with around 20 leaves, *FT* levels were low in all new leaves produced, even those of comparable area to leaves that expressed *FT* in younger plants. This pattern is consistent with a shift away from perception of environmental stimuli and induction of flowering through *FT* as plants age. Although not explicitly tested, the spatial expression profile of *FT* expression seems to increase with leaf age (Takada & Goto, 2003). To confirm the pattern of transcript accumulation, we analyzed the individual leaves of *pFT:GUS* plants aged two to four weeks, measuring the percent surface area showing staining. Within individual plants, GUS staining increased across the leaf surface with leaf age before declining in older leaves, consistent with *FT* transcript accumulation patterns (Figure 3e, S4a-b). Short day plants displayed no staining (Figure S4c). We also sampled the newly emerging leaves and then every fourth leaf of *pFT:GUS* plants having 20 to 25 leaves. Consistent with the mRNA data, newly emerged leaves showed minimal or no staining (Figure S4d). Interestingly, leaves corresponding to peak levels of *FT* transcript showed staining only at the edges. This pattern seems independent of shading by younger leaves, as these leaves remain mostly uncovered. This data suggests leaves accumulate *FT* transcript as they age, but levels decline as leaves begin to senesce. Spatially, leaves produced early can express *FT* across their surface, while *FT* is restricted to the edges of leaves produced later. Using this information, we could quantify the influence *FT* plays in flowering over developmental time. We used a beta function to simulate the proportion of *FT* per unit tissue of each leaf (Yin *et al.*, 1995) based on relative leaf age (*r*) (section S2).

Assessing the FT-Temperature-Response module: Cool-temperature induction of SVP and CO activity explains FT behavior in fluctuating temperatures

Plants sometimes respond to temperature fluctuations differently than their growth in constant temperatures predicts (Yin & Kropff, 1996; Karsai *et al.*, 2013). As temperature fluctuations can suppress and induce *FT*, adding this behavior to the model could improve its predictive capacity under fluctuating temperatures. We created an *FT*-Temperature-Response (FTR) module. Under long days, in 22 °C days and 12 °C nights, *FT* was suppressed at dusk compared to 22 °C constant-temperature conditions, likely through the action of SVP and the FLM-β splice variant (Lee *et al.*, 2007; Posé *et al.*, 2013; Kinmonth-Schultz *et al.*, 2016). Higher dawn levels of *FT*

coincide with higher levels of *CO* mRNA and protein in cool nights (Kinmonth-Schultz *et al.*, 2016). When the temperature drops from night to day, *FT* is induced above that of constant temperature controls, and remains induced after four days (Thines *et al.*, 2014; Kinmonth-Schultz *et al.*, 2016).

Our modifications, termed FM-1.5, captured *FT* patterns observed in warm-day, cool-night conditions (Figure 4a), while *FT* was low in constant, cool conditions consistent with previous observations (Blazquez *et al.*, 2003, data not shown). To determine the amount of *FT* accumulated daily, we compared the area under the curve of simulated and observed *FT* levels. The levels fell well within the variation range of 10 data sets not used in parameterization for constant temperature and 12 °C cool-night conditions (Figure 4b). The observed *FT* levels in 17 °C cool-night conditions were higher than predicted. They showed nighttime induction, but minimal suppression at dusk (Kinmonth-Schultz *et al.*, 2016), indicating a potential nonlinear relationship between *SVP* activity and temperature. However, as daytime levels of *FT* correlate more strongly with flowering time (Kinmonth-Schultz *et al.*, 2016), the lower levels of simulated *FT* in 17 °C and 12 °C cool night conditions relative to the control allowed us to address the relationship between *FT* and leaf tissue production. For conditions where a temperature drop occurs during the day, our model captured the strong induction of *FT* and the relative differences between treatments (Figure 4c-d), ensuring the *FT* dosage was similar to that observed.

Flowering time predictions under dynamic temperature conditions

We adjusted the model so that temperature fluctuations influenced *FT* expression directly and linked *FT* to leaf production. We removed the FM-1 model's thermal time component, then assessed the capacity of FM-1.5 to predict flowering under different temperature conditions. We parameterized the gene expression components using data from plants grown in long day, warm-day, cool-night conditions. We tested the capacity of the model to predict flowering in these conditions. FM-1.5 better predicted both rosette leaf number at bolt and days to bolt (Figure 5a, Table 1) for both strains. The leaf production over time was also similar to that observed, although the model accumulated leaves more quickly early on as it uses a linear rather than exponential relationship (Figure 5b). Col-0 was slightly overestimated for days to bolt (bias = 2.67), indicating potential bias for the rate of leaf production with temperature; however, the overall model behavior across temperature treatments for both leaf number and days to bolt improved (Table 1).

Leaves grow and emerge more slowly under cool temperatures. The simulated delay in cool-night flowering conditions could be due to slower *FT* accumulation. To determine how leaf tissue amount and *FT* expression contributed to these results, we set the temperature perceived by *FT* to be constant at 22 °C, but maintained the link to and the temperature influence on leaf production. We expected that under cool nighttime temperatures, more *FT* produced would cause flowering at a leaf number similar to the constant temperature control. Plants would still flower later due to slower whole-plant *FT* accumulation through leaf production. FM-1.5 predicted a similar leaf number to the control for the 17 °C-night treatment (Table 2). It predicted a lower leaf number for the 12 °C-night treatment, because the leaves that are present continue to produce *FT*, such that it accumulates over time and causes the plants to reach the threshold sooner. As expected, cool-night treatments flowered later.

In some instances, a temperature drop strongly induces *FT* (Schwartz *et al.*, 2009; Kinmonth-Schultz *et al.*, 2016). We wondered whether such an induction could affect flowering times, or if slower whole-plant accumulation of *FT* with slower leaf growth would delay flowering. Previously, we observed *FT* induction in one-week-old plants when the temperature dropped from 22 °C to 12 °C or 17 °C just after dawn in long days. In these conditions, *FT* was strongly upregulated both in 12 °C and 17 °C (Figure 4c, Kinmonth-Schultz et al. 2016). We asked whether the model could predict flowering after exposure to 12 °C in long days for two, four, or six days. Plants were grown in short-days for two-weeks before temperature treatment to ensure they had two to three true leaves and were competent to flower. After treatment, plants were moved to warm, long-day conditions. Control plants were moved directly to warm, long-day conditions at two weeks. Warm, long-day growth chamber temperature conditions were 23.9 °C (day) and 22.8 °C (night), and this was reflected in the model's climate data input. We postulated that a two-day drop to 12 °C would be enough to induce *FT* but not long enough to sufficiently slow growth. As *FT* transcript must accumulate over several days before flowering can occur (Krzymuski *et al.*, 2015), the effect of *FT* produced at 12 °C should complement the *FT* produced in subsequent warm, long days and cause a lower number of leaves at bolt. In a four- or six-day drop to 12 °C, leaf production should slow sufficiently, causing lower whole-plant levels of *FT* and flowering after greater leaf production.

We observed that plants in the two- or four-day treatments flowered at a similar leaf number to plants grown in warm conditions (Table 3), while plants exposed to 12 °C for six days produced approximately 1.5 more leaves before flowering, as expected. Also as expected, the number of days to visible bolt increased by approximately one day with each consecutive two-days at 12 °C. Leaf production declined with each consecutive two-day 12 °C treatment. By dawn of day seven, when all plants had been moved to warm temperatures, there was a clear gradient in leaf number across the treatments and a visible decline in leaf area (Figure S5).

FM-1.5 predicted a similar leaf number and days to bolt to what we had observed for all treatments (Table 3). We observed an increase in leaf number with increasing exposure time to 12 °C. The model captured this behavior. Considering only the 12 °C treatments, slower simulated leaf production caused by cooler temperatures correlates well with the observed number of days to bolt and final leaf number. This is consistent with our proposal that slower growth in cool temperatures contributes to delayed flowering by slowing whole-plant accumulation of *FT*. FM-1 could not capture the increased leaf production in plants exposed to 12 °C for six-days, although it showed a similar pattern of acceleration in the two-day treated plants (Table 3). It did capture a similar delay in number of days to bolt, although the prediction was lower than observed for all treatments. Overall, FM-1.5 behaved similarly to what we observed, suggesting that incorporating the effects of temperature fluctuations on flowering gene accumulations, and linking gene expression to tissue production, could improve model predictions in fluctuating environments.

Model extension: Prediction of flowering under constant temperature conditions and shorter day lengths

We had parameterized the model for fluctuating temperature environments in long days. We asked how well the model could predict flowering in constant temperature conditions and shorter day lengths. We expected that the model would fail to accurately predict flowering in 12-hour

and in short-days as *FT* is expressed at lower levels (Kobayashi *et al.*, 1999). Further, in our simulation, only early leaves express *FT*, so increasing leaf tissue would not improve performance.

As predicted, simulated *FT* failed to reach a threshold (Figure 6a). The model also failed to predict flowering for plants grown at 12 °C in long days from seed, and for plants grown for a week at 22 °C in short-days then moved to 12 °C long-day conditions. This was because simulated *FT* remained suppressed and because leaf tissue development was substantially slowed (Figure 6a-b). SVP suppression of *FT* declines as plants age in fluctuating temperatures (Kinmonth-Schultz *et al.*, 2016), a trend that may contribute to flowering in 12 °C constant temperature conditions. However, once incorporated into our model (Section S6), flowering was still very delayed. The average predicted leaf number was 132.50 compared to 25.83 observed, indicating that factors other than *FT* may be involved in shorter day conditions.

Discussion

Incorporating underlying mechanisms into models could improve their utility for a range of conditions, without requiring recalibration (White, 2009; Boote *et al.*, 2013). Traditional thermal unit models incorporate the influence of day length by modifying the rate of thermal time accumulation. Some mechanistic models use day length and vernalization to influence the number of leaves at which the transition from the vegetative to reproductive phase occurs, while considering temperature's influence on developmental rate (Brown *et al.*, 2013). Our simulations are consistent with this approach. However, our work helps to clarify the molecular mechanisms underlying temperature's influence on these processes. We demonstrate that *FT* levels, as influenced by day length and temperature, determine the developmental timing of a vegetative to reproductive shift, while temperature influences when this occurs by influencing the rate of development and the whole-plant accumulations of *FT*. Temperature should be considered as a factor in determining the developmental stage (leaf number) at which the transition occurs, not only by influencing developmental rate. We further suggest that tissue accumulation through growth is the underlying factor in the accumulation of thermal time as it causes gene products to accumulate. We also demonstrate that leaves do not consistently express *FT*, as there appears to be a shift during development. *FT* is expressed in the first few true leaves produced, but is only expressed at basal levels in the newly formed leaves of older plants. The change in *FT* expression with developmental age was incorporated in our FTR module using leaf age as a proxy (Fig. 3; equations [S2.1] to [S2.3]), an approach that enables us to integrate qualitative (presence/absence) and quantitative (dosage response) aspects of *FT* effects on flowering. This information can help us quantify when *FT* plays a role during development, when *FT* alone is a poor predictor of flowering, and when it may act synergistically or competitively with other flowering factors. Such a mechanistic modelling approach can highlight areas needing additional research.

While FM-1 could capture the decrease in leaf area with decreasing temperature in plants exposed to different constant temperatures, it simulated larger leaf areas for plants grown in fluctuating temperature conditions than the constant temperature control. This is contrary to what has been observed (Pyl *et al.*, 2012), and was due to two factors. First, specific leaf area (SLA) decreased with increasing thermal time (Christophe et al. 2008), such that in simulations of

warmer conditions, plants develop faster, leading to a lower SLA and lower leaf area than plants in cool temperatures. Second, maintenance respiration is lower under cooler temperatures. In FM-1, photosynthesis and respiration rates correlate with the current temperature (Rasse & Tocquin, 2006). The assimilated carbon is pooled and then allocated either to growth or to maintenance respiration. Under fluctuating temperature conditions, when plants have first been exposed to warm temperatures and have accumulated the same amount of carbon as plants in constant warm temperatures, a lower rate of maintenance respiration leaves a larger pool of carbon that can be used for growth. This was beyond the scope of our study; however, it highlights an important knowledge gap in our understanding of carbon use and allocation under fluctuating temperatures and requires further study.

Here, we demonstrated that the influence of *FT* is likely dependent on the leaf tissue available for its production. A likely second factor is the sensitivity of genes at the shoot apex to the FT signal, which may change with climate. For example, in short-days, high temperatures are proposed to reduce activity of SVP at the shoot apex to initiate flowering despite lower levels of *FT* (Fernández *et al.*, 2016). At the shoot apex, SVP suppresses *SUPPRESSOR OF OVEREXPRESSION OF CONSTANS* (*SOC1*), which is positively regulated by *FT*, and which activates *LEAFY* (*LFY*), a key player in the floral transition (Schmid *et al.*, 2003; Lee *et al.*, 2008; Jang *et al.*, 2009). FT also activates *APETALA1* (*AP1*) at the shoot apex (Lee & Lee, 2010). AP1, in turn, is involved in the down regulation of *TERMINAL FLOWERING1* (*TFL1*), a homolog of *FT*. TFL1 is thought to compete with FT for binding with FD to suppress *LFY*, as well as *AP1*, forming a negative feedback loop (Kaufmann *et al.*, 2010; Wickland & Hanzawa, 2015). Both the decrease in SVP and TFL1 would likely decrease the threshold amount of *FT* needed to induce flowering. Like *SVP*, *TFL1* may play a more active role under cooler temperatures, as lines containing the *tfl1* mutation showed a stronger flowering phenotype at 16 °C compared to 23 °C (Kim *et al.*, 2013). Wenden *et al*. (2009) demonstrated that a changing threshold due to different allelic variants of *LATE FLOWERING* in Pea, a homologue of *TFL1* in *Arabidopsis* (Foucher *et al.*, 2003), can contribute to accurate prediction of flowering times (Wenden *et al.*, 2009). Incorporating such a mechanism – influence by climate – may aid our understanding of how climate influences flowering.

Finally, other factors produced in the leaves or plant tissue may contribute to flowering. Early exploration into compounds responsible for floral induction found that photosynthates increase at the shoot apex concurrently or slightly after floral induction (Golembeski *et al.*, 2014). Strains unable to accumulate starch show late flowering, which can be partly restored when sucrose is applied to their meristems (Corbesier *et al.*, 1998). Photosynthates may contribute to flowering both in long and short days (Bernier *et al.*, 1993; Golembeski *et al.*, 2014). Further, gibberellic acid (GA) is involved in inducing flowering in short days (Wilson *et al.*, 1992) as well as under low constant (15 °C) temperatures independently of *FT* (Galvao *et al.*, 2015). The latter may contribute to the earlier than predicted flowering we observed in plants grown from seed at 12 °C. Interestingly, GA biosynthesis is negatively regulated by SVP at the shoot apex (Andres *et al.*, 2014), while GA positively regulates *LFY* at the shoot apex to promote flowering (Blazquez & Weigel, 2000). As a proof of concept, we tested the capacity of a second factor, Factor X, accumulating in later produced leaves (Figure 7). This improved the model predictions for shorter-day lengths. However, this factor acted independently of day length and temperature, which is likely not the case, causing similar predictions for both 12-hour and short day lengths. The observed days to bolt were 58.10 and 79.45 days in 12-hour and short days, respectively.

Adding Factor X yielded model predictions of 53.13 and 53.62 days, respectively. As most mechanistic studies are performed on young plants, we lack a complete picture of how flowering regulators in the leaves and at the shoot apex respond to climate and interact and change over a growing season. Our study provides a baseline on which to explore these seasonal interactions.

Supplementary Data

Section S1: Description of the Framework Model 1

Section S2: Incorporating FT as a function of leaf tissue amount

Section S3: Determining whole-plant FT levels and accumulating FT to a threshold

Section S4: Adjusting leaf area to respond to temperature

Section S5: FT transcript accumulation in fluctuating temperature conditions simulated through influence of SVP and CO activity

Section S6: Model extension: adjustments used to improve model fit in conditions causing late flowering

Table S1: Coefficients values for equations used in FM-1.5.

Figure S1: Graphic representation of FM-1.

Figure S2: Simulated SVP activity in long-day constant temperature and temperature-cycle conditions.

Figure S3: The levels of *CO* transcript after a drop from 22 to 12 °C relative to levels in plants that had remained at 22 °C.

Figure S4. The spatial expression profile of *FT* changes with leaf age.

Figure S5. Leaf production slows during short-term exposure to cool temperatures

Acknowledgements

Many thanks to Drs. Daniel Seaton and Andrew Millar for help with the model and Paul Panipinto for his help on this project. This work was supported in part by a Cooperative Research Program for Agricultural Science and Technology Development (PJ01000707), Rural Development Administration, Republic of Korea and a Specific Cooperative Agreement (58-1265-1-074) between University of Washington and USDA-ARS to S.-H.K, by National Institute of Health grant (GM079712) and partly from Next-Generation BioGreen 21 Program (SSAC, PJ011175, Rural Development Administration, Republic of Korea) to T.I., and by the Frye-Hotson-Rigg Fellowship to H.K.S.

References

Abe M, Kobayashi Y, Yamamoto S, Daimon Y, Yamaguchi A, Ikeda Y, Ichinoki H, Notaguchi M, Goto K, Araki T. **2005**. FD, a bZIP protein mediating signals from the floral pathway integrator FT at the shoot apex. *Science* **309**: 1052–6.

Amasino R. **2010**. Seasonal and developmental timing of flowering. *Plant Journal* **61**: 1001–1013.

Andres F, Porri A, Torti S, Mateos J, Romera-Branchat M, Luis Garcia-Martinez J, Fornara F, Gregis V, Kater MM, Coupland G. **2014**. SHORT VEGETATIVE PHASE reduces gibberellin biosynthesis at the *Arabidopsis* shoot apex to regulate the floral transition. *Proceedings of the National Academy of Sciences* **111**: E2760–E2769.

Asseng S, Ewert F, Rosenzweig C, Jones JW, Hatfield JL, Ruane AC, Boote KJ, Thorburn PJ, Rötter RP, Cammarano D, *et al.* 2013. Uncertainty in simulating wheat yields under climate change. *Nature Climate Change* **3**: 827–832.

Bernier G, Havelange A, Houssa C, Petitjean A, Lejeune P. **1993**. Physiological signals that induce flowering. *Plant Cell* **5**: 1147.

Blazquez M, Ahn J, Weigel D. **2003**. A thermosensory pathway controlling flowering time in *Arabidopsis thaliana*. *Nature Genetics* **33**: 168–171.

Blazquez MA, Weigel D. **2000**. Integration of floral inductive signals in *Arabidopsis*. *Nature* **404**: 889–892.

Boote KJ, Jones JW, White JW, Asseng S, Lizaso JI. **2013**. Putting mechanisms into crop production models. *Plant, Cell and Environment* **36**: 1658–1672.

Brown HE, Jamieson PD, Brooking IR, Moot DJ, Huth NI. **2013**. Integration of molecular and physiological models to explain time of anthesis in wheat. *Annals of Botany* **112**: 1683–1703.

Chew YH, Wenden B, Flis A, Mengin V, Taylor J, Davey CL, Tindal C, Thomas H, Ougham HJ, Reffye P de, *et al.* 2014. Multiscale digital *Arabidopsis* predicts individual organ and whole-organism growth. *Proceedings of the National Academy of Sciences* **111**: E4127–E4136.

Chew YH, Wilczek AM, Williams M, Welch SM, Schmitt J, Halliday KJ. **2012**. An augmented *Arabidopsis* phenology model reveals seasonal temperature control of flowering time. *New Phytologist* **194**: 654–665.

Chuine I. **2000**. A unified model for budburst of trees. *Journal of Theoretical Biology* **207**: 337–347.

Corbesier L, Lejeune P, Bernier G. **1998**. The role of carbohydrates in the induction of flowering in *Arabidopsis thaliana*: comparison between the wild type and a starchless mutant. *Planta* **206**: 131–7.

Corbesier L, Vincent C, Jang S, Fornara F, Fan Q, Searle I, Giakountis A, Farrona S, Gissot L, Turnbull C, *et al.* 2007. FT protein movement contributes to long-distance signaling in floral induction of *Arabidopsis thaliana*. *Science* **316**: 1030–1033.

Fernández-Aparicio M, Huang K, Wafula EK, Honaas LA, Wickett NJ, Timko MP, Depamphilis CW, Yoder JI, Westwood JH. **2013**. Application of qRT-PCR and RNA-Seq analysis for the

identification of housekeeping genes useful for normalization of gene expression values during Striga hermonthica development. *Molecular Biology Reports* **40**: 3395–3407.

Fernández V, Takahashi Y, LeGourrierec J, Coupland G. **2016**. Photoperiodic and thermosensory pathways interact through CONSTANS to promote flowering at high temperature under short days. *Plant Journal*.

Foucher F, Morin J, Courtiade J, Cadioux S, Ellis N, Banfield MJ, Rameau C. **2003**. *DETERMINATE* and *LATE FLOWERING* are two *TERMINAL FLOWER1/CENTRORADIALIS* homologs that control two distinct phases of flowering initiation and development in pea. *Plant Cell* **15**: 2742–2754.

Galvao VC, Collani S, Horrer D, Schmid M. **2015**. Gibberellic acid signaling is required for ambient temperature-mediated induction of flowering in *Arabidopsis thaliana*. *Plant Journal* **84**: 949–962.

Golembeski GS, Kinmonth-Schultz HA, Song YH, Imaizumi T. **2014**. Photoperiodic flowering regulation in *Arabidopsis thaliana*. In: Fornara F, ed. *Molecular Genetics of Floral Transition and Flower Development*. London, UK: Academic Press Ltd-Elsevier Science Ltd, 1–28.

He J, Le Gouis J, Stratonovitch P, Allard V, Gaju O, Heumez E, Orford S, Griffiths S, Snape JW, Foulkes MJ, *et al.* 2012. Simulation of environmental and genotypic variations of final leaf number and anthesis date for wheat. *European Journal of Agronomy* **42**: 22–33.

Jaglo-Ottosen KR, Gilmour SJ, Zarka DG, Schabenberger O, Thomashow MF. **1998**. *Arabidopsis CBF1* overexpression induces *COR* genes and enhances freezing tolerance. *Science* **280**: 104–106.

Jamieson PD, Brooking IR, Semenov MA, Porter JR. **1998a**. Making sense of wheat development: a critique of methodology. *Field Crops Research* **55**: 117–127.

Jamieson PD, Semenov MA, Brooking IR, Francis GS. **1998b**. Sirius: a mechanistic model of wheat response to environmental variation. *European Journal of Agronomy* **8**: 161–179.

Jang S, Torti S, Coupland G. **2009**. Genetic and spatial interactions between FT, TSF and SVP during the early stages of floral induction in *Arabidopsis*. *Plant Journal* **60**: 614–625.

Jones JW, Hoogenboom G, Porter CH, Boote KJ, Batchelor WD, Hunt LA, Wilkens PW, Singh U, Gijsman AJ, Ritchie JT. **2003**. The DSSAT cropping system model. *European Journal of Agronomy* **18**: 235–265.

Karsai I, Igartua E, Casas AM, Kiss T, Soos V, Balla K, Bedo Z, Veisz O. **2013**. Developmental patterns of a large set of barley (*Hordeum vulgare*) cultivars in response to ambient temperature. *Annals of Applied Biology* **162**: 309–323.

Karsai I, Szucs P, Koszegi B, Hayes PM, Casas A, Bedo Z, Veisz O. **2008**. Effects of photo and thermo cycles on flowering time in barley: a genetical phenomics approach. *Journal of Experimental Botany* **59**: 2707–2715.

Kaufmann K, Wellmer F, Muiño JM, Ferrier T, Wuest SE, Kumar V, Serrano-Mislata A, Madueño F, Krajewski P, Meyerowitz EM, *et al.* 2010. Orchestration of Floral Initiation by APETALA1. *Science* **328**: 85–89.

Kim S-H, Gitz DC, Sicher RC, Baker JT, Timlin DJ, Reddy VR. **2007**. Temperature dependence of growth, development, and photosynthesis in maze under elevated CO_2. *Environmental and Experimental Botany* **61**: 224–236.

Kim W, Park TI, Yoo SJ, Jun AR, Ahn JH. **2013**. Generation and analysis of a complete mutant set for the *Arabidopsis FT/TFL1* family shows specific effects on thermo-sensitive flowering regulation. *Journal of Experimental Botany* **64**: 1715–1729.

Kim S-H, Yang Y, Timlin DJ, Fleisher DH, Dathe A, Reddy VR, Staver K. **2012**. Modeling temperature responses of leaf growth, development, and biomass in maize with MAIZSIM. *Agronomy Journal* **104**: 1523–1537.

Kinmonth-Schultz HA, Tong X, Lee J, Song YH, Ito S, Kim S-H, Imaizumi T. **2016**. Cool night-time temperatures induce the expression of *CONSTANS* and *FLOWERING LOCUS T* to regulate flowering in *Arabidopsis*. *New Phytologist* **211**: 208–224.

Kobayashi Y, Kaya H, Goto K, Iwabuchi M, Araki T. **1999**. A pair of related genes with antagonistic roles in mediating flowering signals. *Science* **286**: 1960–1962.

Krzymuski M, Andrés F, Cagnola JI, Seonghoe J, Yanovsky M, Coupland G, Casal JJ. **2015**. The dynamics of *FLOWERING LOCUS T* expression encodes long-day information. *Plant journal* **83**: 952–961.

Kumudini S, Andrade FH, Boote KJ, Brown GA, Dzotsi KA, Edmeades GO, Gocken T, Goodwin M, Halter AL, Hammer GL, *et al.* 2014. Predicting maize phenology: Intercomparison of functions for developmental response to temperature. *Agronomy Journal* **106**: 2087.

Lee J, Lee I. **2010**. Regulation and function of SOC1, a flowering pathway integrator. *Journal of Experimental Botany*: erq098.

Lee J, Oh M, Park H, Lee I. **2008**. SOC1 translocated to the nucleus by interaction with AGL24 directly regulates *LEAFY*. *Plant Journal* **55**: 832–843.

Lee JH, Ryu H-S, Chung KS, Posé D, Kim S, Schmid M, Ahn JH. **2013**. Regulation of temperature-responsive flowering by MADS-Box transcription factor repressors. *Science* **342**: 628–632.

Lee JH, Yoo SJ, Park SH, Hwang I, Lee JS, Ahn JH. **2007**. Role of *SVP* in the control of flowering time by ambient temperature in *Arabidopsis*. *Genes & Development* **21**: 397–402.

Lehenbauer PA. **1914**. Growth of maize seedlings in relation to temperature. *Physiological Researches* **1**: 247–288.

Lutz U, Posé D, Pfeifer M, Gundlach H, Hagmann J, Wang C, Weigel D, Mayer KFX, Schmid M, Schwechheimer C. **2015**. Modulation of ambient temperature-dependent flowering in *Arabidopsis thaliana* by natural variation of *FLOWERING LOCUS M*. *PLoS Genetics* **11**: e1005588.

Makowski D, Asseng S, Ewert F, Bassu S, Durand JL, Li T, Martre P, Adam M, Aggarwal PK, Angulo C, *et al.* 2015. A statistical analysis of three ensembles of crop model responses to temperature and CO_2 concentration. *Agricultural and Forest Meteorology* **214**: 483–493.

Mathieu J, Yant LJ, Mürdter F, Küttner F, Schmid M. **2009**. Repression of flowering by the miR172 target SMZ. *PLoS Biology* **7**: e1000148.

Parent B, Turc O, Gibon Y, Stitt M, Tardieu F. **2010**. Modelling temperature-compensated physiological rates, based on the co-ordination of responses to temperature of developmental processes. *Journal of Experimental Botany* **61**: 2057–2069.

Piper EL, Smit MA, Boote KJ, Jones JW. **1996**. The role of daily minimum temperature in modulating the development rate to flowering in soybean. *Field Crops Research* **47**: 211–220.

Posé D, Verhage L, Ott F, Yant L, Mathieu J, Angenent GC, Immink RGH, Schmid M. **2013**. Temperature-dependent regulation of flowering by antagonistic FLM variants. *Nature* **503**: 414–417.

Pyl E-T, Piques M, Ivakov A, Schulze W, Ishihara H, Stitt M, Sulpice R. **2012**. Metabolism and growth in *Arabidopsis* depend on the daytime temperature but are temperature-compensated against cool nights. *Plant Cell* **24**: 2443–2469.

Rasse DP, Tocquin P. **2006**. Leaf carbohydrate controls over *Arabidopsis* growth and response to elevated CO_2: an experimentally based model. *New Phytologist* **172**: 500–513.

Rensing L, Ruoff P. **2002**. Temperature effect on entrainment, phase shifting, and amplitude of circadian clocks and its molecular bases. *Chronobiology International* **19**: 807–864.

Ritchie J, Otter S. **1985**. Description and performance of CERES-Wheat. A user-oriented wheat model. *US Department of Agriculture,* ARS **38**: 159–175.

Salazar JD, Saithong T, Brown PE, Foreman J, Locke JCW, Halliday KJ, Carré IA, Rand DA, Millar AJ. **2009**. Prediction of photoperiodic regulators from quantitative gene circuit models. *Cell* **139**: 1170–1179.

Schmid M, Uhlenhaut NH, Godard F, Demar M, Bressan R, Weigel D, Lohmann JU. **2003**. Dissection of floral induction pathways using global expression analysis. *Development* **130**: 6001–12.

Schwartz C, Balasubramanian S, Warthmann N, Michael TP, Lempe J, Sureshkumar S, Kobayashi Y, Maloof JN, Borevitz JO, Chory J, *et al.* 2009. Cis-regulatory changes at *FLOWERING LOCUS T* mediate natural variation in flowering responses of *Arabidopsis thaliana*. *Genetics* **183**: 723–732.

Seaton DD, Smith RW, Song YH, MacGregor DR, Stewart K, Steel G, Foreman J, Penfield S, Imaizumi T, Millar AJ, *et al.* 2015. Linked circadian outputs control elongation growth and flowering in response to photoperiod and temperature. *Molecular Systems Biology* **11**: 1–19.

Segal IH. **1976**. *Biochemical Calculations: How to Solve Mathematical Problems in General Biochemistry*. Canada: John Wiley and Sons.

Song Y-H, Shim J-S, Kinmonth-Schultz HA, Imaizumi T. **2015**. Photoperiodic flowering: time measurement mechanisms in leaves. *Annual Review of Plant Biology* **66**: 441–464.

Takada S, Goto K. **2003**. TERMINAL FLOWER2, an Arabidopsis homolog of *HETEROCHROMATIN PROTEIN1*, counteracts the activation of *FLOWERING LOCUS T* by constans in the vascular tissues of leaves to regulate flowering time. *Plant Cell* **15**: 2856–65.

Thines BC, Youn Y, Duarte MI, Harmon FG. **2014**. The time of day effects of warm temperature on flowering time involve PIF4 and PIF5. *Journal of Experimental Botany* **65**: 1141–1151.

Welch SM, Roe JL, Dong Z. **2003**. A genetic neural network model of flowering time control in *Arabidopsis thaliana*. *Agronomy Journal* **95**: 71--81.

Wenden B, Dun EA, Hanan J, Andrieu B, Weller JL, Beveridge CA, Rameau C. **2009**. Computational analysis of flowering in pea (*Pisum sativum*). *New Phytologist* **184**: 153–167.

White JW. **2009**. Combining ecophysiological models and genomics to decipher the GEM-to-P problem. *NJAS - Wageningen Journal of Life Sciences* **57**: 53–58.

Wickland DP, Hanzawa Y. **2015**. The FLOWERING LOCUS T/TERMINAL FLOWER 1 Gene Family: Functional Evolution and Molecular Mechanisms. *Molecular Plant* **8**: 983–997.

Wilczek AM, Roe JL, Knapp MC, Cooper MD, Lopez-Gallego C, Martin LJ, Muir CD, Sim S, Walker A, Anderson J, *et al.* 2009. Effects of genetic perturbation on seasonal life history plasticity. *Science* **323**: 930–934.

Wilson RN, Heckman JW, Somerville CR. **1992**. Gibberellin is required for flowering in *Arabidopsis thaliana* under short days. *Plant Physiology* **100**: 403–408.

Yan L, Fu D, Li C, Blechl A, Tranquilli G, Bonafede M, Sanchez A, Valarik M, Yasuda S, Dubcovsky J. **2006**. The wheat and barley vernalization gene *VRN3* is an orthologue of *FT*. *Proceedings of the National Academy of Sciences* **103**: 19581–19586.

Yin X, Kropff M. **1996**. The effect of temperature on leaf appearance in rice. *Annals of Botany* **77**: 215–221.

Yin X, Kropff MJ, McLaren G, Visperas RM. **1995**. A nonlinear model for crop development as a function of temperature. *Agricultural and Forest Meteorology* **77**: 1–16.

Zheng B, Biddulph B, Li D, Kuchel H, Chapman S. **2013**. Quantification of the effects of *VRN1* and *Ppd-D1* to predict spring wheat (*Triticum aestivum*) heading time across diverse environments. *Journal of Experimental Botany* **64**: 3747–3761.

Table 1. Comparison of fit between observed and predicted flowering times in days to bolt and leaf number at bolt among FM-1, FM-1 when night and day temperatures have the same influence on thermal time, and FM-1.5 for Columbia-0 and Landsberg *erecta*.

		FM-1	FM-1 (Night = Day)	FM-1.5
Days to Bolt	**RMSE**	5.32	4.16	3.30
	Bias	-3.96	-3.09	1.39
Leaf Number	**RMSE**	5.43	4.99	2.78
	Bias	1.02	1.79	-0.71

Table 2. Comparison of observed flowering times (Obs. Data) in days to bolt and leaf number at bolt in long days in 12, 17, and 22 °C nighttime temperatures (NT) to the modeled fit in FM-1.5 and in FM-1.5 with *FT* being held constant at 22 °C levels.

	Treatment	**Obs. data**	**FM-1.5**	***FM-1.5* (*FT* constant)**
Days to Bolt	**NT22 °C**	32.27	36.67	36.67
	NT17 °C	38.6	41.25	38.50
	NT12 °C	40.08	43.29	39.46
Leaf Number	**NT22 °C**	14.77	15	15
	NT17 °C	20.5	19	15
	NT12 °C	20.79	18	13

Table 3. Statistical analysis of observed flowering times and comparison among observed and predicted flowering by FM-1 (original model) and FM-1.5 in leaf number and days to bolt in long days after 2, 4, or 6 days exposure to 12 ˚C relative to plants grown in constant, warm temperatures (control).

	treatment	Obs. Data	n	Robust S.E.	Robust *z*	*P*-Value	C.I. of dif. (Lower)	C.I. of dif. (Upper)	FM-1	FM-1.5
Days to Bolt	**Control**	35.00	11	0.62	31.10				33.67	35.63
	12 ˚C, 2 days	36.00	15	0.60	1.73	0.08	-0.65	2.73	34.63	36.46
	12 ˚C, 4 days	37.31	14	0.42	5.54	0.00	0.87	3.80	35.75	37.63
	12 ˚C, 6 days	38.64	14	0.35	7.85	0.00	2.24	5.02	37.04	39.58
Leaf Number	**Control**	13.73	11	0.52	19.59				25.00	14.00
	12 ˚C, 2 days	13.13	15	0.34	-1.21	0.23	-0.81	1.65	24.00	13.00
	12 ˚C, 4 days	13.64	14	0.36	0.49	0.63	-1.07	1.42	24.00	14.00
	12 ˚C, 4 days	15.14	14	0.39	3.47	0.00	0.08	2.64	25.00	15.00

Figure Legends

Figure 1. Schematic of Model FM-1.5. Temperature (through *CONSTANS* and *SHORT VEGETATIVE GROWTH/FLOWERING LOCUS M*), day length, and the circadian clock regulate expression of *FLOWERING LOCUS T* (*FT*) in the Photoperiodism and Phenology modules per unit tissue. The leaf number and relative leaf age, outputs of the Functional-Structural-Plant module, are used to determine the capacity of each leaf to express *FT*, and leaf area is used to determine the amount of leaf tissue present. *FT* is summed across all leaves in a plant and added to the whole-plant *FT* from the previous time step. The model ceases leaf production and determines the days to bolt (DtB) when *FT* reaches a pre-set threshold set by using the leaf number for plants grown in long-days and at 22 °C. Red illustrates where adjustments made to the original model (FM-1). The bold, italic numerals correspond to the numbers in the model description in the main text.

Figure 2. FM-1 predicts earlier than observed days to bolt. The difference between predicted and observed results in days to bolt in Columbia-0 (Col) and Landsberg *erecta* (L*er*) in long days when nighttime temperatures have a lower influence than daytime temperatures on accumulation of thermal time (a). The predicted and observed final leaf numbers (b). The difference between predicted and observed results in days to bolt when daytime and nighttime temperatures have the same influence accumulation of thermal time. All are plotted over the three nighttime temperatures. Daytime temperature was 22 °C.

Figure 3. *FT* is expressed only in the first few true leaves produced. Leaves of plants aged two (a), four (b), and six (c) weeks old and grown in short days were exposed to long days or short days (d) for three days and harvested at 16 hours after dawn on the third day to determine *FT* amount per leaf. The colors in (d) correspond to the colors and ages in panels (a-c). *FT* levels were determined by absolute copy number and normalized within a replicate. The simulated proportion of *FT* per unit leaf tissue (cm^{-2}, solid lines) for each plant age is shown. This value was used in FM-1.5 as a modifier to adjust the amount of *FT* produced by each leaf. Percent of the leaf area showing staining in *pFT:GUS* plants (e). For all, the two cotyledons and first two true leaves were pooled for each sample as they emerge in pairs. Leaves that failed to yield 2μg total RNA were excluded. For each plant inset, the italicized number indicated the relative leaf age of the cotyledons. The shading of the bar graphs (dark to light) indicates relative leaf age (youngest to oldest) and corresponds to the shading in the plant insets. Scale bars = 0.5 cm.

Figure 4. Suppression of *FT* by SVP activity and induction by CO can capture the behavior of *FT* in fluctuating temperatures. The predicted (sim.) and observed (obs.) *FT* gene expression when the nighttime temperature (NT) was 22 °C and 12 °C (a). Daytime temperature was 22 °C. The total predicted (simulation) and observed (training and testing data) *FT* expression over a 24-hour period calculated as the area under the curve (AUC) for three nighttime temperature conditions (b). The observed *FT* expression when temperatures drop at dawn from 22 °C to 12 °C, and then remain at 12 °C continuously (cont.) as originally shown in Kinmonth-Schultz *et al.* 2016 (c) and the simulated values in these same conditions (d). The white and black bars spanning the tops of figures a, c, and d indicate lights on and lights off.

Figure 5. Incorporating temperature regulation of *FT* and linking *FT* to leaf tissue production improves model prediction in fluctuating temperatures. The difference between predicted and observed results in days to bolt in Columbia-0 (Col) and Landsberg *erecta* (L*er*) in long days

plotted over 12, 17, and 22 °C nighttime temperatures (a). Predicted (sim.) and observed (obs.) Number of leaves produced over time in 12 and 22 °C nighttime temperatures (NT) (b). Daytime temperature was 22 °C.

Figure 6. Accumulation of *FT* with development cannot predict flowering in shorter day lengths or in cool constant temperatures. Simulated (sim.) *FT* accumulated with leaf tissue production, considering leaf number, age, and area, in long days (LD), 12-hour days (MD), and short days (SD) at 22 °C, and in long days at 12 °C after growth for one week at 22 °C in short days (a). *FT* expression is influenced by day length and temperature fluctuations. The horizontal black line is the threshold of *FT* determined using plants grown in long-day, 22 °C conditions. The simulated accumulated leaf area in these same conditions (b) is larger for shorter day lengths as these plants were grown at higher light intensities, but lower for plants grown at cool constant temperatures.

Figure 7. A second florigin-like compound may increase in newly formed leaves of older plants. Simulated *FT* expression (solid line) in a plant with 20 leaves grown in short-day conditions, is high only in the first few true leaves produced. Adding a second factor, Factor X (dash-dotted line), that increases in later produced leaves, improved FM-1.5 model performance in conditions in which *FT* expression is low and, therefore, does not accumulate to a threshold.

Figure 1.

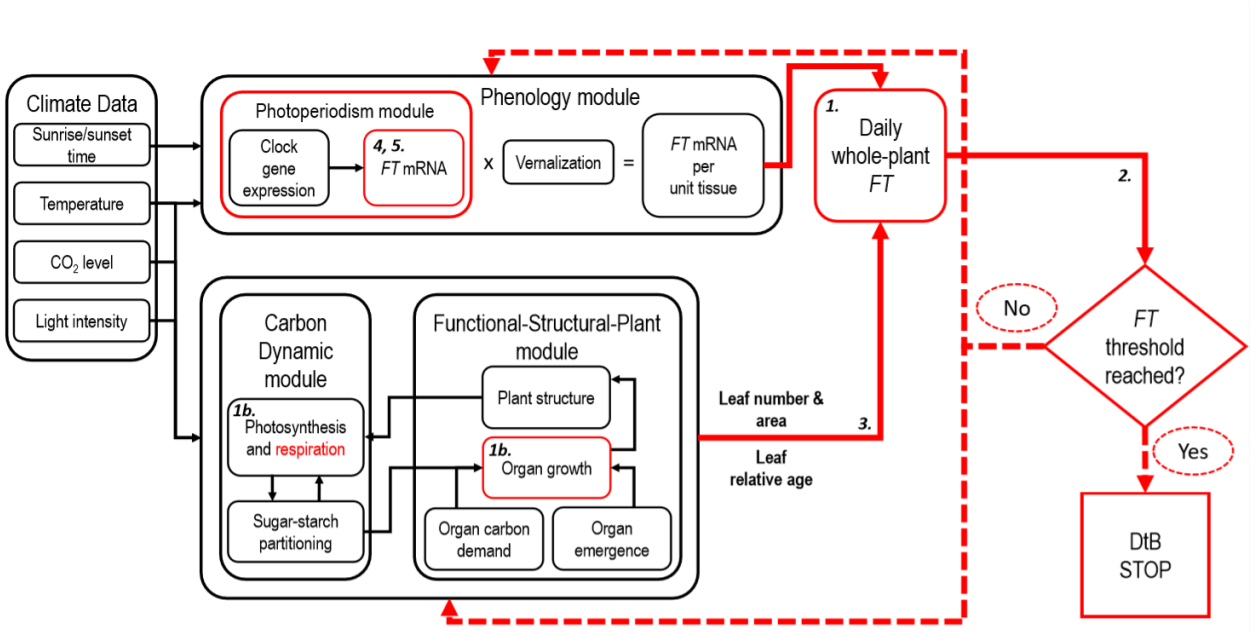
Climate Data
Sunrise/sunset time
Temperature
CO_2 level
Light intensity
Photoperiodism module
Clock gene expression
4, 5. FT mRNA
Phenology module
x
Vernalization
=
FT mRNA per unit tissue
1. Daily whole-plant FT
2.
No
FT threshold reached?
Yes
DtB STOP
Carbon Dynamic module
1b. Photosynthesis and respiration
Sugar-starch partitioning
Functional-Structural-Plant module
Plant structure
1b. Organ growth
Organ carbon demand
Organ emergence
Leaf number & area
3.
Leaf relative age

Figure 2.

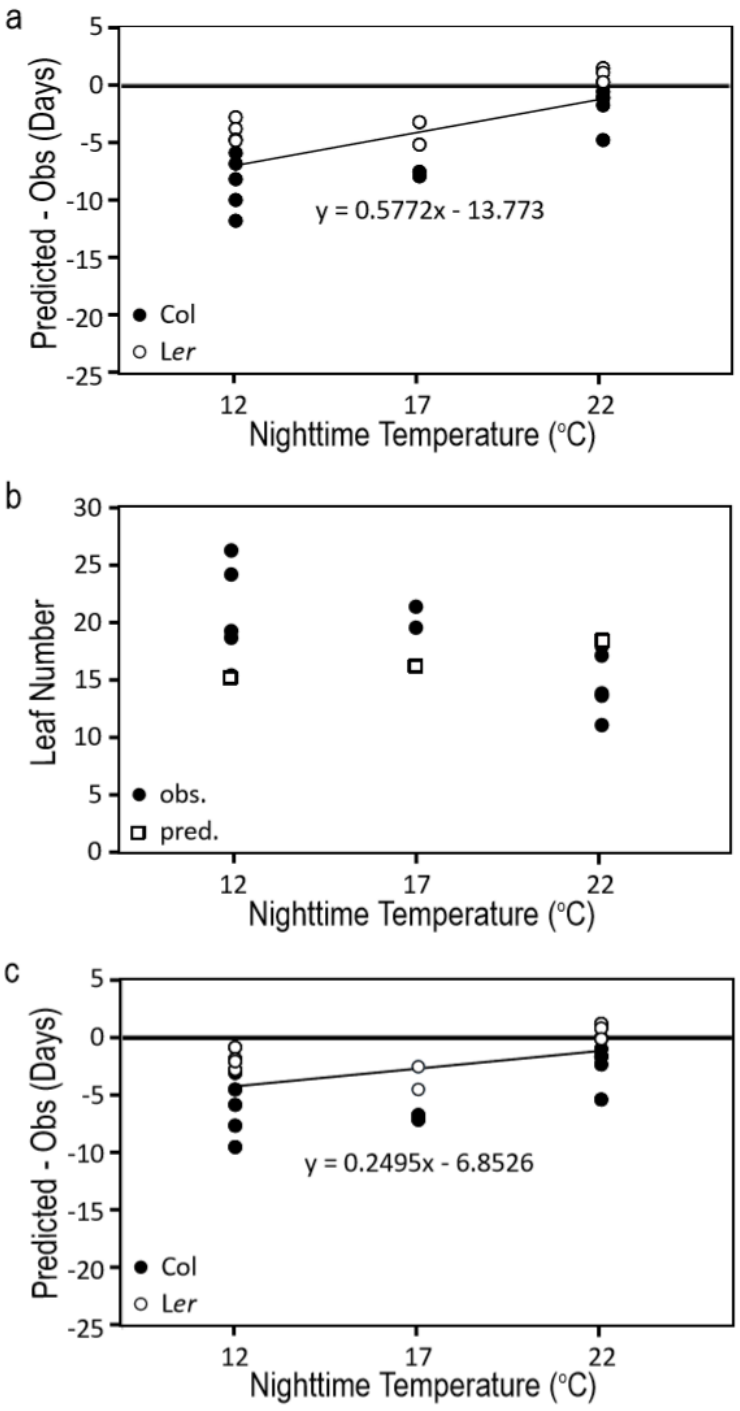
a
Predicted - Obs (Days)
5
0
-5
-10
-15
-20
-25
y = 0.5772x - 13.773
Col
Ler
12
17
22
Nighttime Temperature (°C)
b
Leaf Number
30
25
20
15
10
5
0
obs.
pred.
12
17
22
Nighttime Temperature (°C)
c
Predicted - Obs (Days)
5
0
-5
-10
-15
-20
-25
y = 0.2495x - 6.8526
Col
Ler
12
17
22
Nighttime Temperature (°C)

Figure 3.

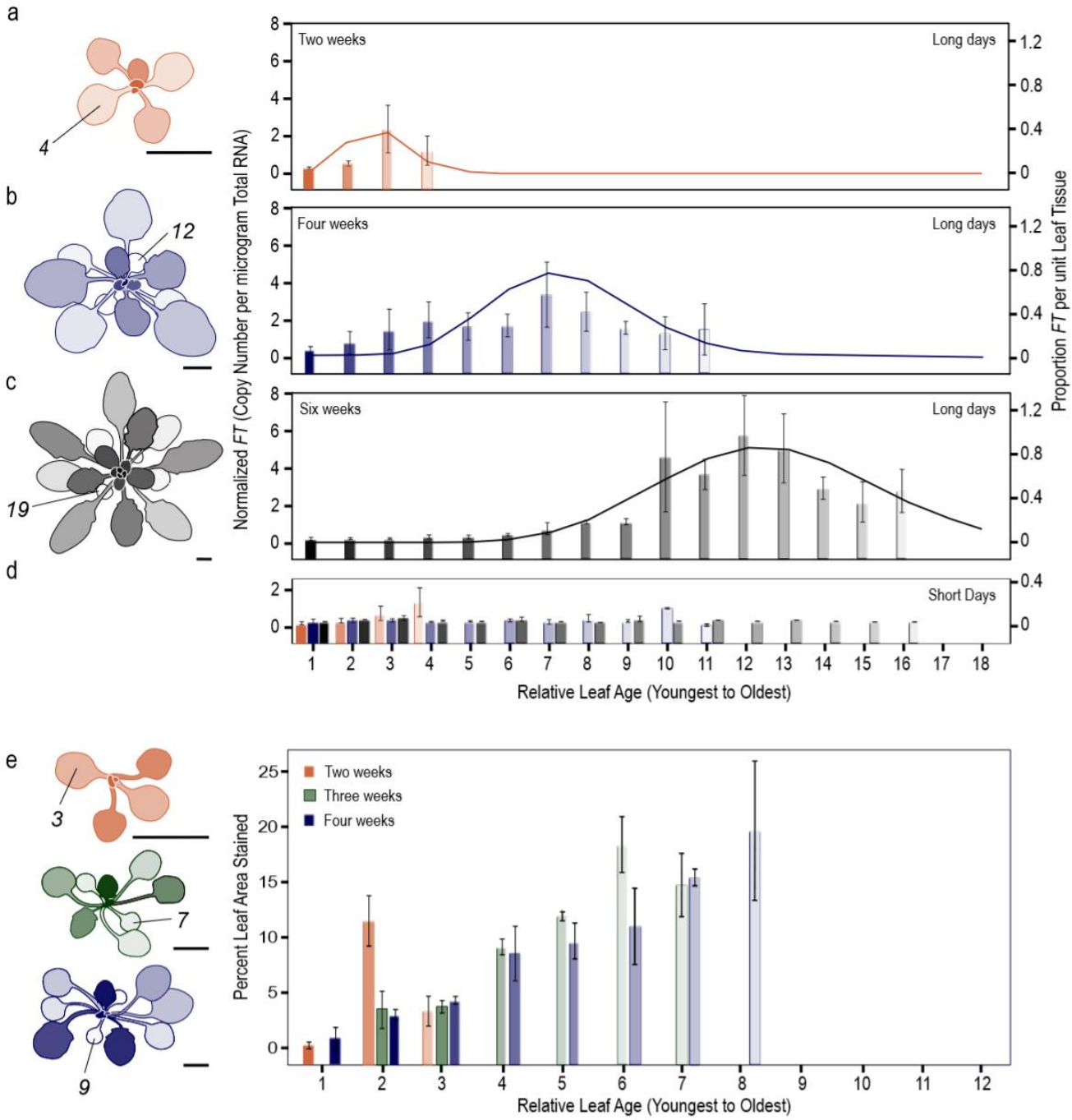
a
4
b
12
c
19
d
e
3
7
9
Two weeks
Long days
Four weeks
Long days
Six weeks
Long days
Short Days
Normalized FT (Copy Number per microgram Total RNA)
Proportion FT per unit Leaf Tissue
Relative Leaf Age (Youngest to Oldest)
Two weeks
Three weeks
Four weeks
Percent Leaf Area Stained
Relative Leaf Age (Youngest to Oldest)

Figure 4.

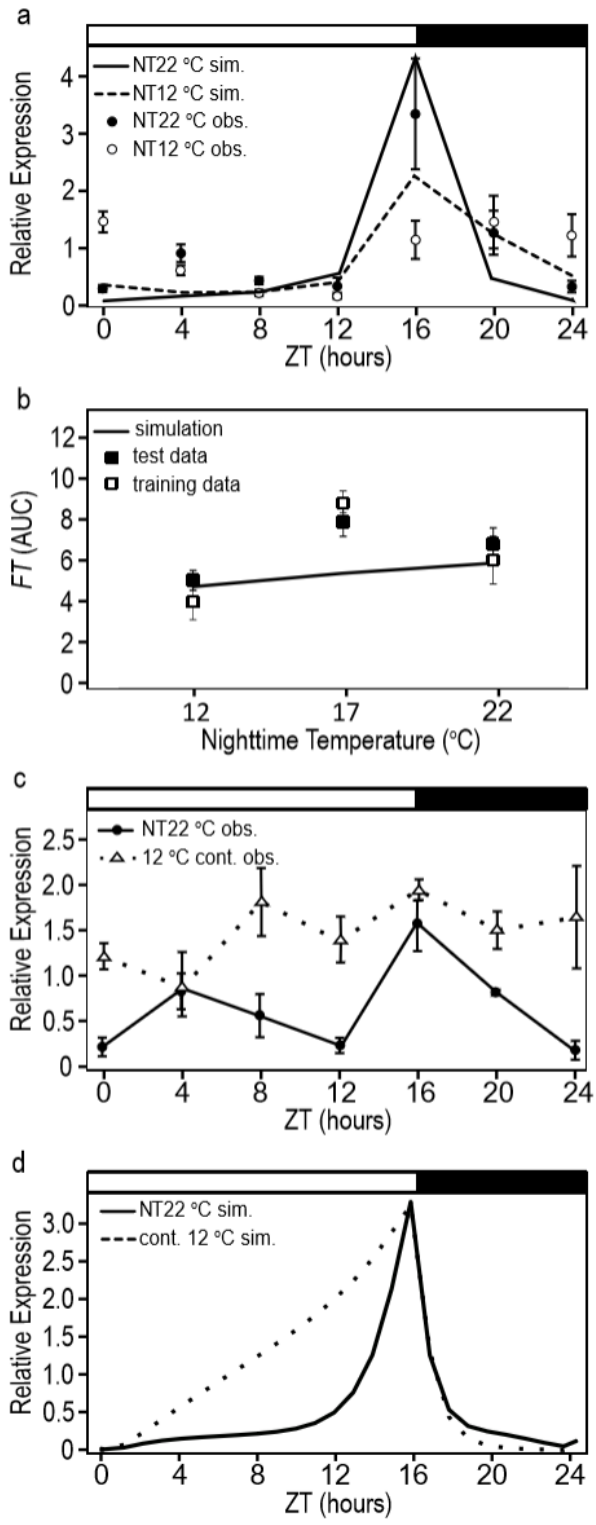
a
NT22 °C sim.
NT12 °C sim.
NT22 °C obs.
NT12 °C obs.
Relative Expression
ZT (hours)
b
simulation
test data
training data
FT (AUC)
Nighttime Temperature (°C)
c
NT22 °C obs.
12 °C cont. obs.
Relative Expression
ZT (hours)
d
NT22 °C sim.
cont. 12 °C sim.
Relative Expression
ZT (hours)

Figure 5.

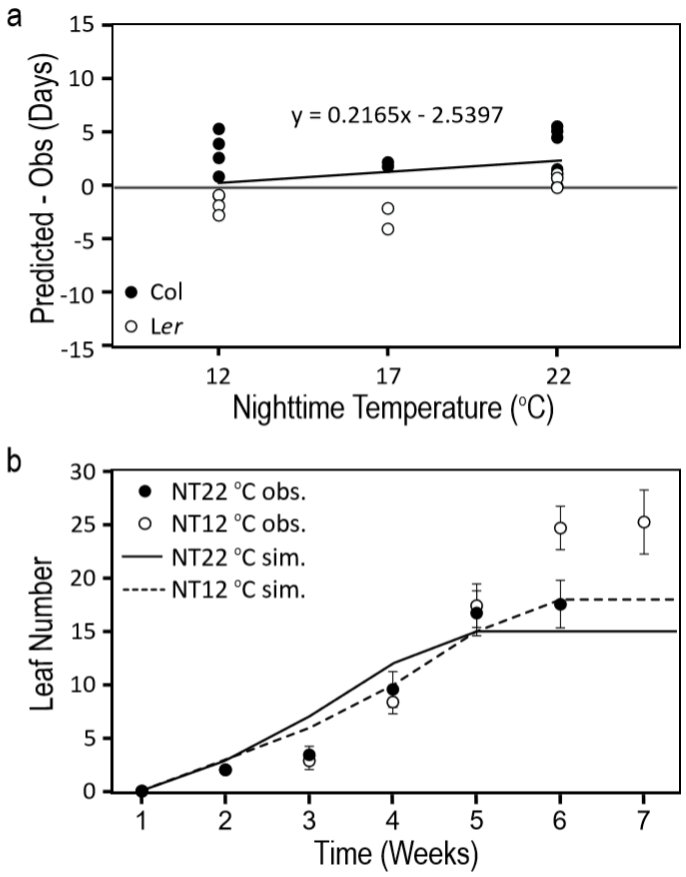
a
Predicted - Obs (Days)
y = 0.2165x - 2.5397
Col
Ler
Nighttime Temperature (°C)
b
Leaf Number
NT22 °C obs.
NT12 °C obs.
NT22 °C sim.
NT12 °C sim.
Time (Weeks)

Figure 6.

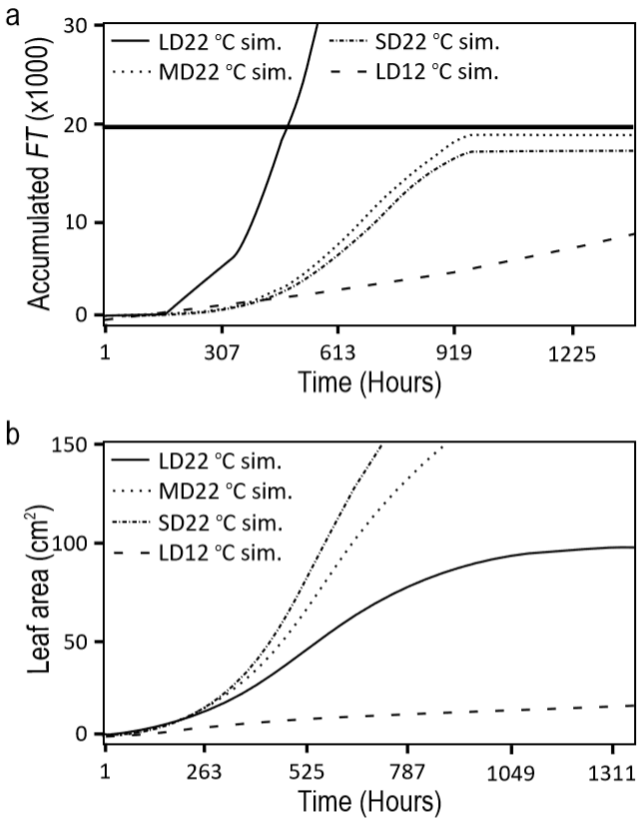
a
LD22 °C sim.
MD22 °C sim.
SD22 °C sim.
LD12 °C sim.
Accumulated FT (x1000)
30
20
10
0
1
307
613
919
1225
Time (Hours)
b
LD22 °C sim.
MD22 °C sim.
SD22 °C sim.
LD12 °C sim.
Leaf area (cm²)
150
100
50
0
1
263
525
787
1049
1311
Time (Hours)

Figure 7.

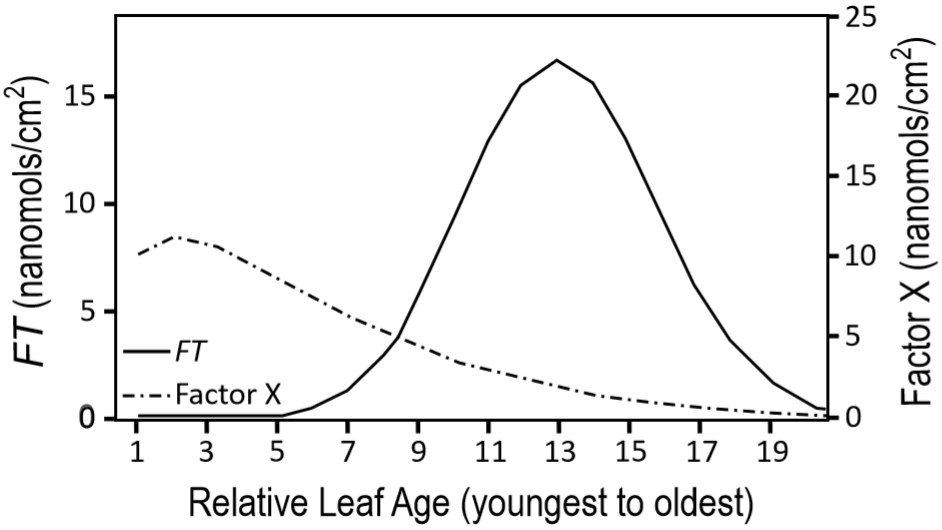
FT (nanomols/cm2)
Factor X (nanomols/cm2)
FT
Factor X
Relative Leaf Age (youngest to oldest)
0
5
10
15
20
25
1
3
5
7
9
11
13
15
17
19

Supplemental Material

Model Description

S1. Description of the Framework Model 1

The Framework Model (FM-1, Figure S1, Chew *et al.*, 2014) combines plant growth and mechanistic flowering regulation for *Arabidopsis.* The model is run in two phases. In the first phase, the climate data is called and the timing of the flowering (Days to bolt, DtB) is determined by two modules. The Photoperiodism module describes the circadian clock and day length control of *FT* transcript accumulation (Salazar *et al.*, 2009). The Phenology module describes the integrated influence of day length, ambient temperature, and vernalization (Wilczek *et al.*, 2009; Chew *et al.*, 2012). *FT* transcript accumulation, output from the Photoperiodism module, is fit to a linear function describing the degree to which day length influences the timing of flowering, and yields a value between zero and one. Climate information is input into the Phenology module which accumulates thermal units (degrees Celsius at each time step) over time. The amount of thermal units at each time step is modified by the day length and by vernalization to produce Modified Photothermal Units (MPTUs). Vernalization, like day length, yields a value between zero and one. These modules are run until a threshold level of MPTUs is reached. The number of days taken to reach this threshold is used to determine the stopping point of vegetative growth and onset of flowering in the second phase. In the second phase, the climate data is called again and used to determine the rate of photosynthesis, respiration, organ initiation and growth. Vegetative growth is determined by the rate of photosynthesis and carbon partitioning between roots and shoots (Carbon Dynamic module, Rasse & Tocquin, 2006), and includes the rate of organ production as a function of climate parameters (Functional-Structural Plant module). Specifically, leaf area is influence by temperature and light intensity, while the rate of leaf production is influenced by temperature. Each phase is initiated at sowing.

S2. Incorporating FT as a function of leaf tissue amount

To simulate the proportion of *FT* per unit tissue of each leaf, we used a beta function (Yin *et al.*, 1995) based on relative leaf age (*r*), with the youngest emerged leaf being one (equation [S2.1] to [S2.3], Figure 3a-c, main text).

[S2.1] $$\beta_{FT} = \max\left(0,\ \beta_{FTmx}\left[\left(\frac{r}{R_{opt}}\right)\left(\frac{R_{crit}-r}{R_{crit}-R_{opt}}\right)^{\left(\frac{R_{crit}-R_{opt}}{R_{opt}}\right)}\right]^{a}\right)$$

β_{FT} yields a value between zero and one. β_{FTmx} describes the maximum value that can be attained by a leaf of a single plant, R_{opt} is the relative age at which that maximum value is attained, R_{crit} is the oldest leaf that can express *FT*, *a* describes the steepness of the curvature. The beta function

oscillates if the independent variable spans a broad range. To avoid this behavior, we set β_{FT} to be zero below and above the relative ages where β_{FT} attains a minimum. β_{FTmx} and R_{opt} are dependent on the total number of leaves on a plant (l), as described below, avoiding the need to reparameterize for plants of different ages.

[S2.2] $$\beta_{FTmx} = 1 - \left(\frac{b}{l} \right)$$

[S2.3] $$R_{opt} = cl$$

b and c are coefficients. All parameter values are listed in Table S1.

S3. Determining whole-plant FT levels and accumulating FT to a threshold

To link *FT* transcript accumulation to leaf tissue production, the Phenology module is called at each time step (Figure 1, main text). We consider the output of the Phenology module to be the amount of *FT* produced per unit leaf tissue (*FT*, nmol cm^{-2}). This value is adjusted by the capacity of each leaf to express *FT* (β_{FT}, unit-less modifier), along with the leaf area (*LA*, cm^2), as shown below.

[S3.1] $$FT_{leaf} = LA \text{ x } \beta_{FT} \text{ x } FT$$

At each time step, FT_{leaf} (nmol $leaf^{-1}$) is determined for each leaf, summed across all leaves, and added to the value from the previous time step to determine whole-plant *FT* levels. Such accumulation of *FT* is consistent with the observation that several inductive long-days or several days of artificial induction of *FT* are needed to induce a flowering response (Corbesier *et al.*, 2007; Krzymuski *et al.*, 2015; Kinmonth-Schultz *et al.*, 2016). The model then runs until a threshold level of *FT* is reached. As with FM-1, this version considers relative levels of *FT*.

Note that within the Phenology module, we removed the equation relating *FT* amount as an area under the curve to day length from FM-1 (Chew *et al.*, 2014 see SOM Eq. 3.7.1) and instead use direct accumulation of *FT*. That equation had been used to modify the rate of thermal time accumulation by the influence of day length. We maintained the vernalization component from FM-1, as vernalization should modify overall levels of *FT* (Helliwell *et al.*, 2006; Searle *et al.*, 2006). The latter, while not applicable to our conditions, maintains the flexibility of the model in other conditions. This value falls between zero and one and now modifies the levels of *FT* produced within the Phenology model, rather than modifying the rate of thermal unit accumulation. We removed the thermal time component from the Phenology module entirely, as temperature is now incorporated through *FT* accumulation and the rate of leaf development.

S4. Adjusting leaf area to respond to temperature

We used leaf area to determine the amount of leaf tissue present as *FT* induction is dependent on light intercepted by the leaf. While FM-1 could capture the decrease in leaf area with decreasing

temperature in plants exposed to different constant temperatures, it simulated larger leaf areas for plants grown in fluctuating temperature conditions than the constant temperature control. This is contrary to observed behavior as plants seem to accumulate similar biomass under fluctuating temperatures relative to a constant, warm temperature control, but have a lower Specific Leaf Area (SLA, $m^2\ g^{-1}$) (Pyl *et al.*, 2012). This problem occurred for two reasons. First, SLA decreases with increasing thermal time (i.e. developmental time, Christophe et al. 2008). This relationship was used in FM-1 and caused a lower SLA and lower leaf area in plant simulations of warmer conditions as plants develop faster. Second, maintenance respiration is lower under cooler temperatures. Under fluctuating temperature conditions, when plants have first been exposed to warm temperatures and have accumulated the same amount of stored carbon as the control, a lower rate of maintenance respiration leaves a larger pool of carbon that can be used for growth. To address these issues, we adjusted the Specific Leaf Area (SLA, m2/g-1) to decline with decreasing temperature (using a relationship from Pyl et al. 2012 Figure 1e), and removed the temperature sensitivity of maintenance respiration.

S5. FT transcript accumulation in fluctuating temperature conditions simulated through influence of SVP and CO activity

Under long days, in 22 °C day and 12 °C night, fluctuating temperature conditions, *FT* was suppressed at dusk compared to 22 °C constant-temperature conditions (Kinmonth-Schultz et al. 2016) likely through the action of SVP and the FLM-β splice variant. This is consistent with prior observations under constant temperatures (Blazquez *et al.*, 2003; Lee *et al.*, 2007, 2013; Posé *et al.*, 2013). SVP protein levels increase shortly after exposure to cool temperatures (Kinmonth-Schultz et al. 2016), as does the ratio of *FLM-β* to *FLM-δ* splice variants (Posé *et al.*, 2013). FLM-β facilitates SVP binding. SVP and FLM-β protein levels increase with decreasing temperatures (Lee *et al.*, 2013). While both SVP and FLM-β are present at 23 °C, a transfer from 23 °C to 27 °C results in a decay of SVP that occurs within 12-hs after being moved to 27 °C (Lee *et al.*, 2013). We use a single term to simulate the combined behavior of SVP and FLM-β termed "SVP activity". Consistent with the observed behavior of these proteins, we modeled SVP activity to increase in response to a decrease in temperature, as shown below.

[S5.1] $$SVP_{new}(t) = \min\left\{SVP_{mx},\ \max\left[0,\ \left(d - \left(VT_{SVP}T(t)\right)\right)\right]\right\}$$

SVP_{new} is the newly synthesized protein (nmol), SVP_{mx} is the maximum rate of synthesis in response to decreasing temperature, VT_{SVP} describes the degree of decrease of SVP synthesis in response to an increase in temperature, d is the intercept, used to adjust the overall amount of SVP synthesized, T is the temperature (°C), and t is time (h) in this and all subsequent equations. $t = 0$ at sewing. Values and units of each coefficient can be found in Table S1. In order to capture the suppression of *FT* at dusk, we caused the decay rate for SVP to be slightly lower than its production at cooler temperatures. This caused SVP activity to remain higher at 22 °C after a 12 °C night than in constant warm temperatures, even after several hs of exposure (Figure S2). The decay rate is modeled using a Michaelis-Menten function dependent on the concentration of SVP

present as shown below (equation [S5.2]). v_{SVP} is the maximum rate of decay and k_{SVP} is the Michaelis-Menten constant describing the concentration of SVP at which the rate of decay is ½ v_{SVP}.

[S5.2] $$SVP(t) = SVP_{new}(t) \cdot \exp\left(e \cdot SVP(t-1)\right) - v_{SVP}\frac{SVP(t-1)}{k_{SVP_1} + SVP(t-1)}$$

It is biologically likely that SVP activity would plateau rather than continue to accumulate, for example through spatial limitations of the SVP binding sites on the *FT* promoter. We caused SVP activity to decline at a rate proportional to the amount of SVP present, the rate of which is defined by coefficient *e* in equation [S5.2]. This causes SVP activity to plateau rather than continue to accumulate. Although we were interested in the response of *FT* to cool temperatures rather than the behavior of SVP activity *per se*, the relative levels in simulated SVP activity between 27 °C and 22 °C (1.5 to 5.3, a 3.5-fold change), and between 12 °C and 22 °C (5.3 to 38.8 a 7.3-fold change) was similar to the fold changes observed for SVP bound to genomic regions of *FT* across similar temperatures (Figure S2, Lee *et al.* 2013).

Under long days, in 22 °C day and 12 °C night, fluctuating temperature conditions, levels of *FT* are higher at dawn coinciding with higher levels of *CO* mRNA and protein in cool nights. It is possible that the SVP/FLM-β complex and CO act competitively at the *FT* promoter (Bratzel & Turck, 2015), with CO overcoming suppression by SVP/FLM-β at night when it's levels are high. FM-1 already describes the relationship between *FT* and CO protein in the Photoperiod module (Chew *et al.*, 2014). We adjusted this interaction by modifying the Michaelis-Menten function for competitive inhibition (Segal, 1976) of *FT* transcription in FM-1, such that the induction of *FT* by CO is influenced by the activity of SVP and FLM-β as below.

[S5.3] $$FT(t) = v_{CO_{p1}}\frac{CO_p(t-1)}{k_{CO_{p1}}\left(1+\frac{SVP(t-1)}{k_{SVP_2}}\right)+CO_p(t-1)} - v_{FT}\frac{FT(t-1)}{k_{FT}+FT(t-1)}$$

The lower case *v* and *k* are Michaelis-Menten constants either describing the rate of synthesis of *FT* as influenced by CO protein (CO_p) or SVP, or the degradation of *FT* as described for decay of SVP above (equation [S5.2]).

Like SVP activity, *CO* transcript accumulation is induced by cool temperatures (Kinmonth-Schultz *et al.*, 2016). However, it seems to respond to changes in temperature. To note changes in temperature, the model queries the temperature at each time step. If the current temperature is higher than the temperature at the previous time step, the current temperature is set as the maximum temperature. Induction of *CO* seems to respond to the degree of temperature change as a drop of 10 °C yielded a greater increase in *CO* transcript accumulation than did a drop of 5 °C (Kinmonth-Schultz *et al.*, 2016). We made induction of *CO* mRNA (*KT*) linearly related to the temperature difference between the maximum and current temperature (*delta T*) as shown below (equation [S5.4]).

[S5.4] $$KT = KT_o \cdot delta\ T \cdot \exp\left(-f\left(t_{delta\ T}\right)\right)$$

Coefficient *f* describes the rate at which induction of *CO* changes with *delta T*, and $t_{delta\ T}$ is the time (days) since the change in temperature occurred. *KT* is used to modify the relationship between *CO* mRNA (CO_m) and CO protein (CO_p), as shown below (equation [S5.5]).

[S5.5] $$CO_p(t) = v_{CO_{p2}}\left(KT(t) + CO_m(t)\right)^g - v_{CO_{p3}}\frac{CO_p(t-1)}{k_{CO_{p2}} + CO_p(t-1)}(1 - L(t))$$

The coefficient *g* describes the strength of CO protein induction from *CO* mRNA. This term is needed to cause upregulation of CO protein at night, as CO protein is degraded more heavily at night (Song *et al.*, 2015). This was done instead of modifying the degradation rate, as temperature seems to influence CO primarily through transcriptional regulation (Kinmonth-Schultz *et al.*, 2016). All other aspects of equation [S5.5] remained the same as that used in FM-1 (Chew *et al.*, 2014, see S.O.M. equation [S3.4.14]). *FT* can be induced by a drop in temperature in the light as well as in the dark (Schwartz *et al.*, 2009; Thines *et al.*, 2014). If the change to cool temperatures occurs during the day, and the temperature then remains cool, *FT* is strongly elevated four days after the change in temperature occurred (Kinmonth-Schultz *et al.*, 2016). *CO* is slightly higher as well. The model as thus far described, showed this behavior. However, simulated *FT* was strongly elevated and flowering occurred extremely early (five leaves, data not shown). We addressed this problem in two ways. First, instead of remaining high after a change to cool temperatures occurs, induction of *CO* would likely decline over time if the temperature afterwards remains stable. We do observe a decline over time (Figure S3), and the rate of decline is described by *g* above (equation [S5.4]). The time since a change in temperature occurred is described by $t_{g_{temp}}$. Second, we lowered *g* in equation [S5.5] above if the change in temperature occurred during the day. This was done to reduce the strength of CO protein induction and to cause the relative *FT* amounts between the treatment and control groups to be similar to those observed. Likely, the model fails to capture some regulation of *CO* or *FT* that occurs during the day. That regulation is beyond the scope of this study.

S6. Model extension: adjustments used to improve model fit in conditions causing late flowering

The version of the model described in section S1 to S5, version FM-1.5, predicts delayed flowering for plants exposed to cool constant temperatures and to plants exposed to 12-h day lengths. These conditions are known to delay flowering relative to warm temperatures or long days (Blazquez *et al.*, 2003; Kobayashi & Weigel, 2007). In FM-1.5, simulated *FT* is lower in cool constant temperatures relative to warm temperatures and in shorter day lengths relative to long days, consistent with previous observations (Kobayashi *et al.*, 1999; Blazquez *et al.*, 2003). However, as FM-1.5 predicts flowering based entirely on *FT* levels as observed in young plants, it likely fails to capture changing dynamics of floral regulators over developmental time. We explored two possible mechanisms which could accelerate flowering beyond that which was predicted by the model. First, suppression of *FT* by *SVP* seems to be more pronounced in young

plants, parallel with a change in the *FLM-β* to *FLM-δ* ratio (Kinmonth-Schultz *et al.*, 2016). To cause *SVP* activity to decline over time we modified equation [S5.2] as follows:

[S6.1] $$SVP(t) = SVP_{new}(t) \cdot \exp\left[\left(e \cdot \exp\left(h(t_{age})\right)\right) SVP(t-1)\right] - v_{SVP} \frac{SVP(t-1)}{k_{SVP} + SVP(t-1)}$$

This modification, described by *g* in equation S6.1 above, adjusted the maximum level of SVP activity relative to plant age (t_{age}). This value was fit from the change in peak *FT* expression over two weeks (Kinmonth-Schultz *et al.*, 2016). Second, just as *FT* seems to be expressed primarily in the first few true leaves, a second florigen-like compound such as photosynthates or gibberellic acid, as discussed in the main text, could increase in leaves produced later. We simulated this second hypothetical, Factor X, similarly to what we did in equations [S2.1] to [S2.3] as shown below.

[S6.2] $$\beta_X = \max\left(0,\ \beta_{Xmx}\left[\left(\frac{r}{R_{opt_2}}\right)\left(\frac{R_{crit_2} - r}{R_{crit_2} - R_{opt_2}}\right)^{\left(\frac{R_{crit_2} - R_{opt_2}}{R_{opt_2}}\right)}\right]^m\right)$$

[S6.3] $$\beta_{Xmx} = l \cdot n$$

[S6.4] $$R_{opt_2} = o \cdot l$$

B_{Xmx} describes the maximum amount of Factor X that can be attained by a leaf of a single plant, R_{opt_2} is the relative age at which that maximum value is attained, R_{crit_2} is the oldest leaf that can express *FT*, *m* describes the steepness of the curvature. *n* and *o* relate total leaf number with the maximum level of Factor X that can be attained and the leaf, by relative age, that attains that max value.

Table S1: Coefficients values for equations used in FM-1.5.

Eq.	Coef.	Description	Value	Units
2.1	R_{crit}	Oldest leaf capable of expressing *FT*	30	
2.1	a	Describes the curvature of the slope as *FT* increases and decreases with leaf age	12	
2.2	b	Term relating the maximum level of *FT* expression to total leaf number	2.25	
2.3	c	Term relating total leaf number to which leaf (based on relative leaf age) expresses the highest level of *FT*	0.65	
5.1	SVP_{mx}	Maximum rate of SVP protein	12	nmol h^{-1}
5.1	d	Intercept in the negative linear relation between SVP synthesis and temperature	16	nmol
5.1	VT_{SVP}	The degree of decrease of SVP protein in response to an increase in temperature	0.35	nmol $^{\circ}C^{-1}$
5.2	e	The rate at which SVP activity declines relative to the total SVP present	-0.003	nmol $nmol^{-1}$
5.2	v_{SVP}	Maximum rate of decay of SVP activity	8.85	nmol h^{-1}
5.2	k_{SVP_1}	The concentration of SVP at which the rate of decay is ½ v_{SVP}	0.55	nmol
5.3	$v_{CO_{p1}}$	Maximum rate of *FT* mRNA synthesis with CO protein	40	nmol h^{-1}
5.3	$k_{CO_{p1}}$	The concentration of CO protein at which the rate of *FT* synthesis is ½ $v_{CO_{p1}}$	4.5	nmol
5.3	k_{SVP_2}	The equilibrium constant describing the strength with which SVP binds to *FT* regulatory regions	6	nmol
5.3	v_{FT}	Maximum rate of *FT* mRNA decay	70	nmol h^{-1}
5.3	k_{FT}	The concentration of *FT* at which the rate of decay is ½ v_{FT}	62	nmol
5.4	KT_o	The change in *CO* mRNA production with the difference between the maximum and current temperature	0.2561	nmol $^{\circ}C^{-1}$
5.4	f	Rate at which induction of CO declines over time	0.261	nmol day^{-1}
5.5	$v_{CO_{p2}}$	Rate of CO protein production with *CO* mRNA amount	0.3	nmol h^{-1}
5.5	g	Strength of CO protein induction from *CO* mRNA, when the temperature drops during the night	2.45	
5.5	g^*	Strength of CO protein induction from *CO* mRNA, when the temperature drops during the day	1.556	
5.5	$v_{CO_{p3}}$	Maximum rate of CO protein decay	44.55	nmol h^{-1}
5.5	$k_{CO_{p2}}$	Concentration of CO protein at which the decay	2	nmol

		rate is ½ $v_{CO_{p3}}$		
6.1	e	Rate at which SVP activity declines relative to the total SVP activity	0.002	nmol nmol^{-1}
6.1	h	Rate at which SVP activity declines with plant age	0.0414	nmol day^{-1}
S6.2	R_{crit_2}	Oldest leaf capable of expressing Factor X	60	
S6.2	m	Describes the curvature of Factor X as it increases and decreases with leaf age	12	
S6.2	n	Relates the maximum value of Factor X to total leaf number (l)	0.6	
S6.2	o	Relates total leaf number with the leaf (by relative leaf age) that expresses the highest value of Factor X	0.1	

Figure S1. Graphic representation of FM-1.

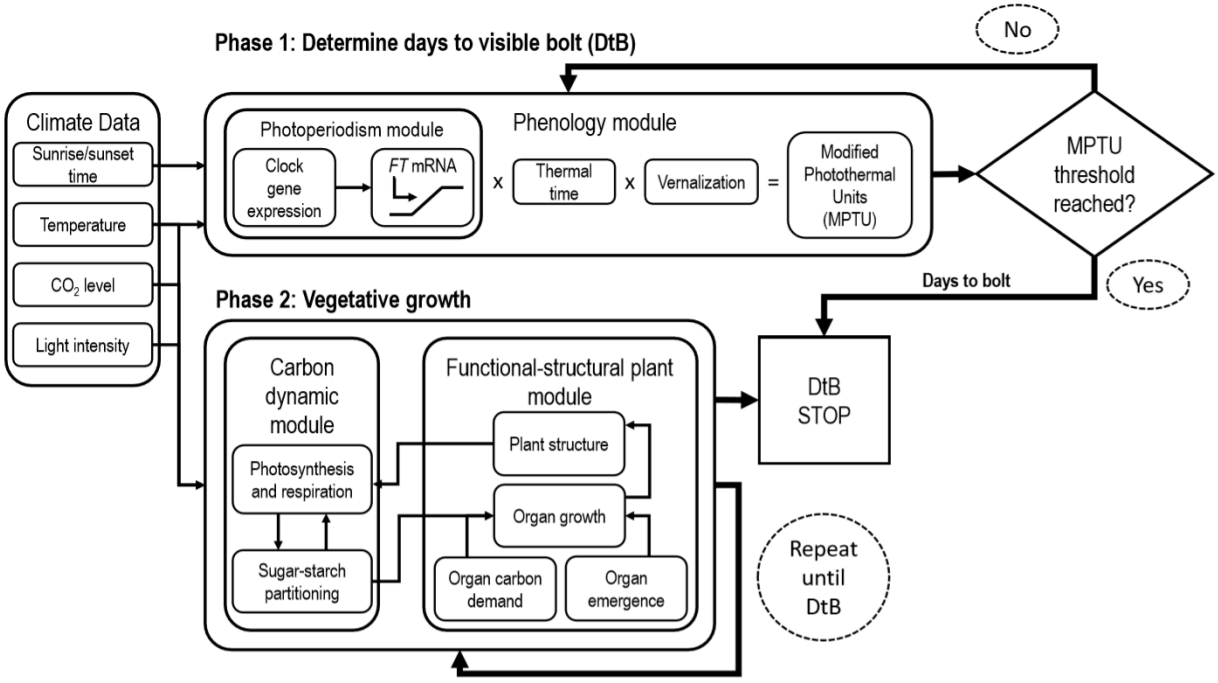

Figure S2. Simulated SVP activity in long-day constant temperature (22 ˚C) and temperature-cycle conditions (22-12 ˚C and 27-22 ˚C). The cooler temperature lasted for the duration of the night. Arrows indicate the SVP activity levels that are observed at 12, 22, and 27 ˚C.

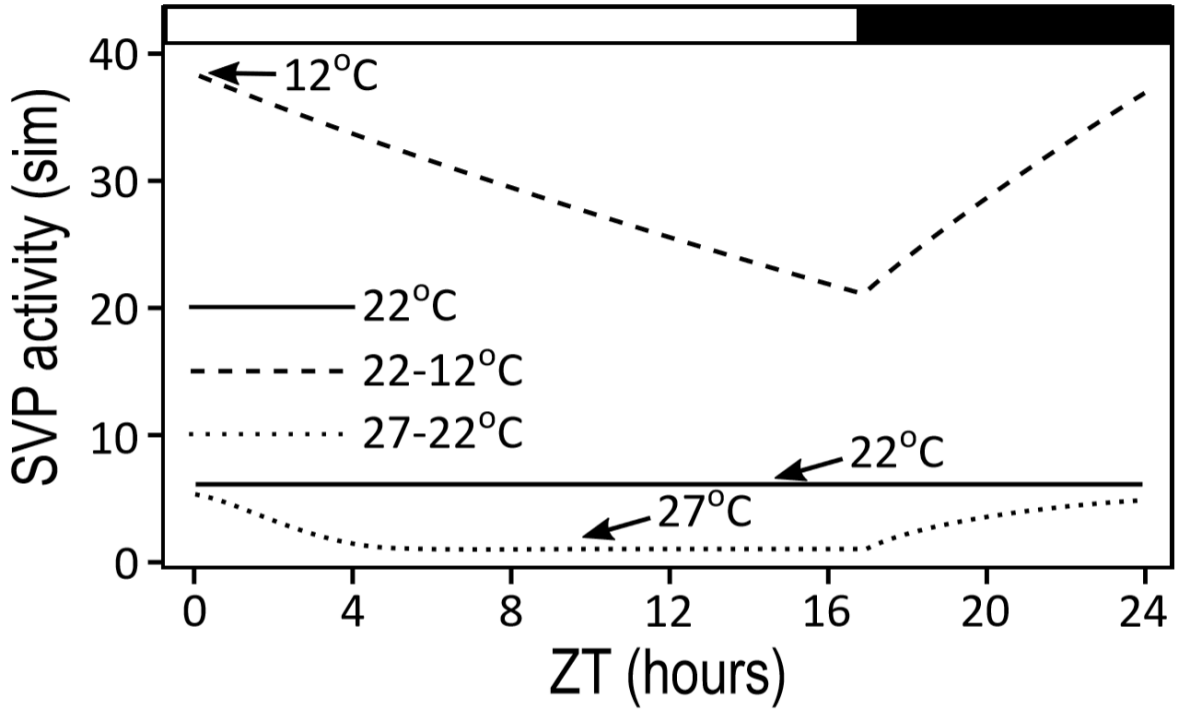

Figure S3. The levels of *CO* transcript after a drop from 22 to 12 ˚C relative to levels in plants that had remained at 22 ˚C. The drop from 22 to 12 ˚C occurred just after dawn on day 1. The daily averages of three time points (ZT0, 8, and 16) were compared.

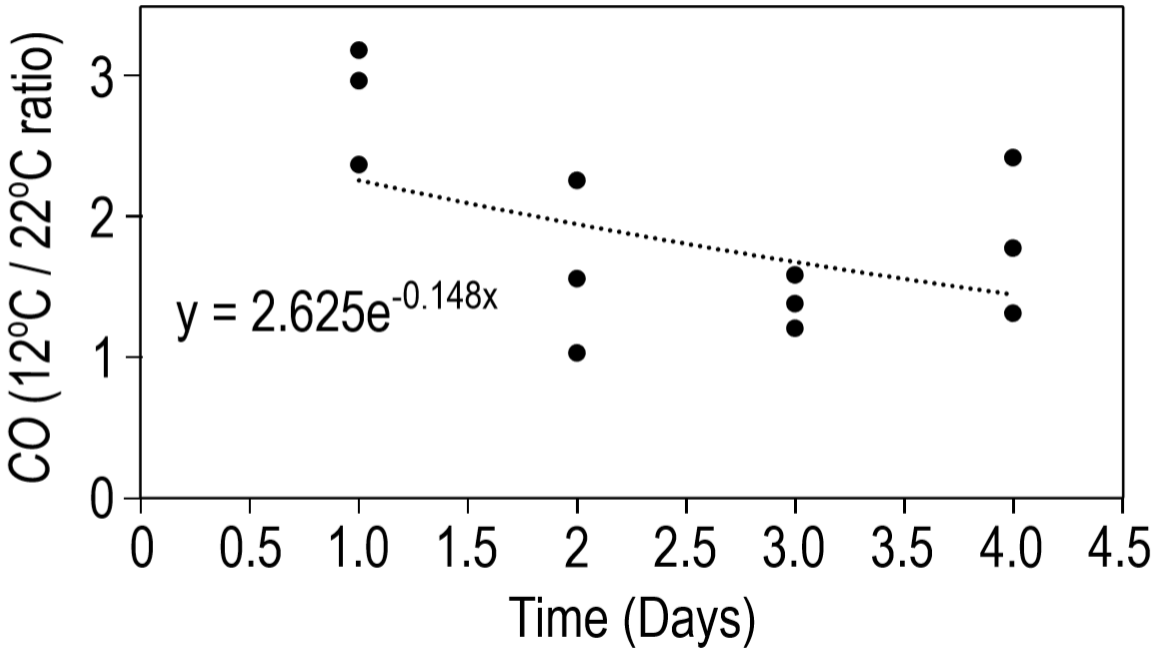

Figure S4. The spatial expression profile of *FT* changes with leaf age. The staining pattern of *pFT:GUS* plants aged two, three, four, and six weeks 16 hours after dawn after exposure to long days or short days for three days. Images were compiled from smaller microscope images as leaves were too large for a single frame. The traced images were used to determine percent leaf area stained, the un-traced images are shown for comparison. Leaves are ordered by relative leaf age, with one being the youngest. Scale bars = 2.5 mm unless indicated by an asterisk (* = 1 mm, ** = 0.5 mm).

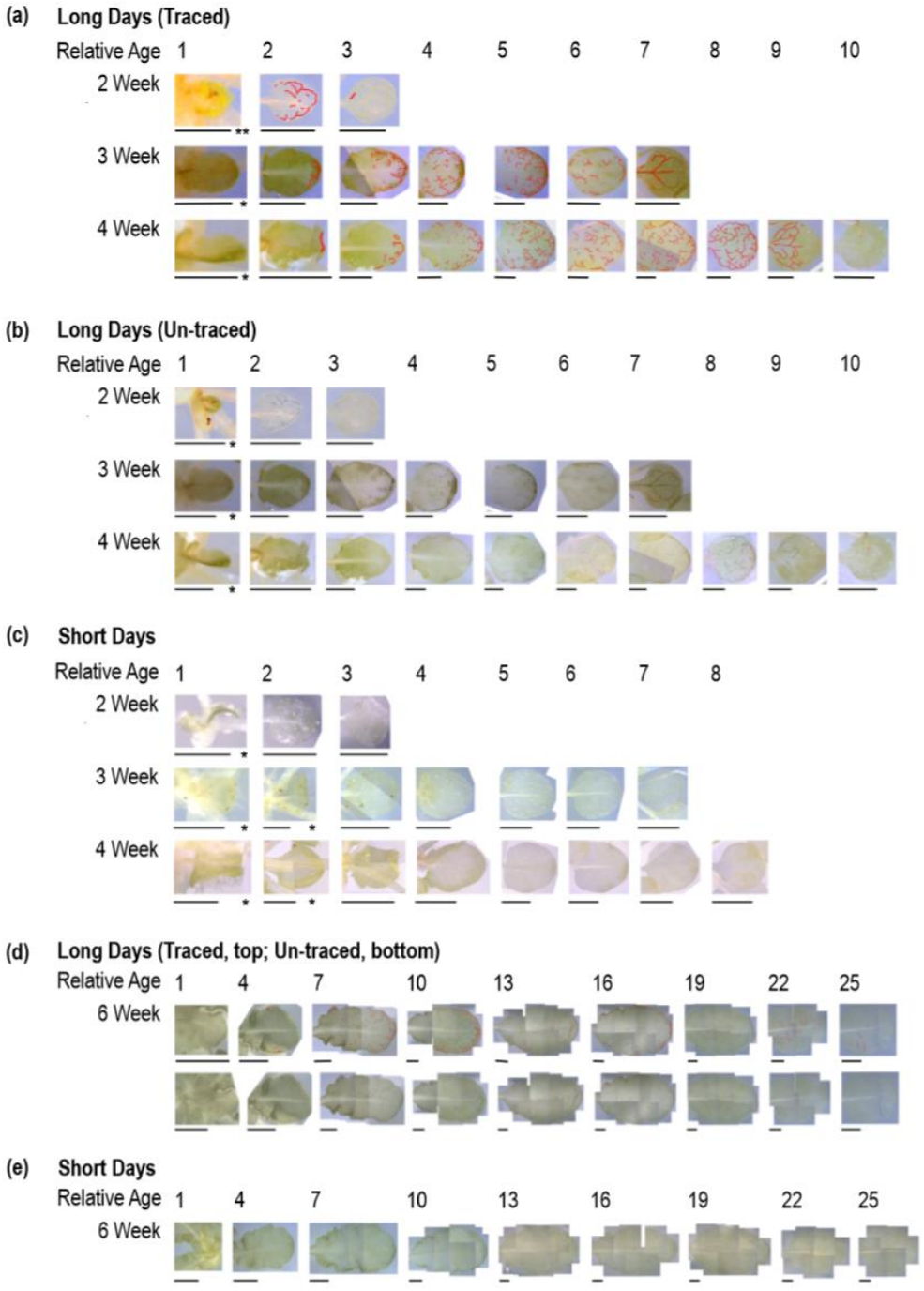

Figure S5. Leaf production slows during short-term exposure to cool temperatures. The average leaf number of plants exposed to 12 °C for two, four, or six days in long days relative to the warm-temperature (23.7 °C day, 22.9 °C night) control.

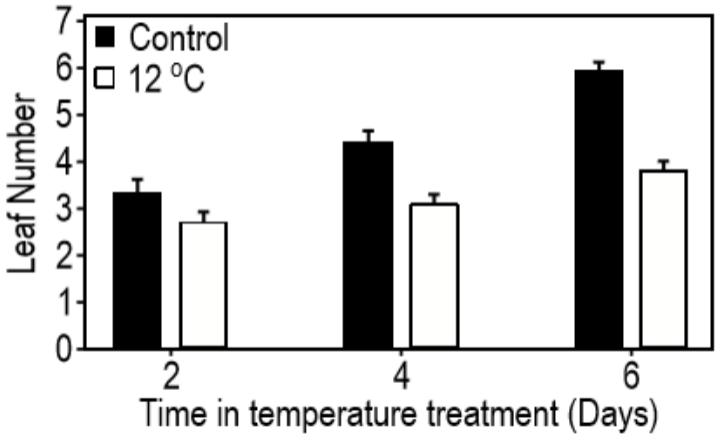

References

Blazquez M, Ahn J, Weigel D. **2003**. A thermosensory pathway controlling flowering time in *Arabidopsis thaliana*. *Nature Genetics* **33**: 168–171.

Bratzel F, Turck F. **2015**. Molecular memories in the regulation of seasonal flowering: from competence to cessation. *Genome Biology* **16**: 192.

Chew YH, Wenden B, Flis A, Mengin V, Taylor J, Davey CL, Tindal C, Thomas H, Ougham HJ, Reffye P de, *et al.* 2014. Multiscale digital *Arabidopsis* predicts individual organ and whole-organism growth. *Proceedings of the National Academy of Sciences* **111**: E4127–E4136.

Chew YH, Wilczek AM, Williams M, Welch SM, Schmitt J, Halliday KJ. **2012**. An augmented *Arabidopsis* phenology model reveals seasonal temperature control of flowering time. *New Phytologist* **194**: 654–665.

Corbesier L, Vincent C, Jang S, Fornara F, Fan Q, Searle I, Giakountis A, Farrona S, Gissot L, Turnbull C, *et al.* 2007. FT protein movement contributes to long-distance signaling in floral induction of *Arabidopsis thaliana*. *Science* **316**: 1030–1033.

Helliwell CA, Wood CC, Robertson M, James Peacock W, Dennis ES. **2006**. The *Arabidopsis thaliana* FLC protein interacts directly in vivo with *SOC1* and *FT* chromatin and is part of a high-molecular-weight protein complex. *Plant Journal* **46**: 183–192.

Kinmonth-Schultz HA, Tong X, Lee J, Song YH, Ito S, Kim S-H, Imaizumi T. **2016**. Cool night-time temperatures induce the expression of *CONSTANS* and *FLOWERING LOCUS T* to regulate flowering in *Arabidopsis*. *New Phytologist* **211**: 208–224.

Kobayashi Y, Kaya H, Goto K, Iwabuchi M, Araki T. **1999**. A pair of related genes with antagonistic roles in mediating flowering signals. *Science* **286**: 1960–1962.

Kobayashi Y, Weigel D. **2007**. Move on up, it's time for change--mobile signals controlling photoperiod-dependent flowering. *Genes & Development* **21**: 2371–2384.

Krzymuski M, Andrés F, Cagnola JI, Seonghoe J, Yanovsky M, Coupland G, Casal JJ. **2015**. The dynamics of *FLOWERING LOCUS T* expression encodes long-day information. *Plant journal* **83**: 952–961.

Lee JH, Ryu H-S, Chung KS, Posé D, Kim S, Schmid M, Ahn JH. **2013**. Regulation of temperature-responsive flowering by MADS-Box transcription factor repressors. *Science* **342**: 628–632.

Lee JH, Yoo SJ, Park SH, Hwang I, Lee JS, Ahn JH. **2007**. Role of *SVP* in the control of flowering time by ambient temperature in *Arabidopsis*. *Genes & Development* **21**: 397–402.

Posé D, Verhage L, Ott F, Yant L, Mathieu J, Angenent GC, Immink RGH, Schmid M. **2013**. Temperature-dependent regulation of flowering by antagonistic FLM variants. *Nature* **503**: 414–417.

Pyl E-T, Piques M, Ivakov A, Schulze W, Ishihara H, Stitt M, Sulpice R. **2012**. Metabolism and growth in *Arabidopsis* depend on the daytime temperature but are temperature-compensated against cool nights. *Plant Cell* **24**: 2443–2469.

Rasse DP, Tocquin P. **2006**. Leaf carbohydrate controls over *Arabidopsis* growth and response to elevated CO_2: an experimentally based model. *New Phytologist* **172**: 500–513.

Salazar JD, Saithong T, Brown PE, Foreman J, Locke JCW, Halliday KJ, Carré IA, Rand DA, Millar AJ. **2009**. Prediction of photoperiodic regulators from quantitative gene circuit models. *Cell* **139**: 1170–1179.

Schwartz C, Balasubramanian S, Warthmann N, Michael TP, Lempe J, Sureshkumar S, Kobayashi Y, Maloof JN, Borevitz JO, Chory J, *et al.* 2009. Cis-regulatory changes at *FLOWERING LOCUS T* mediate natural variation in flowering responses of *Arabidopsis thaliana*. *Genetics* **183**: 723–732.

Searle I, He Y, Turck F, Vincent C, Fornara F, Kröber S, Amasino RA, Coupland G. **2006**. The transcription factor FLC confers a flowering response to vernalization by repressing meristem competence and systemic signaling in Arabidopsis. *Genes & Development* **20**: 898–912.

Segal IH. **1976**. *Biochemical Calculations: How to Solve Mathematical Problems in General Biochemistry*. Canada: John Wiley and Sons.

Song Y-H, Shim J-S, Kinmonth-Schultz HA, Imaizumi T. **2015**. Photoperiodic flowering: time measurement mechanisms in leaves. *Annual Review of Plant Biology* **66**: 441–464.

Thines BC, Youn Y, Duarte MI, Harmon FG. **2014**. The time of day effects of warm temperature on flowering time involve PIF4 and PIF5. *Journal of Experimental Botany* **65**: 1141–1151.

Wilczek AM, Roe JL, Knapp MC, Cooper MD, Lopez-Gallego C, Martin LJ, Muir CD, Sim S, Walker A, Anderson J, *et al.* 2009. Effects of genetic perturbation on seasonal life history plasticity. *Science* **323**: 930–934.

Yin X, Kropff MJ, McLaren G, Visperas RM. **1995**. A nonlinear model for crop development as a function of temperature. *Agricultural and Forest Meteorology* **77**: 1–16.

Chapter 5

Concluding thoughts: It comes down to scale

Chapter 5

Concluding thoughts: It comes down to scale

The interactions of internal and external stimuli regulate plant development

My aim has been to understand how complex internal and external cues converge to regulate developmental shifts in plants. I began by exploring three known circadian outputs – diurnal growth, flowering, and cold response (Kinmonth-Schultz *et al.*, 2013). Through this review, I discussed that whether a process is under tight control of the circadian clock depends on the dynamics of the immediate environment. For example, leaf growth seems to be buffered to dynamic fluctuations in temperature, showing a consistent rhythmic rate of expansion throughout its growth cycle (Poiré *et al.*, 2010; Pantin *et al.*, 2011). Root growth does not have the same degree of buffering, perhaps because the temperature of the soil is more stable, but also because root growth must respond to a heterogeneous environment in which available nutrients and water resources may be patchy (Walter *et al.*, 2009). However, even rhythmic processes buffered by the circadian clock vary in their timing depending on environmental limitations. Rhythmic leaf growth peaks during the day in young *Arabidopsis* leaves when plants are photosynthesizing, because carbon, needed to build cell walls, is the limiting factor (Pantin *et al.*, 2011). Peak growth occurs at night in older plants, when stomata are closed and water loss is decreased, because turgor, needed to drive cell expansion, is highest.

Similar changes in rhythmic growth occur in the hypocotyls of young seedlings in *Arabidopsis* dependent on light quality, sucrose availability, and temperature (Stewart *et al.*, 2011; Nomoto *et al.*, 2013). The known mechanisms regulating hypocotyl growth help explain how a circadian-controlled process may still respond flexibly to the environment. Hypocotyl growth is regulated through the *PHTYTOCHROME INTERACTING FACTORS* (*PIF*) *4* and *5* which are degraded under red light through PHYTOCHROME B (PHYB) in a clock-dependent manner (Nusinow *et al.*, 2011). This gating limits *PIF4* and *PIF5* expression to shaded conditions during long days or to around dawn in short days (Farré, 2012). However, sucrose can also stabilize the PIF5 protein throughout the day (Stewart *et al.*, 2011). Considering both leaf and hypocotyl growth, it appears that the circadian clock serves both to buffer growth responses to dynamic environments, while also restricting the perception of some environmental cues to specific times of the day.

The mechanisms regulating flowering are well understood for several environmental cues in isolation, and many affect a few key flowering regulator genes. The flowering pathway, therefore, can be used to explain how several environmental cues might converge on a clock-mediated output to regulate development (Kinmonth-Schultz *et al.*, 2013). We focused on *FLOWERING LOCUS T* (*FT*), a key component of photoperiodic (day length) perception in plants (Song *et al.*, 2015). *FT* expression levels are tightly linked to flowering, and it is a key component of florigen, the messenger responsible for carrying environmental signals perceived in the leaves to the shoot apex where flowering is induced (Corbesier *et al.*, 2007). To restrict the expression of *FT* to long days, the expression of its transcriptional activator, *CONSTANS* (*CO*), is repressed in the morning by CYCLING DOF FACTORs (CDFs). The CDFs are degraded in the afternoon in response to light in long days through the FLAVIN-BINDING, KELCH REPEAT, F-BOX 1 (FKF1)-GIGANTEA (GI) complex (Sawa *et al.*, 2007). This releases repression on *CO*, facilitating *FT* expression. *FKF1* and *GI* are both regulated by the circadian clock (Sawa *et al.*, 2007). To ensure the CO protein signal is relegated to the long-day afternoon, the CO protein is rapidly degraded in the dark by the action of the CONSTITUTIVE

PHOTOMORPHOGENIC 1 (COP1) and SUPPRESSOR OF PHYA-105 1 (SPA1) E3 ubiquitin ligase complex (Zuo *et al.*, 2011). Light quality, and possibly temperature, affects flowering through the Phytochrome family of proteins (phyB, phyD, and phyE) and through *PHYTOCHROME AND FLOWERING TIME 1* (*PFT1*), which regulate *CO* as well as *FT* independently of CO (Iñigo *et al.*, 2012). Cool ambient temperatures also act to suppress *FT* dependently and independently of CO through HIGH EXPRESSION OF OSMOTICALLY RESPONSIVE GENES (HOS1) and through SHORT VEGETATIVE PHASE (SVP) (Lee *et al.*, 2007, 2012; Jung *et al.*, 2012). Heat and drought increase the expression of *FLOWERING BHLH3* (*FBH3*), which is a family member of *CO* transcriptional activators (Rizhsky *et al.*, 2004). Finally, plant carbon status as well as exogenous sucrose application can affect circadian clock genes as well as *FT* (Usadel *et al.*, 2008; Dalchau *et al.*, 2011).

There are several questions that follow from these studies. How do these mechanisms interact under a complex environment? Which pathways dominate? When might they act synergistically or antagonistically? Many of these studies were done in stable temperature environments (e.g. Sawa *et al.*, 2007). If temperature fluctuations were applied, they were often applied daily for the life of the plant (e.g. Lee *et al.*, 2012). Often, conditions were such that one pathway was saturated, dominating the flowering response (e.g. the photoperiodic pathway in long days, Sawa *et al.*, 2007). These studies have yielded valuable insight; however, we are missing a more accurate portrayal of what may be happening in nature. A simpler question, which I begin to address below, is how do plants respond to multiple environmental cues when experienced in tandem? A more complex question, which remains to be answered, is how do environmental cues change over the lifetime of a plant? For example, when do summer annuals germinate, and how many leaves are they able to produce before day lengths become saturating? If long day lengths are not experienced until later in development, perhaps day length interacts with other pathways rather than dominating as is the case when seedlings germinate in long-day conditions. How does temperature change from germination to flowering? To better understand flowering in natural environments, we need to explore these complex interactions.

How do plants sense and respond to multiple environmental factors?

To begin addressing plant response in complex environments, I asked the following in my third (Kinmonth-Schultz *et al.*, 2016) and fourth chapters: How do plants sense and respond to two environmental cues experienced together? Is it possible to predict plant response in a dynamic natural environment? In my first chapter, I proposed that a response in a complex environment could be decomposed into separate, predictable plant responses. To address this, I asked how the key flowering regulator gene, *FT*, would respond under different day length conditions, when the temperature fluctuated, such that the days were warm and the nights were cool. These conditions are closer to that experienced by plants grown in natural environments.

Prior to beginning this study, we understood the photoperiodic (day length) regulation of *FT*, as described in the preceding section, under constant temperature conditions (Golembeski *et al.*, 2014). We understood as well, that growth in cool constant temperature conditions represses *FT* through the action of *SVP* and *FLOWERING LOCUS M-β* (*FLM-β*) delays flowering (Blazquez *et al.*, 2003; Lee *et al.*, 2007; 2013; Pose *et al.*, 2013). We did not yet know how temperature cycles would affect *FT* and plant response when they were overlaid onto diurnal light dark cycles. From the prior data, we expected that *FT* would simply be suppressed after exposure to

cool-night temperatures. Surprisingly, we found a different pattern. *FT* was suppressed at dusk as expected; however, it was higher at dawn compared to the constant, warm temperature control (Figure 5.1). We demonstrated that this pattern could be decomposed into two separate processes. First, a drop in temperature that occurs during a 24-hour period seems to induce the transcription of *CO* through the activity of the FBH family of transcriptional activators (Ito *et al.*, 2012). The induction of *CO* mRNA and the subsequent production of CO protein is higher than that of CO protein degradation even at night, causing *FT* to be induced. This pattern of *FT* induction, is consistent with that of *FT* from plants grown in temperature cycle conditions in constant light. In those conditions, *FT* is high during the cool period of the cycle (Schwartz *et al.*, 2009). Second, both SVP and the FLM-β splice variant that aids SVP binding to the *FT* regulator regions are higher under cooler temperatures (Lee *et al.*, 2007, 2013; Posé *et al.*, 2013). This leads to suppression of *FT* under cool constant as well as fluctuating temperature environments.

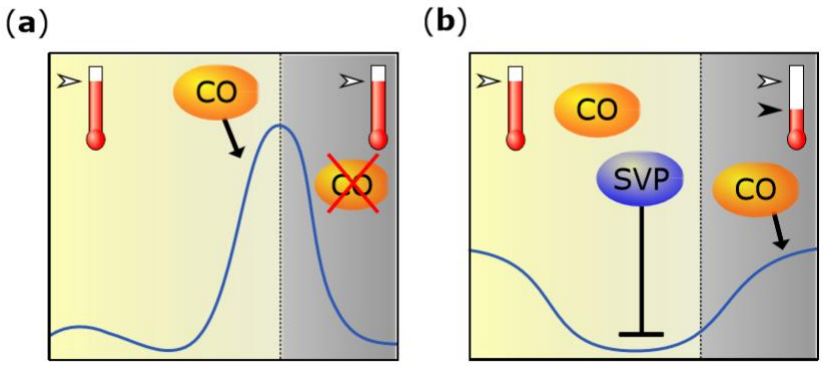

Figure 5.1. The behavior of *FT* in warm-day, cool-night conditions can be explained by the suppressive and inductive actions of SVP and CO, respectively. Under constant, warm temperatures CO protein induces *FT* expression (blue line) at the end of the day in long days (a). CO protein is degraded at night causing a rapid decline of *FT* in the dark. In warm-day cool night conditions, a drop from warm to cool temperatures stabilizes SVP protein and induces *CO* leading to higher levels of CO protein at night (b). Consequently, *FT* is suppressed by SVP and induced by CO.

I incorporated these two mechanisms into an existing model of *FT* photoperiodic regulation (Salazar *et al.*, 2009; Chew *et al.*, 2014) and confirmed that they could recapitulate the pattern of *FT* response that we had observed in plants. Further, I clarified how this might occur. In order for an accurate simulation of the *FT* transcriptional profile, we assumed, first, that CO and SVP might act competitively at the *FT* regulatory regions. This is consistent with our emerging understanding of the complex regulation of the *FT* gene (Bratzel & Turck, 2015). Second, for SVP and FLM-β to suppress *FT* at dusk after 16 hours of warm temperatures, the degradation rate of their activity must be lower than production such that their activity is still high after several hours of warm temperatures (Figure 5.2).

There remain several questions regarding temperature regulation of *FT*. What causes the strong induction of *CO* and how do the FBHs act in this process? One possible upstream mechanism for this is a change in membrane fluidity. Tension imposed on the cell membrane can induce gene expression changes, as in the pathogen response (Monshausen & Haswell, 2013). Rapid declines in temperature affect the fluidity and therefore surface tension of the membrane (Murata & Los,

1997). Further, how might the response of *CO* differ when temperature ramps gradually over the course of the day? Our model would show an induction of *CO* in these conditions, but does this occur in plants. Finally, does SVP, indeed, remain on *FT* regulatory regions over time as is predicted from our model?

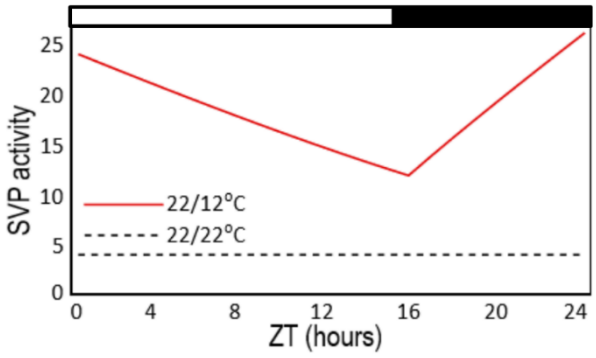

Figure 5.2. A degradation rate of SVP activity that is lower than its production is needed to explain suppression of *FT* at dusk in simulation. Even after several hours of exposure to 22 ˚C temperatures, simulated SVP remains higher at dusk after exposure to at 12 ˚C night (red line) than when in constant 22 ˚C temperatures (dashed, black line). The white and black bar indicates day and night.

Integrating molecular and whole-plant responses to temperature can explain flowering in fluctuating temperature environments

While we could describe the mechanistic regulation of *FT* in more natural warm-day, cool-night conditions it was not clear how this affected flowering. Flowering was delayed in these conditions relative to a constant, warm temperature control. However, flowering affects numerous plant processes, including plant growth and development (Parent *et al.*, 2010). How much of the delay that we observed was due to *FT* levels? I explored this question in two ways. First, I asked whether *FT* levels could correlate to flowering across multiple conditions (Kinmonth-Schultz *et al.*, 2016). I found that transcriptional levels of *FT* can be highly predictive of flowering across a range of day-length, temperature, and mutant lines (Figure 5.3). Qualitative observations linking *FT* expression to flowering had been made (Corbesier *et al.*, 2007; Fernández *et al.*, 2016). Simulation of *FT* area from models built based on observations of *FT* in long- and short-days, also correlated well with flowering in other day lengths (Salazar *et al.*, 2009). However, this was the first time that *FT* was quantitatively linked to flowering times across a range of conditions.

Second, I considered accumulation of *FT* over time with plant development, again using a mathematical modeling approach. *FT* is produced in the leaves. From there it moves to the shoot apex where it induces the floral transition (Corbesier *et al.*, 2007). The rate of leaf production is strongly related to temperature (Parent *et al.*, 2010). As more leaves are produced, the amount of *FT* that is perceived at the shoot apex should increase. Under cooler temperatures, whole-plant

FT levels should be affected both by the direct regulation of *FT* gene expression as described in the preceding section and by slower leaf emergence and expansion. The Framework Model 1 (Chew *et al.*, 2014) describes photoperiodic regulation of *FT* as well as leaf growth and development as a function of temperature. The original version, FM-1, utilized thermal time to predict the timing of flowering. Thermal time is the accumulation of thermal units, or degrees Celsius per unit time, such that flowering is predicted to be faster during a warm growing season than a cool one. FM-1 modulates the rate of accumulation of thermal time by day length through *FT* resulting in Modified Photothermal Units (MPTUs), such that flowering is predicted to occur most quickly when temperatures are warm and days are long.

I replaced the MPTU component of the model with direct accumulation of *FT* with leaf tissue production. I incorporated temperature regulation of simulated *FT* expression as described in the preceding section. This approach better predicted flowering in fluctuating temperature environments in long days than did the thermal unit approach (Figure 5.4).

As I mention in chapter one, some form of thermal time has been widely incorporated into models used to predict plant phenological shifts (Lehenbauer, 1914; Ritchie & Otter, 1985; Jamieson *et al.*, 1998a,b; Chuine, 2000; Jones *et al.*, 2003; Wilczek *et al.*, 2009; He *et al.*, 2012; Kumudini *et al.*, 2014). Frequently, day length and vernalization are incorporated by modifying the rate of accumulation of thermal time. However, these model often need to be reparameterized for new conditions (Piper *et al.*, 1996). For example, using thermal time, FM-1 fits well in some conditions when the influence of nighttime temperatures is excluded or reduced (Wilczek *et al.*, 2009; Chew *et al.*, 2012). For our warm-day, cool-night conditions, FM-1 better predicted flowering when nighttime temperatures were reincorporated.

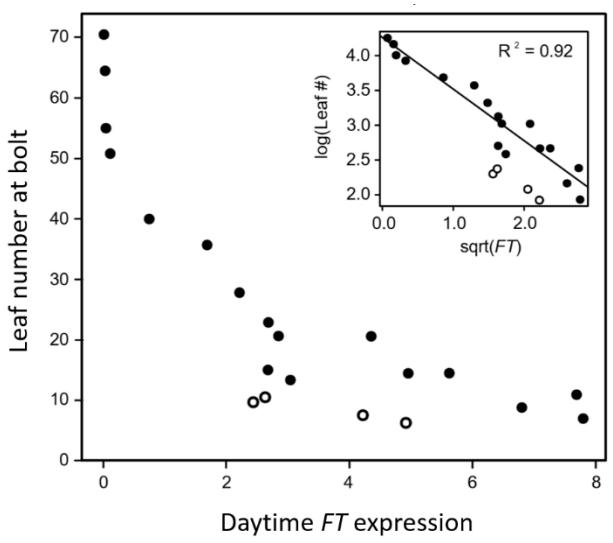

Figure 5.3. *FT* levels correlate with the timing of flowering. The timing of flowering, determined by the number of leaves produced before a visible flowering stalk (bolt) is produced is plotted over daytime *FT* expression, calculated as the area under the curve over a 24-hour period. Inset the linearized form of this data showing the correlation. Black circles are wild-type and mutant plants from the Columbia-0 background grown in multiple day length and ambient temperature conditions. The open circles are two other wild-type strains Landsberg *erecta*, and Wassilewskija-2 in long days in two different temperature conditions.

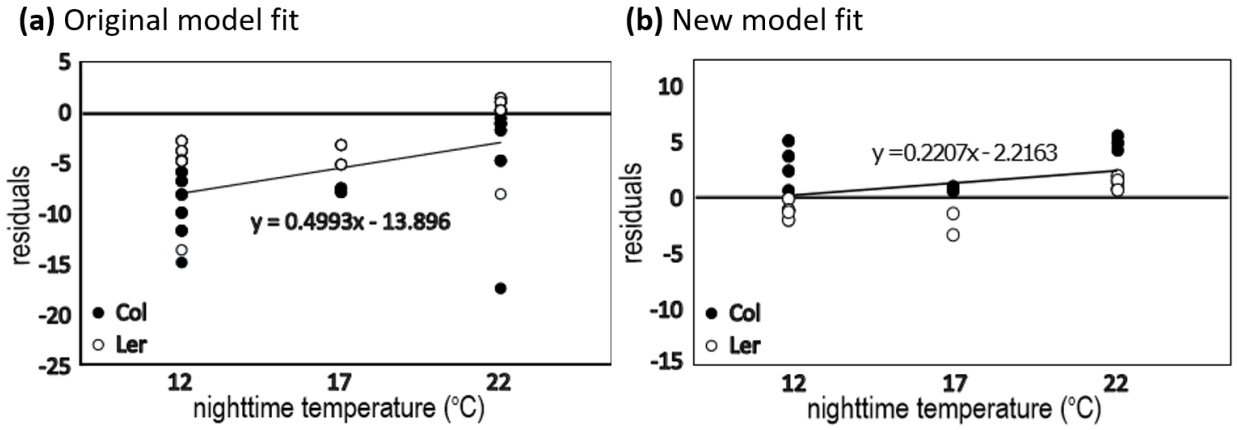

Figure 5.4. Simulating *FT* accumulation as a function of temperature and leaf tissue production improves the modeled fit compared to a Modified Photothermal Unit (MPTU) approach. The difference between predicted and observed days to bolt (residuals) plotted over three nighttime temperature treatments. Daytime temperatures were 22˚C. The original model (FM-1) predicted earlier than observed flowering in both 12 and 17 ˚C nighttime temperature conditions for Columbia-0 (Col) and Landsberg *erecta* (Ler) (a). This trend was reduced when MPTUs were replaced with direct temperature regulation of *FT* gene coupled with accumulation of *FT* with leaf tissue growth (b).

Incorporating the underlying mechanisms of plant response could reduce the need to reparameterize (White, 2009; Boote *et al.*, 2013). Our approach – direct temperature regulation of *FT* coupled with whole-plant *FT* accumulation – is consistent with models that use day length and vernalization to influence the final leaf number, while temperature influences the developmental rate (Brown *et al.*, 2013). *FT* is a known component underlying the influence of day length and vernalization on final leaf number (Amasino, 2010; Song *et al.*, 2015), and our approach suggests that direct temperature regulation of *FT* should be considered as a factor in these models as well. We further suggest that growth, resulting in the accumulation of gene products, is the underlying factor in the accumulation of thermal time.

Several questions remain that could help to clarify this approach. Do all leaves that express *FT* contribute to flowering? In grains, such as in rice, the flag leaf which is situated just below the spike, contributes a majority of the photosynthates to the developing grains (Li *et al.*, 1998). Could there be a similar distribution for florigen? How does FT protein or the effect of FT at the shoot apex accumulate over time? Whole plant analysis of *FT* mRNA shows that it cycles, rising from and declining to basal levels each day. However, the *FT* expression must be induced for several consecutive days for flowering to occur (Corbesier *et al.*, 2007; Krzymuski *et al.*, 2015; Kinmonth-Schultz *et al.*, 2016). Either the protein or the effects of FT on the chromatin of shoot-apex genes accumulate. How stable is this effect? Answering these questions will help clarify spatial as well as temporal regulation of *FT* and its influence on flowering in fluctuating natural environments.

Analyzing flowering regulation over a range of spatial and temporal scales

Considering both molecular regulation as well as whole-plant integration of *FT* can improve model predictions of flowering in some conditions. Taking such a whole-plant scale approach also provides an avenue on which to build further mechanistic understanding of climactic regulation throughout the growing season. In chapter four, we demonstrated that *FT* is highest in the first few true leaves produced, while later leaves produce only basal levels of *FT*. As leaves age, their *FT* levels also decline. When this behavior is incorporated into the model, whole-plant levels of *FT* eventually decline as the plant produces more and more leaves. This results in a plateau of accumulated *FT* (Figure 5.5). If *FT* plateaus before the threshold is reached, flowering does not occur. This is the case when *FT* is suppressed in shorter day lengths or under cool, constant temperatures. Had we not considered leaf age in *FT* expression, *FT* would eventually reach the threshold in all conditions, predicting flowering.

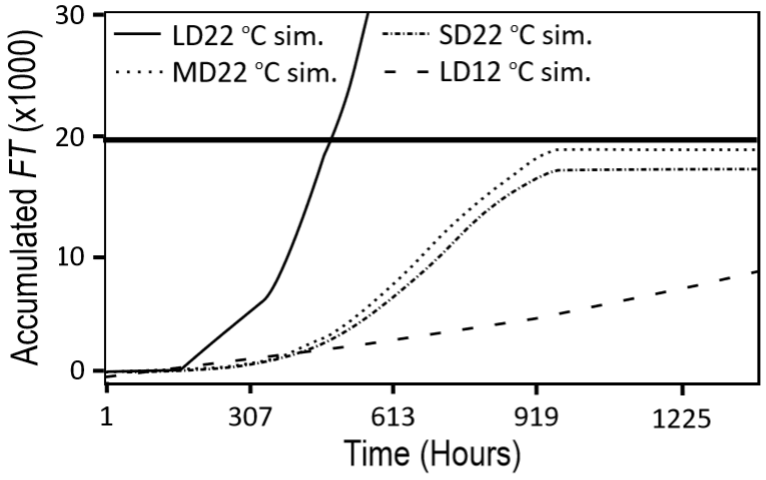

Figure 5.5. Simulated flowering occurs when accumulated *FT* reaches a pre-set threshold. Simulated (sim.) *FT* accumulates most quickly in long-day, warm temperature conditions (LD22 ˚C). It does not reach the plateau in short- (SD) or 12-hour (MD) day lengths, or in long days under cool temperatures (LD12 ˚C). The horizontal black bar is the pre-set threshold of *FT* determined by flowering times in LD22 ˚C conditions.

The fact that the model fails in these conditions is expected. *FT* is highest long-day conditions and other factors are thought to play a role as plants age (Blazquez & Weigel, 2000; Fornara & Coupland, 2009). Using a modeling approach, we can explore how these different flowering regulators interact with themselves and with climate throughout the lifetime of the plant. As *FT* declines, other factors may increase in the leaves or other plant tissues. Sucrose was long thought to be a florigen as carbon metabolites were found to increase at the shoot apex around the time of the floral induction (Golembeski *et al.*, 2014). Now, TREHELOSE-6-PHOSPHATE, a carbon metabolite intermediate, is thought to function both in long and short days to regulate flowering. In short days, it is thought to act directly at the shoot apex to control levels of *SQUAMOSA PROMOTER BINDNG PROTEIN-LIKE* (*SPL*) gene family members as well as miR156 (Wahl *et al.*, 2013), components of the age-dependent pathway (Fornara & Coupland, 2009). Carbon metabolism, in terms of both growth and pools of non-structural carbohydrates is affected by climate in complex ways (Wingler, 2015; Pilkington *et al.*, 2015). While it seems that long-day

photoperiods may override this pathway (Fornara & Coupland, 2009), it would be interesting to understand how the both pathways interact in intermediate day lengths. Further, like *FT*, gibberellic acid (GA) is a graft-transmissible signal (Regnault *et al.*, 2016). GA is involved in inducing flowering in short days (Wilson *et al.*, 1992) as well as under low constant (15 ˚C) temperatures independently of *FT* (Galvao *et al.*, 2015). GA may act down stream of NO FLOWERING IN SHORT DAY (NFL) (Sharma *et al.*, 2016). Interestingly, GA biosynthesis is negatively regulated by SVP at the shoot apex (Andres *et al.*, 2014), while GA positively regulates *LFY* at the shoot apex to promote flowering (Blazquez & Weigel, 2000).

In addition to other florigen-like factors, a second factor that may contribute to flowering as plants age is sensitivity of genes at the shoot apex to the florigen signal. This, again, is likely influenced by climate. For example, in short-days, high temperatures are proposed to reduce activity of SVP at the shoot apex, causing flowering despite lower levels of *FT* (Fernández *et al.*, 2016). At the shoot apex, SVP suppresses *SUPPRESSOR OF OVEREXPRESSION OF CONSTANS* (*SOC1*), which is positively regulated by *FT*, and which activates *LEAFY* (*LFY*), a key player in the floral transition (Schmid *et al.*, 2003; Lee *et al.*, 2008; Jang *et al.*, 2009). FT also activates *APETALA1* (*AP1*) at the shoot apex (Lee & Lee, 2010). AP1, in turn, is involved in the down regulation of *TERMINAL FLOWERING1*, a homolog of *FT*. TFL1 is thought to compete with FT for binding with FD, causing suppression of *LFY*, as well as *AP1*, forming a negative feedback loop (Kaufmann *et al.*, 2010; Wickland & Hanzawa, 2015). Both the decrease in SVP and TFL1 would likely decrease the threshold amount of *FT* needed to induce flowering. Like *SVP*, *TFL1* may play a more active role under cooler temperatures, as lines containing the *tfl1* mutation showed a stronger flowering phenotype at 16 ˚C compared to 23 ˚C (Kim *et al.*, 2013). Wenden *et al*. demonstrate that a changing threshold due to different allelic variants of *LATE FLOWERING* in Pea, a homologue of *TFL1* in *Arabidopsis* (Foucher *et al.*, 2003), can contribute to accurate prediction of flowering times (Wenden *et al.*, 2009). I propose that climate can act to influence flowering in a similar manner.

Considering both mobile, florigen-like signals and threshold sensitivity at the shoot apex, a more likely model would be one in which a few different floral signals increase at the shoot apex over time, coupled with a decline of the threshold needed to induce flowering. Which floral signal is dominant would depend on the climactic cues. The threshold requirement at the shoot apex would likely change both with climate and with developmental time. An important next step is to determine how the levels of flowering regulators change in later produced leaves and at the shoot apex over the lifetime of the plant.

When considering temporal seasonal scales, it is necessary to consider how climactic factors might change in their interactions over the season. Molecular analyses of flowering pathway components are often done on young plants, in conditions in which one factor may be saturating (such as in long day lengths), or in stable conditions (e.g. Blazquez *et al.*, 2003; Sawa *et al.*, 2007). In nature, day length, light quality, and temperature are all constantly changing. Here insights can be gained from agricultural studies performed to understand the complex interactions between multiple cues. For example, detailed analysis of wheat led to the observation that long-day photoperiods suppress flowering in the fall in winter annuals, while promoting flowering after vernalization has occurred (Brooking & Jamieson, 2002). Similar interactions between climate variables have been observed in other plants. Fluctuating ambient temperatures may be enough to overcome the vernalization requirement in *Arabidopsis*

(Burghardt *et al.*, 2016), while longer vernalization times can allow flowering in shorter photoperiods in *Beta vulgaris* ssp. Maritima (Van Dijk, 2009).

The reasons for some of these climactic interactions is unclear, and for this, considering longer, evolutionary time scales may be useful. For example, day length or light-intensity can influence dormancy or the onset of the cold response (Franklin & Whitelam, 2007). Likely, this is because cold temperatures and light quality changes occurred simultaneously and predictably over several generations. Approaching some of these other climactic interactions in a similar way could yield new insights. One proposed reason that high temperatures reduce SVP at the shoot apex and promote flowering despite lower levels of *FT* is to enable flowering under drought conditions as an avoidance mechanism (Fernández *et al.*, 2016). This behavior is consistent with the different growth habits of *Brassica rapa* populations from wet and dry sites (Franks *et al.*, 2007; Franks & Weis, 2008). Those that had experienced drought for several generations flowered earlier and at a smaller size than those that had not. It would be interesting to compare the protein profiles of SVP homologs and expression of flowering genes at the shoot apex between these two populations both in well-watered and drought conditions, and over developmental time. Some comparisons of natural populations are already yielding differences in known regulators, such as with the cold response (Gehan *et al.*, 2015).

Phenological regulation is clearly complex. Internal and external factors converge to regulate the timing of phenological events. Systematically considering different scales of regulation – molecular, physiological, and whole plant, as well as seasonal and evolutionary time – could improve our understanding. Mathematical models can aid in this process, while detailed observations of agricultural crops over the growing season could yield new insights for molecular studies.

Finally, I would like to come back to the need I stated in chapter one: to be able to better predict plant response in complex environments. A common resistance to incorporating detailed molecular mechanisms into models is that doing so requires several new parameters (Zheng *et al.*, 2013). This is true. Basic thermal time models have two to four parameters (Kumudini *et al.*, 2014), while molecular pathways need terms describing the rate of induction, degradation, or the relationships between genes (Welch *et al.*, 2003; Salazar *et al.*, 2009). For these reasons, I do not suggest that full molecular pathways be incorporated into crop models. Crop modelers can begin with the models they have, and adjust them based on insights gained from mechanistic models in model species (e.g. Brown *et al.*, 2013). For example, our model demonstrated that short-term drops in temperature could promote flowering to some degree through induction of *FT*. Based on this, temperature fluctuations could be given a net positive influence on the developmental time (leaf number) at which the vegetative to reproductive shift occurs, while average temperatures could still influence the rate of leaf emergence. Mechanistic models can also help to clarify the influence different allelic variants to determine the weight of parameters used to describe different cultivars in more traditional crop models (e.g. Zheng *et al.*, 2013). Finally, if modelers find that adding mechanistic regulation would be useful, it may not be necessary to add full pathways. For example, in our model, temperature influences CO directly rather than through regulation of FBH and other upstream components. Using such a gradual, additive, *á la carte* approach would be more tenable than trying to build – and run – a complex mechanistic plant simulation.

References

Andres F, Porri A, Torti S, Mateos J, Romera-Branchat M, Luis Garcia-Martinez J, Fornara F, Gregis V, Kater MM, Coupland G. **2014**. SHORT VEGETATIVE PHASE reduces gibberellin biosynthesis at the *Arabidopsis* shoot apex to regulate the floral transition. *Proceedings of the National Academy of Sciences* **111**: E2760–E2769.

Blazquez M, Ahn J, Weigel D. **2003**. A thermosensory pathway controlling flowering time in *Arabidopsis thaliana*. *Nature Genetics* **33**: 168–171.

Blazquez MA, Weigel D. **2000**. Integration of floral inductive signals in *Arabidopsis*. *Nature* **404**: 889–892.

Boote KJ, Jones JW, White JW, Asseng S, Lizaso JI. **2013**. Putting mechanisms into crop production models. *Plant, Cell and Environment* **36**: 1658–1672.

Bratzel F, Turck F. **2015**. Molecular memories in the regulation of seasonal flowering: from competence to cessation. *Genome Biology* **16**: 192.

Brooking IR, Jamieson PD. **2002**. Temperature and photoperiod response of vernalization in near-isogenic lines of wheat. *Field Crops Research* **79**: 21–38.

Brown HE, Jamieson PD, Brooking IR, Moot DJ, Huth NI. **2013**. Integration of molecular and physiological models to explain time of anthesis in wheat. *Annals of Botany* **112**: 1683–1703.

Burghardt LT, Runcie DE, Wilczek AM, Cooper MD, Roe JL, Welch SM, Schmitt J. **2016**. Fluctuating, warm temperatures decrease the effect of a key floral repressor on flowering time in Arabidopsis thaliana. *New Phytologist* **210**: 564–576.

Chew YH, Wenden B, Flis A, Mengin V, Taylor J, Davey CL, Tindal C, Thomas H, Ougham HJ, Reffye P de, *et al.* 2014. Multiscale digital *Arabidopsis* predicts individual organ and whole-organism growth. *Proceedings of the National Academy of Sciences* **111**: E4127–E4136.

Chew YH, Wilczek AM, Williams M, Welch SM, Schmitt J, Halliday KJ. **2012**. An augmented *Arabidopsis* phenology model reveals seasonal temperature control of flowering time. *New Phytologist* **194**: 654–665.

Chuine I. **2000**. A unified model for budburst of trees. *Journal of Theoretical Biology* **207**: 337–347.

Corbesier L, Vincent C, Jang S, Fornara F, Fan Q, Searle I, Giakountis A, Farrona S, Gissot L, Turnbull C, *et al.* 2007. FT protein movement contributes to long-distance signaling in floral induction of *Arabidopsis thaliana*. *Science* **316**: 1030–1033.

Dalchau N, Baek SJ, Briggs HM, Robertson FC, Dodd AN, Gardner MJ, Stancombe MA, Haydon MJ, Stan G-B, Gonçalves JM, *et al.* 2011. The circadian oscillator gene *GIGANTEA*

mediates a long-term response of the *Arabidopsis thaliana* circadian clock to sucrose. *Proceedings of the National Academy of Sciences* **108**: 5104–5109.

Farré EM. **2012**. The regulation of plant growth by the circadian clock. *Plant Biology* **14**: 401–410.

Fernández V, Takahashi Y, LeGourrierec J, Coupland G. **2016**. Photoperiodic and thermosensory pathways interact through CONSTANS to promote flowering at high temperature under short days. *Plant Journal*.

Fornara F, Coupland G. **2009**. Plant Phase Transitions Make a SPLash. *Cell* **138**: 625–627.

Foucher F, Morin J, Courtiade J, Cadioux S, Ellis N, Banfield MJ, Rameau C. **2003**. *DETERMINATE* and *LATE FLOWERING* are two *TERMINAL FLOWER1/CENTRORADIALIS* homologs that control two distinct phases of flowering initiation and development in pea. *Plant Cell* **15**: 2742–2754.

Franklin KA, Whitelam GC. **2007**. Light-quality regulation of freezing tolerance in Arabidopsis thaliana. *Nature Genetics* **39**: 1410–1413.

Franks SJ, Sim S, Weis AE. **2007**. Rapid evolution of flowering time by an annual plant in response to a climate fluctuation. *Proceedings of the National Academy of Sciences* **104**: 1278–1282.

Franks SJ, Weis AE. **2008**. A change in climate causes rapid evolution of multiple life-history traits and their interactions in an annual plant. *Journal of Evolutionary Biology* **21**: 1321–1334.

Galvao VC, Collani S, Horrer D, Schmid M. **2015**. Gibberellic acid signaling is required for ambient temperature-mediated induction of flowering in *Arabidopsis thaliana*. *Plant Journal* **84**: 949–962.

Gehan MA, Park S, Gilmour SJ, An C, Lee C-M, Thomashow MF. **2015**. Natural variation in the C-repeat binding factor cold response pathway correlates with local adaptation of Arabidopsis ecotypes. *Plant Journal* **84**: 682–693.

Golembeski GS, Kinmonth-Schultz HA, Song YH, Imaizumi T. **2014**. Photoperiodic flowering regulation in *Arabidopsis thaliana*. In: Fornara F, ed. *Molecular Genetics of Floral Transition and Flower Development*. London, UK: Academic Press Ltd-Elsevier Science Ltd, 1–28.

He J, Le Gouis J, Stratonovitch P, Allard V, Gaju O, Heumez E, Orford S, Griffiths S, Snape JW, Foulkes MJ, *et al.* 2012. Simulation of environmental and genotypic variations of final leaf number and anthesis date for wheat. *European Journal of Agronomy* **42**: 22–33.

Iñigo S, Alvarez MJ, Strasser B, Califano A, Cerdán PD. **2012**. PFT1, the MED25 subunit of the plant Mediator complex, promotes flowering through CONSTANS dependent and independent mechanisms in Arabidopsis. *Plant Journal* **69**: 601–612.

Ito S, Song YH, Josephson-Day AR, Miller RJ, Breton G, Olmstead RG, Imaizumi T. **2012**. FLOWERING BHLH transcriptional activators control expression of the photoperiodic flowering regulator *CONSTANS* in *Arabidopsis*. *Proceedings of the National Academy of Sciences* **109**: 3582–3587.

Jamieson PD, Brooking IR, Semenov MA, Porter JR. **1998a**. Making sense of wheat development: a critique of methodology. *Field Crops Research* **55**: 117–127.

Jamieson PD, Semenov MA, Brooking IR, Francis GS. **1998b**. Sirius: a mechanistic model of wheat response to environmental variation. *European Journal of Agronomy* **8**: 161–179.

Jang S, Torti S, Coupland G. **2009**. Genetic and spatial interactions between FT, TSF and SVP during the early stages of floral induction in *Arabidopsis*. *Plant Journal* **60**: 614–625.

Jones JW, Hoogenboom G, Porter CH, Boote KJ, Batchelor WD, Hunt LA, Wilkens PW, Singh U, Gijsman AJ, Ritchie JT. **2003**. The DSSAT cropping system model. *European Journal of Agronomy* **18**: 235–265.

Jung J-H, Seo PJ, Park C-M. **2012**. The E3 ubiquitin ligase HOS1 regulates *Arabidopsis* flowering by mediating CONSTANS degradation under cold stress. *Journal of Biological Chemistry* **287**: 43277–43287.

Kaufmann K, Wellmer F, Muiño JM, Ferrier T, Wuest SE, Kumar V, Serrano-Mislata A, Madueño F, Krajewski P, Meyerowitz EM, *et al.* 2010. Orchestration of Floral Initiation by APETALA1. *Science* **328**: 85–89.

Kim W, Park TI, Yoo SJ, Jun AR, Ahn JH. **2013**. Generation and analysis of a complete mutant set for the *Arabidopsis FT/TFL1* family shows specific effects on thermo-sensitive flowering regulation. *Journal of Experimental Botany* **64**: 1715–1729.

Kinmonth-Schultz HA, Golembeski GS, Imaizumi T. **2013**. Circadian clock-regulated physiological outputs: dynamic responses in nature. *Seminars in cell & developmental biology* **24**: 407–413.

Kinmonth-Schultz HA, Tong X, Lee J, Song YH, Ito S, Kim S-H, Imaizumi T. **2016**. Cool night-time temperatures induce the expression of *CONSTANS* and *FLOWERING LOCUS T* to regulate flowering in *Arabidopsis*. *New Phytologist* **211**: 208–224.

Krzymuski M, Andrés F, Cagnola JI, Seonghoe J, Yanovsky M, Coupland G, Casal JJ. **2015**. The dynamics of *FLOWERING LOCUS T* expression encodes long-day information. *Plant journal* **83**: 952–961.

Kumudini S, Andrade FH, Boote KJ, Brown GA, Dzotsi KA, Edmeades GO, Gocken T, Goodwin M, Halter AL, Hammer GL, *et al.* 2014. Predicting maize phenology: Intercomparison of functions for developmental response to temperature. *Agronomy Journal* **106**: 2087.

Lee JH, Kim JJ, Kim SH, Cho HJ, Kim J, Ahn JH. **2012**. The E3 ubiquitin ligase HOS1 regulates low ambient temperature-responsive flowering in *Arabidopsis thaliana*. *Plant and Cell Physiology*.

Lee J, Lee I. **2010**. Regulation and function of SOC1, a flowering pathway integrator. *Journal of Experimental Botany*: erq098.

Lee J, Oh M, Park H, Lee I. **2008**. SOC1 translocated to the nucleus by interaction with AGL24 directly regulates *LEAFY*. *Plant Journal* **55**: 832–843.

Lee JH, Ryu H-S, Chung KS, Posé D, Kim S, Schmid M, Ahn JH. **2013**. Regulation of temperature-responsive flowering by MADS-Box transcription factor repressors. *Science* **342**: 628–632.

Lee JH, Yoo SJ, Park SH, Hwang I, Lee JS, Ahn JH. **2007**. Role of *SVP* in the control of flowering time by ambient temperature in *Arabidopsis*. *Genes & Development* **21**: 397–402.

Lehenbauer PA. **1914**. Growth of maize seedlings in relation to temperature. *Physiological Researches* **1**: 247–288.

Li Z, Pinson SRM, Stansel JW, Paterson AH. **1998**. Genetic dissection of the source-sink relationship affecting fecundity and yield in rice (shape Oryza sativa L.). *Molecular Breeding* **4**: 419–426.

Monshausen GB, Haswell ES. **2013**. A force of nature: molecular mechanisms of mechanoperception in plants. *Journal of Experimental Botany*: ert204.

Murata N, Los DA. **1997**. Membrane fluidity and temperature perception. *Plant Physiology* **115**: 875–879.

Nomoto Y, Kubozono S, Miyachi M, Yamashino T, Nakamichi N, Mizuno T. **2013**. A circadian clock- and PIF4-mediated double coincidence mechanism is implicated in the thermosensitive photoperiodic control of plant architectures in *Arabidopsis thaliana*. *Plant & Cell Physiology* **53**: 1965–1973.

Nusinow DA, Helfer A, Hamilton EE, King JJ, Imaizumi T, Schultz TF, Farré EM, Kay SA. **2011**. The ELF4-ELF3-LUX complex links the circadian clock to diurnal control of hypocotyl growth. *Nature* **475**: 398–402.

Pantin F, Simonneau T, Rolland G, Dauzat M, Muller B. **2011**. Control of Leaf Expansion: A Developmental Switch from Metabolics to Hydraulics. *Plant Physiology* **156**: 803–815.

Parent B, Turc O, Gibon Y, Stitt M, Tardieu F. **2010**. Modelling temperature-compensated physiological rates, based on the co-ordination of responses to temperature of developmental processes. *Journal of Experimental Botany* **61**: 2057–2069.

Pilkington SM, Encke B, Krohn N, Höhne M, Stitt M, Pyl E-T. **2015**. Relationship between starch degradation and carbon demand for maintenance and growth in Arabidopsis thaliana in different irradiance and temperature regimes. *Plant, Cell & Environment* **38**: 157–171.

Piper EL, Smit MA, Boote KJ, Jones JW. **1996**. The role of daily minimum temperature in modulating the development rate to flowering in soybean. *Field Crops Research* **47**: 211–220.

Poiré R, Wiese-Klinkenberg A, Parent B, Mielewczik M, Schurr U, Tardieu F, Walter A. **2010**. Diel time-courses of leaf growth in monocot and dicot species: endogenous rhythms and temperature effects. *Journal of Experimental Botany* **61**: 1751–1759.

Posé D, Verhage L, Ott F, Yant L, Mathieu J, Angenent GC, Immink RGH, Schmid M. **2013**. Temperature-dependent regulation of flowering by antagonistic FLM variants. *Nature* **503**: 414–417.

Regnault T, Davière J-M, Achard P. **2016**. Long-distance transport of endogenous gibberellins in *Arabidopsis*. *Plant Signaling & Behavior* **11**: e1110661.

Ritchie J, Otter S. **1985**. Description and performance of CERES-Wheat. A user-oriented wheat model. *US Department of Agriculture,* ARS **38**: 159–175.

Rizhsky L, Liang H, Shuman J, Shulaev V, Davletova S, Mittler R. **2004**. When defense pathways collide. The response of Arabidopsis to a combination of drought and heat stress. *Plant Physiology* **134**: 1683–1696.

Salazar JD, Saithong T, Brown PE, Foreman J, Locke JCW, Halliday KJ, Carré IA, Rand DA, Millar AJ. **2009**. Prediction of photoperiodic regulators from quantitative gene circuit models. *Cell* **139**: 1170–1179.

Sawa M, Nusinow DA, Kay SA, Imaizumi T. **2007**. FKF1 and GIGANTEA complex formation is required for day-length measurement in *Arabidopsis*. *Science* **318**: 261–265.

Schmid M, Uhlenhaut NH, Godard F, Demar M, Bressan R, Weigel D, Lohmann JU. **2003**. Dissection of floral induction pathways using global expression analysis. *Development* **130**: 6001–12.

Schwartz C, Balasubramanian S, Warthmann N, Michael TP, Lempe J, Sureshkumar S, Kobayashi Y, Maloof JN, Borevitz JO, Chory J, *et al.* 2009. Cis-regulatory changes at *FLOWERING LOCUS T* mediate natural variation in flowering responses of *Arabidopsis thaliana*. *Genetics* **183**: 723–732.

Sharma N, Xin R, Kim D-H, Sung S, Lange T, Huq E. **2016**. NO FLOWERING IN SHORT DAY (NFL) is a bHLH transcription factor that promotes flowering specifically under short-day conditions in Arabidopsis. *Development* **143**: 682–690.

Song Y-H, Shim J-S, Kinmonth-Schultz HA, Imaizumi T. **2015**. Photoperiodic flowering: time measurement mechanisms in leaves. *Annual Review of Plant Biology* **66**: 441–464.

Stewart JL, Maloof JN, Nemhauser JL. **2011**. PIF genes mediate the effect of sucrose on seedling growth dynamics. *PloS one* **6**: e19894.

Usadel B, Blasing OE, Gibon Y, Retzlaff K, Hohne M, Gunther M, Stitt M. **2008**. Global transcript levels respond to small changes of the carbon status during progressive exhaustion of carbohydrates in Arabidopsis rosettes. *Plant Physiology* **146**: 1834–1861.

Van Dijk H. **2009**. Evolutionary change in flowering phenology in the iteroparous herb Beta vulgaris ssp. maritima: a search for the underlying mechanisms. *Journal of Experimental Botany* **60**: 3143–3155.

Wahl V, Ponnu J, Schlereth A, Arrivault S, Langenecker T, Franke A, Feil R, Lunn JE, Stitt M, Schmid M. **2013**. Regulation of flowering by trehalose-6-phosphate signaling in Arabidopsis thaliana. *Science* **339**: 704–707.

Walter A, Silk WK, Schurr U. **2009**. Environmental Effects on Spatial and Temporal Patterns of Leaf and Root Growth. *Annual Review of Plant Biology* **60**: 279–304.

Welch SM, Roe JL, Dong Z. **2003**. A genetic neural network model of flowering time control in *Arabidopsis thaliana*. *Agronomy Journal* **95**: 71--81.

Wenden B, Dun EA, Hanan J, Andrieu B, Weller JL, Beveridge CA, Rameau C. **2009**. Computational analysis of flowering in pea (*Pisum sativum*). *New Phytologist* **184**: 153–167.

White JW. **2009**. Combining ecophysiological models and genomics to decipher the GEM-to-P problem. *NJAS - Wageningen Journal of Life Sciences* **57**: 53–58.

Wickland DP, Hanzawa Y. **2015**. The *FLOWERING LOCUS T/TERMINAL FLOWER 1* gene family: functional evolution and molecular mechanisms. *Molecular Plant* **8**: 983–997.

Wilczek AM, Roe JL, Knapp MC, Cooper MD, Lopez-Gallego C, Martin LJ, Muir CD, Sim S, Walker A, Anderson J, *et al.* 2009. Effects of genetic perturbation on seasonal life history plasticity. *Science* **323**: 930–934.

Wilson RN, Heckman JW, Somerville CR. **1992**. Gibberellin is required for flowering in *Arabidopsis thaliana* under short days. *Plant Physiology* **100**: 403–408.

Wingler A. **2015**. Comparison of signaling interactions determining annual and perennial plant growth in response to low temperature. *Plant Physiology* **5**: 794.

Zheng B, Biddulph B, Li D, Kuchel H, Chapman S. **2013**. Quantification of the effects of *VRN1* and *Ppd-D1* to predict spring wheat (*Triticum aestivum*) heading time across diverse environments. *Journal of Experimental Botany* **64**: 3747–3761.

Zuo Z, Liu H, Liu B, Liu X, Lin C. **2011**. Blue light-dependent interaction of CRY2 with SPA1 regulates COP1 activity and floral initiation in Arabidopsis. *Current biology* **21**: 841–847.